Aus dem Institut für Biomaterialforschung, Helmholtz-Zentrum Geesthacht

Synthesis and Characterization of Thermosensitive Hydrogels Derived From Polysaccharides

Dissertation

zur Erlangung des akademischen Grades
"doctor rerum naturalium"

(Dr. rer. nat.)
in der Wissenschaftsdisziplin
"Materialien in den Lebenswissenschaften"

eingereicht an der
Mathematisch-Naturwissenschaftlichen Fakultät
der Universität Potsdam

von

Harshal Diliprao Santan
aus Nanded (Maharashtra), Indien

Potsdam, den 26.06.2013

Published online at the
Institutional Repository of the University of Potsdam:
URL http://opus.kobv.de/ubp/volltexte/2014/6979/
URN urn:nbn:de:kobv:517-opus-69793
http://nbn-resolving.de/urn:nbn:de:kobv:517-opus-69793

Statement of Originality

I, Harshal Santan, formally submit the dissertation entitled “Synthesis and Characterization of Thermosensitive Hydrogels Derived from Polysaccharides” to the Department of Mathematics and Natural Sciences University of Potsdam, Germany, for the acquirement of the academic degree of Doctor of Natural Sciences (Dr. rer. nat.) in Materials for Life Science.

I hereby certify that this submission is entirely my own original work and that, to the best of my knowledge and belief, it contains no material previously published or written by another person, except where due reference is made in the thesis itself. Neither the dissertation, nor any sections thereof, has been previously submitted for a degree or other qualification to any other University or Institution. Any contribution made to the research by other, with whom I worked at HZG or elsewhere, is explicitly acknowledged in the thesis.

Contents

Abstract

In this work, thermosensitive hydrogels having tunable thermo-mechanical properties were synthesized. Generally the thermal transition of thermosensitive hydrogels is based on either a lower critical solution temperature (LCST) or critical micelle concentration/ temperature (CMC/ CMT). The temperature dependent transition from sol to gel with large volume change may be seen in the former type of thermosensitive hydrogels and is negligible in CMC/ CMT dependent systems. The change in volume leads to exclusion of water molecules, resulting in shrinking and stiffening of system above the transition temperature. The volume change can be undesired when cells are to be incorporated in the system. The gelation in the latter case is mainly driven by micelle formation above the transition temperature and further colloidal packing of micelles around the gelation temperature. As the gelation mainly depends on concentration of polymer, such a system could undergo fast dissolution upon addition of solvent. Here, it was envisioned to realize a thermosensitive gel based on two components, one responsible for a change in mechanical properties by formation of reversible netpoints upon heating without volume change, and second component conferring degradability on demand. As first component, an ABA triblockcopolymer (here: Poly(ethylene glycol)-*b*-poly(propylene glycol)-*b*-poly(ethylene glycol) (PEPE) with thermosensitive properties, whose sol-gel transition on the molecular level is based on micellization and colloidal jamming of the formed micelles was chosen, while for the additional macromolecular component crosslinking the formed micelles biopolymers were employed.

The synthesis of the hydrogels was performed in two ways, either by physical mixing of compounds showing electrostatic interactions, or by covalent coupling of the components. Biopolymers (here: the polysaccharides hyaluronic acid, chondroitin sulphate, or pectin, as well as the protein gelatin) were employed as additional macromolecular crosslinker to simultaneously incorporate an enzyme responsiveness into the systems. In order to have strong ionic/electrostatic interactions between PEPE and polysaccharides, PEPE was aminated to yield predominantly mono- or di-substituted PEPEs. The systems based on aminated PEPE physically mixed with HA showed an enhancement in the mechanical properties such as, elastic modulus (G′) and viscous modulus (G″) and a decrease of

the gelation temperature (T_{gel}) compared to the PEPE at same concentration. Furthermore, by varying the amount of aminated PEPE in the composition, the T_{gel} of the system could be tailored to 27-36 °C. The physical mixtures of HA with di-amino PEPE (HA·di-PEPE) showed higher elastic moduli G′ and stability towards dissolution compared to the physical mixtures of HA with mono-amino PEPE (HA·mono-PEPE). This indicates a strong influence of electrostatic interaction between –COOH groups of HA and $–NH_2$ groups of PEPE.

The physical properties of HA with di-amino PEPE (HA·di-PEPE) compare beneficially with the physical properties of the human vitreous body, the systems are highly transparent, and have a comparable refractive index and viscosity. Therefore, this material was tested for a potential biological application and was shown to be non-cytotoxic in eluate and direct contact tests. The materials will in the future be investigated in further studies as vitreous body substitutes. In addition, enzymatic degradation of these hydrogels was performed using hyaluronidase to specifically degrade the HA. During the degradation of these hydrogels, increase in the T_{gel} was observed along with decrease in the mechanical properties. The aminated PEPE were further utilised in the covalent coupling to Pectin and chondroitin sulphate by using EDC as a coupling agent. Here, it was possible to adjust the T_{gel} (28-33 °C) by varying the grafting density of PEPE to the biopolymer. The grafting of PEPE to Pectin enhanced the thermal stability of the hydrogel. The Pec-*g*-PEPE hydrogels were degradable by enzymes with slight increase in T_{gel} and decrease in G′ during the degradation time.

The covalent coupling of aminated PEPE to HA was performed by DMTMM as a coupling agent. This method of coupling was observed to be more efficient compared to EDC mediated coupling. Moreover, the purification of the final product was performed by ultrafiltration technique, which efficiently removed the unreacted PEPE from the final product, which was not sufficiently achieved by dialysis. Interestingly, the final products of these reaction were in a gel state and showed enhancement in the mechanical properties at very low concentrations (2.5 wt%) near body temperature. In these hydrogels the resulting increase in mechanical properties was due to the combined effect of micelle packing (physical interactions) by PEPE and covalent netpoints between PEPE and HA. PEPE alone or the physical mixtures of the same components were not able to show thermosensitive behavior at concentrations below 16 wt%. These thermosensitive hydrogels also showed on-

demand solubilisation by enzymatic degradation. The concept of thermosensitivity was introduced to 3D architectured porous hydrogels, by covalently grafting the PEPE to gelatin and crosslinking with LDI as a crosslinker. Here, the grafted PEPE resulted in a decrease in the helix formation in gelatin chains and after fixing the gelatin chains by crosslinking, the system showed an enhancement in the mechanical properties upon heating (34-42 °C) which was reversible upon cooling. A possible explanation of the reversible changes in mechanical properties is the strong physical interactions between micelles formed by PEPE being covalently linked to gelatin. Above the transition temperature, the local properties were evaluated by AFM indentation of pore walls in which an increase in elastic modulus (E) at higher temperature (37 °C) was observed. The water uptake of these thermosensitive architectured porous hydrogels was also influenced by PEPE and temperature (25 °C and 37 °C), showing lower water up take at higher temperature and vice versa. In addition, due to the lower water uptake at high temperature, the rate of hydrolytic degradation of these systems was found to be decreased when compared to pure gelatin architectured porous hydrogels. Such temperature sensitive architectured porous hydrogels could be important for e.g. stem cell culturing, cell differentiation and guided cell migration, etc.

Altogether, it was possible to demonstrate that the crosslinking of micelles by a macromolecular crosslinker increased the shear moduli, viscosity, and stability towards dissolution of CMC-based gels. This effect could be likewise be realized by covalent or non-covalent mechanisms such as, micelle interactions, physical interactions of gelatin chains and physical interactions between gelatin chains and micelles. Moreover, the covalent grafting of PEPE will create additional net-points which also influence the mechanical properties of thermosensitive architectured porous hydrogels. Overall, the physical and chemical interactions and reversible physical interactions in such thermosensitive architectured porous hydrogels gave a control over the mechanical properties of such complex system. The hydrogels showing change of mechanical properties without a sol-gel transition or volume change are especially interesting for further study with cell proliferation and differentiation.

Zusammenfassung

In der vorliegenden Arbeit wurden thermosensitive Hydrogele mit einstellbaren thermo-mechanischen Eigenschaften synthetisiert. Im Allgemeinen basiert der thermische Übergang thermosensitiver Gele auf einer niedrigsten kritischen Löslichkeitstemperatur (LCST) oder kritischer Mizellkonzentration bzw. –temperatur (CMC/ CMT). Der temperaturabhängige Übergang von Sol zu Gel mit großer Volumenänderung wurde im ersten Fall bei thermosensitiven Hydrogelen beobachtet und ist vernachlässigbar für CMC/ CMT abhängige Systeme. Die Änderung des Volumens führt zum Ausschluss von Wassermolekülen, was zum Schrumpfen und Versteifen des Systems oberhalb der Übergangstemperatur führt. Die Volumenänderung kann unerwünscht sein, wenn Zellen in das Gel eingeschlossen werden sollen. Die Gelierung im zweiten Fall beruht hauptsächlich auf der Mizellbildung oberhalb der Übergangstemperatur und weiterem kolloidalem Packen von Mizellen im Bereich der Gelierungstemperatur. Weil die Gelierung hauptsächlich von der Polymerkonzentration abhängt, kann sich das Gel bei Zugabe von Lösungsmittel leicht wieder lösen. Hier sollten thermosensitive Gele entwickelt werden, die auf zwei Komponenten beruhen. Eine Komponente sollte aus einem ABA-Triblockcopolymer mit thermosensitiven Eigenschaften bestehen, dem Poly(ethylen glycol)-*b*-Poly(propylenglycol)-*b*-Poly(ethylen glycol) (PEPE), dessen Sol-Gel-Übergang auf Mizellierung und kolloidalem Jamming der gebildeten Mizellen basiert, und einer weiteren makromolekularen Komponente, einem Biopolymer, dass die Mizellen vernetzt. Auf diese Weise sollten thermosensitive Gele realisiert werden, die keine oder nur eine kleine Volumenänderung während der Änderung der mechanischen Eigenschaften zeigen, die stabiler gegenüber Verdünnung sein sollten als klassische Hydrogele mit einem CMC-basierten Übergang und die jedoch gezielt abgebaut werden können.

Die Hydrogele wurden auf zwei Arten vernetzt, entweder durch physikalisches Vermischen, bei dem die Vernetzung durch elektrostatische Wechselwirkungen erfolgte, oder durch kovalente Kopplung der beiden Komponenten. Als makromolekulare Komponente zur Vernetzung der Mizellen wurden Biopolymere (hier: die Polysaccharide Hyaluronsäure (HA), Chondroitinsulfat oder Pektin oder das Protein Gelatin) verwendet, um die Hydrogele enzymatisch abbaubar zu gestalten. Um eine starke ionische/elektrostatische Wechselwirkung zwischen dem PEPE und

den Polysacchariden zu erzielen, wurde PEPE aminiert, um hauptsächlich monoaminiertes bzw. diaminiertes PEPE einsetzen zu können. Die Gele, die auf der physikalischen Mischung von aminierten PEPE mit HA bestehen, zeigten im Vergleich zu PEPE bei gleicher Konzentration eine Zunahme der mechanischen Eigenschaften, wie beispielsweise dem elastischem Modulus (G′) und dem Viskositätsmodulus (G″) bei gleichzeitiger Abnahme der Gelierungstemperatur (T_{gel}). Durch Variation des Gehalts an aminierten PEPE-, konnte die T_{gel} in einem Bereich von 27-36 °C eingestellt werden. Interessanterweise zeigten die physikalischen Mischungen mit diaminierten PEPE (HA·di-PEPE) höhere mechanische Eigenschaften (elastischer Modulus G′) und eine höhere Stabilität gegenüber Verdünnungseffekten als Mischungen mit monoaminiertem PEPE (HA·mono-PEPE). Dies zeigt den starken Einfluss der elektrostatischen Wechselwirkungen zwischen der Carboxylgruppe der HA und der Amingruppe von PEPE. Die physikalischen Eigenschaften HA·di-PEPE sind vergleichbar mit den physikalischen Eigenschaften des Glaskörpers im Auge hinsichtlich Transparenz, Brechungsindex und Viskosität. Deswegen wurde das Material hinsichtlich seiner biologischen Anwendung getestet und zeigte sich sowohl im Überstand als auch im direkten Kontakt als nicht-zytotoxisch. Zukünftig wird dieses Material in weiteren Untersuchungen bezüglich seiner Eignung als Glaskörperersatz geprüft werden. Zusätzlich konnte der enzymatische Abbau der Hydrogele mit Hyaluronidase gezeigt werden, die spezifisch HA abbaut. Beim Abbau der Hydrogele stieg T_{gel} bei gleichzeitiger Abnahme der mechanischen Eigenschaften.

Aminiertes PEPE wurde zusätzlich zur kovalenten Bindung unter Verwendung von EDC als Aktivator an Pektin und Chondroitinsulfat eingesetzt. T_{gel} konnte auf 28 – 33 °C eingestellt werden durch Variation der Pfropfungsdichte am Biopolymer bei gleichzeitiger Zunahme der thermischen Stabilität. Die Pec-*g*-PEPE Hydrogele waren enzymatisch abbaubar, was zu einer leichten Erhöhung von T_{gel} und zu einer Abnahme von G′ führte.

Die kovalente Bindung der aminierten PEPE an HA erfolgte unter Verwendung von DMTMM als Aktivator, der sich in diesem Fall als effektiver als EDC herausstellte. Die Reinigung mittels Ultrafiltration führte zu einer deutlich besseren Aufreinigung des Produkts als mittels Dialyse. Die gegrafteten Systeme waren in Nähe der Körpertemperatur bereits im Gelstadium und zeigten eine Erhöhung der mechanischen Eigenschaften bereits bei sehr geringen Konzentrationen von 2.5

Gew.%. Die höheren mechanischen Eigenschaften dieser Hydrogele erklären sich durch die Kombination der Mizellbildung (physikalische Wechselwirkung) des PEPE und der Bildung kovalenter Netzpunkte zwischen PEPE und HA. PEPE bzw. entsprechende physikalische Mischungen derselben Komponenten zeigten kein thermosensitives Verhalten bei einer Konzentration unterhalb von 16 Gew%. Diese thermosensitiven Hydrogele zeigten auch eine Löslichkeit auf Abruf durch enzymatischen Abbau.

Das Konzept der Thermosensitivität wurde in 3D strukturierte, poröse Hydrogele (T-ArcGel) eingeführt, bei dem PEPE kovalent an Gelatin gebunden wurde und mit LDI vernetzt wurde. Das gepfropfte PEPE führte zu einer Erniedrigung der Helixbildung der Gelatinketten. Nach Fixierung der Gelatinketten durch Vernetzung zeigte das System eine Erhöhung der mechanischen Eigenschaften bei Erwärmung (34-42 °C). Dieses Phänomen war reversibel beim Abkühlen. Eine mögliche Erklärung der reversiblen Änderungen bezüglich der mechanischen Eigenschaften sind die starken physikalischen Wechselwirkungen zwischen den Mizellen des PEPE, die kovalent an Gelatin gebunden wurden. Ferner wurde durch AFM Untersuchungen festgestellt, dass bei Temperaturerhöhung (37 °C) die örtlichen elastischen Moduli (E) der Zellwände zugenommen haben. Zusätzlich wurde die Wasseraufnahme der T-ArcGele durch PEPE und die Temperatur (25 °C und 37 °C) beeinflusst und zeigte eine niedrigere Wasseraufnahme bei höherer Temperatur und umgekehrt. Durch die niedrigere Wasseraufnahme bei hohen Temperaturen erniedrigte sich die Geschwindigkeit des hydrolytischen Abbaus im Vergleich zu dem strukturierten Hydrogel aus reiner Gelatin. Diese temperatursensitiven ArcGele könnten bedeutsam sein für Anwendungen im Bereich Stammzellkultivierung, Zelldifferenzierung und gerichteter Zellmigration.

Zusammenfassend konnte bei den thermosensitiven Hydrogelen gezeigt werden, dass die Vernetzung von Mizellen mit einem makromolekularen Vernetzer die Schermoduli, Viskosität und Löslichkeitsstabilität im Vergleich zu reinen ABA-Triblockcopolymeren mit CMC-Übergang erhöht. Dieser Effekt konnte durch kovalente und nichtkovalente Mechanismen, wie beispielsweise Mizell-Wechselwirkungen, physikalische Interaktionen von Gelatinketten und physikalische Interaktionen von Gelatinketten und Mizellen, realisiert werden. Das Pfropfen von PEPE führte zu zusätzlichen Netzpunkten, die die mechanischen Eigenschaften der thermosensitiven architekturisierten, porösen Hydrogele beeinflussten. Insgesamt

ermöglichten die physikalischen und chemischen Bindungen und die reversiblen physikalischen Wechselwirkungen in den strukturierten, porösen Hydrogelen eine Kontrolle der mechanischen Eigenschaften in diesem sehr komplexen System. Die Hydrogele, die eine Veränderung ihrer mechanischen Eigenschaften ohne Volumenänderung oder Sol-Gel-Übergang zeigen sind besonders interessant für Untersuchungen bezüglich Zellproliferation und –differenzierung.

List of Abbreviations

AFM	Atomic Force Microscopy
CLSM	Confocal Laser Scanning Microscopy
CS	Chondroitin Sulfate
°C	Degree Celsius
DMF	*N*,*N*-Dimethylformamide
DMSO	Dimethylsulfoxide
DMTMM	4-(4,6-dimethoxy-1,3,5-triazin-2-yl)-4-methylmorpholinium chloride
DSC	Differential Scanning Calorimetry
E	Young's modulus
E_c	Compression modulus
ECM	Extracellular matrix
EDC	1-Ethyl-3-(3-dimethylaminopropyl)carbodiimide
EtOH	Ethanol
FT-IR	Fourier Transform Infrared Spectroscopy
G'	Elastic modulus
G''	Viscous modulus
GPC	Gel Permeation Chromatography
HA	Hyaluronic acid
LAL test	Limulus Amebocyte Lysate Test
MALDI-TOF	Matrix-assisted Laser Desorption/Ionization Time of Flight Mass Spectrometry
M_n	Number average molecular weight
M_p	Peak average molecular weight
NMR	Nuclear Magnetic Resonance Spectroscopy
PBS	Phosphate buffered saline
PEG	Poly(ethylene glycol)
PEC	Pectin
PPG	Poly(propylene glycol)
SAXS	Small Angle X-ray Scattering
SEM	Scanning Electron Microscope
T_{gel}	Gelation Temperature
T_g	Glass transition temperature
T_m	Melting temperature
T_{sw}	Switching temperature
TGA	Thermogravimetric Analysis
TMDSC	Temperature modulated DSC
TNBS	Trinitrobenzenesulfonic acid
WAXS	Wide Angle X-ray Scattering
σ_{max}	Compressive stress

List of figures

List of Schemes

List of Tables

Acknowledgements

I would like to express my sincere gratitude to my supervisor, Prof. Andreas Lendlein, for giving me the opportunity to carry out my PhD work at the HZG and for his valuable guidance and support throughout these years. I would also like to thank my group leader, Dr. Axel Neffe, for supporting me during my work, for his suggestions, advices, and for helping me with my thesis.

I would like to express my gratitude to Dr. Stefan Kamlage, Dr. Benjamin Pierce, Dr. Karola Luetzow, and Dr. Giuseppe Tripodo for supporting me and for their special kindness and availability to discuss my work with them.

It is a pleasure for me to thank all the people without whom this thesis would have not been completed: thank you to Dr. H. Kosmella for the mechanical tests, Susanne Schwanz for the thermal analyses, Dr. Ulrich Noechel for the WAXS and SAXS measurements and also for his helpful suggestions, Dr. T. Weigel for the µCT analysis and Frau Heike Schmidt for the NMR measurements. I would also like to thank Karoline Trescher for the CLSM images, and Dr. Toralf Roch for the cytotoxicity tests, Oliver Frank for the AFM measurements, and Dr. Michael Schroeter for his support regarding the thesis submission. I wish to extent my thanks to all members of BMM and BMF.

I would like to express my sincere gratitude to Prof. Stefan Mundlos, for being my second supervisor and for his valuable suggestions and support during each mentoring committee meetings.

A special thanks goes to Simi and Lucile with whom I started my PhD and also to Maik, with whom, I shared the office and enjoyed sharing this experienced with you all. I would also like to thank my friends (Stefania, Maik, Konstanze, Tilman, Tim, Susanna, Candy) for the nice time and for all the fun during these years. I wish to thank all the PhD students for having a great time with you all.

A special thank goes to my parents, my wife Shweta, and my loving son Ojas for their support, endless love, and understanding throughout these years.

1. Introduction

Polymeric biomaterials are intended for in vivo applications, either as an implant or in extracorporeal systems. They substitute, temporarily or permanently, a part of the living system or at least function in intimate contact with cells, tissues or body fluids, without negatively interfering with the biological processes [1–3]. In addition, smart materials which can response to the small change in their environment have attracted research to develop new materials which can be used in different biomedical applications. These materials require chemical and mechanical properties based on the targeted applications. Synthetic polymers have been used in this context, as their properties can be easily adjusted by changing their copolymer composition, molecular weight, or architecture. However, even such widely applied polymers such as poly(lactic-*co*-glycolic acid) (PLGA) have shown drawbacks, such as change of pH of their environment during degradation[4]. Biopolymers such as polysaccharides or proteins give pH neutral degradation and can provide further functionalities such as cell adhesion[5], but suffer from batch to batch variation, poor mechanical properties, and their properties are more difficult to control than of synthetic polymers. Therefore, recently the development of materials combining biopolymers and synthetic polymers has attracted the interest of researchers[6–9]. A further approach is the incorporation of stimuli sensitive “smart” structures in these materials to increase the applicability and/or display on-demand functionality. Stimuli sensitive or smart materials are one of the examples of such system which respond with a large change in the properties to a small change in their physical or chemical environment[10–17]. In this context, the combination and composition of polymeric system is very important, which on further

physical or chemical functionalization may lead to a material with tunable/controlled properties.

1.1 Introduction to Hydrogels

In the recent studies, stimuli sensitive systems have been reported for various biomedical applications such as, drug delivery, cell encapsulation, and tissue engineering[18–21]. For these applications, often soft materials are of interest and very often hydrogels were studied. Fundamentally, hydrogels are three-dimensional polymeric networks, which are insoluble in water but have the capacity to take up large amounts of water. Their ability to absorb water (swelling of hydrogels) is due to the presence of hydrophilic groups (e.g. -OH, -COOH, $-CONH_2$, $-SO_3H$, $-NH_2$, -CONH-), which also affect the chemical potential of the hydrogels. Due to the hydrophilic nature, high water content, soft and rubbery consistency, permeability to small molecules, and resemblance to tissues, hydrogels can be exploited for biomedical and biotechnological applications[22,23]. Hydrogels can be physically crosslinked or chemically crosslinked systems[21,24]. Physically crosslinked hydrogels may dissolve by addition of excess of water, while the chemically crosslinked one remains unaffected. This can be explained by the difference between a permanent and temporary hydrogel system, which is based on type of bonding within the polymeric molecules. In both cases, a wide range of polymer compositions has been used to synthesize different types of hydrogels. The amount of water in the hydrogel influences the properties of hydrogel such as swelling, permeability of other small molecules, and stability (degradation). Specifically in chemically crosslinked hydrogels, the polymer chains are covalently coupled to each other via crosslinking agents. As the chemical crosslinking process is often irreversible, it makes the resulting hydrogel insoluble in solvents; this limits their usage in many

applications[25,26]. Moreover, the crosslinking agents used are mainly toxic and are hard to remove completely from the final product. In contrast, the physically crosslinked hydrogels have physical netpoints associated with intra or intermolecular interactions such as chains entanglement, hydrophobic/hydrophilic interactions, crystallinity, or hydrogen bonding. The physical netpoints could be induced by an external stimuli like, pH, temperature, light, ionic strength, and electric field; and show reversible effect upon removal of external stimuli[16,27,28]. Hence, the physically crosslinked hydrogels have wide uses in biomedical applications.

In general, hydrogels are treated as neither a solution nor a solid, but display properties of both, which resembles naturally occurring systems such as vitreous humour, cartilage, blood clots, etc. The key success of hydrogels as a biomaterial is their viscoelastic behavior, and permeability of small molecules (e.g. proteins) while maintaining their shape for the required time of application.

In the field of synthetic polymers forming hydrogels, Poly(ethylene glycol) (PEG) (Figure 1) based hydrogels have attracted much attention because of their biocompatibility and hydrophilic properties[29–36]. Their chain length can be modified and biological molecules can be chemically attached. PEG or poly(ethylene oxide) is chemically synonymous, but historically PEG has tended to refer to shorter polymers and PEO to high-molecular adducts.

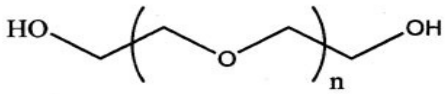

Figure 1. A general representation of hydrophilic Poly(ethylene oxide)

PEG or PEO is a neutral, non-toxic, synthetic polymer. Its water solubility at room temperature is caused by its strong tendency to form hydrogen bonds with water. In recent development, thermosensitive hydrogels derived from PEG system have been extensively used for structurally mimicking the ECM[30,34,37]. In some cases, the

disulfide crosslinking method was used for the preparation of blended HA–gelatin hydrogels to form a synthetic, covalently linked mimic of the ECM[9,38].

1.2 Hydrogels derived from natural polymers

Polysaccharides and proteins, especially the ones present in or derived from the extracellular matrix (ECM) such as, hyaluronic acid, chondroitin sulphate, gelatin etc. are examples of naturally occurring hydrogel forming polymers[39–44]. Hyaluronic acid (HA), for example is a major component of ECM, vitreous humor, and of synovial fluid in joints. It has attractive physical properties such as viscoelastic behavior and unique rheological properties which created a special interest in development of hydrogels derived from HA. Naturally occurring HA is typically a very high molecular weight polysaccharide with molecular weight up to 10-20 MDa. Structurally, the HA is a polysaccharide with a repeating disaccharide unit of D-glucuronic acid and D-*N*-acetyl glucosamine connected with β (1→3) and β (1→4) linkages. HA is a very hydrophilic molecule which forms hydrogen bonding with water molecules and also have intra and inter molecular hydrogen bonding in presence of water. This property allows it to hold very large amounts of water, which is used by nature to regulate the water content in tissues. Very high molecular weight HA in solution is very viscous even at low concentrations (1-2 wt%). Due to this viscoelastic behavior HA is widely used in different biomedical applications. As HA is a polyelectrolyte, the solution properties are affected by ionic strength. The pure HA is water soluble, but has a short residence time in situ which limits the use of HA in biomedical applications.

Other naturally occurring polymers like chondroitin sulphate, pectin, and gelatin are mainly in a gel phase at low temperature and form solution at high temperature. The chemical functionalization of these polymers with synthetic polymers can be useful in

producing hydrogels with tunable mechanical properties and specifically, by physical mixing and covalent coupling with thermosensitive polymers may be useful in producing thermosensitve hydrogels with natural polymer as an backbone.

1.3 Temperature sensitive hydrogels

In recent studies, special types of hydrogels, which undergo (reversible) phase or volume transition upon very minute changes in their external environment, have attracted interest for biomedical applications. Such hydrogels are referred as stimuli sensitive hydrogels, and they can respond to pH, temperature, ionic strength, UV, etc. Figure 2 gives the schematic representation of the phase transition in stimuli sensitive hydrogels. Their response to a stimulus is demonstrated as a dramatic change in shape, surface characteristics, or mechanical properties. Such environmental sensitive hydrogels are ideal candidates for developing self-regulated drug delivery systems[20,45] and also have promising applications in controlled drug delivery applications by changing to a gel structure in response to environmental stimuli, which can be exploited e.g. for fixation of an implant in the body as to influence material-cell interactions.

Generally, temperature sensitive hydrogels showing a reversible sol-gel transition upon increase in temperature are based on two main types, hydrogels having a lower critical solution temperature (LCST) or hydrogels having a critical micelle temperature (CMC). The LCST based hydrogels show shrinking when the temperature increases above the LCST. Generally, water solubility of polymers increases with an increase in temperature and certain hydrogels formed by interpenetrating polymer networks composed of poly[acrylamide–*co*-(butyl methacrylate)] and poly(acrylic acid) exhibit swelling at high temperature and shrinking at low temperature[9]. However, polymers

exhibiting an LCST, show inverse solubility behavior with an increase in temperature. These hydrogels are made-up of polymer chains that either have moderately hydrophobic groups or a mixture of hydrophilic and hydrophobic segments. Poly(*N*-isopropylacrylamide) is the most extensively studied thermosensitive polymer exhibiting LCST in the range of 31-33 °C[46,47]. Thermosensitive polymers having a wide range of LCST based on *N*-alkyl acrylamide homopolymers and copolymers have been investigated. Hydrogels made of polymers having an LCST are highly swollen below LCST and collapse completely above LCST. Below the LCST, hydrogels swell as a result of hydrogen bonding between hydrophilic groups of polymer and water. However, hydrogen bonding weakens above LCST and hydrophobic interactions dominate which results in shrinking of the hydrogel.

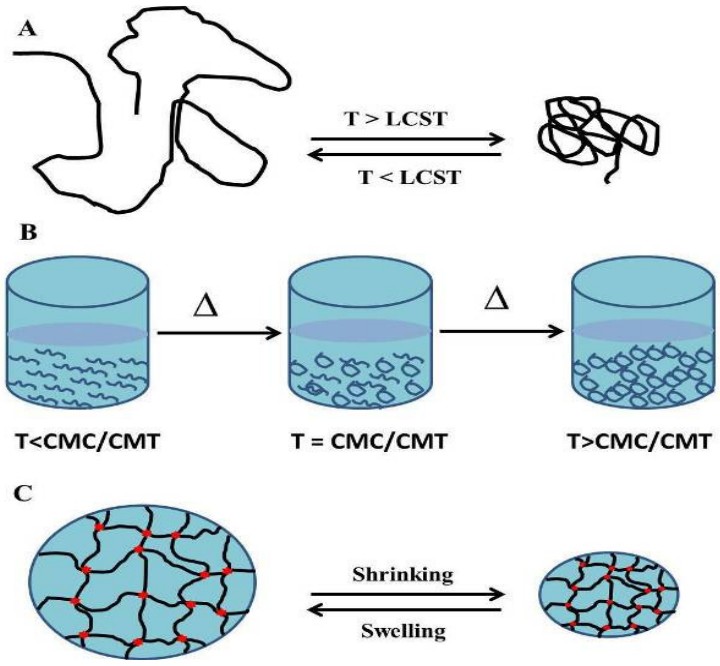

Figure 2. The phase transition in stimuli sensitive polymers based on, **A**. LCST, **B**. CMC, **C**. cross-linked system with LCST.

.

The main cause of thermally induced phase separation is the breaking of polymer-water hydrogen bonding and formation of polymer-polymer bonding at the critical

temperature. PEG systems show also a LCST[48]. The hydrophilic character with surface-wetting properties is especially important for prevention of protein adsorption and induction of blood compatibility in biomedical applications.

1.4 Introduction to CMC Based Thermosensitive Hydrogels

Certain polymers form polymeric micelles in aqueous solution when the concentration of the polymer increases above a certain concentration, named the critical micelle concentration (CMC). At the CMC, hydrophobic segments of block copolymers start to associate to minimize the contact with water molecules, leading to the formation of a core-shell micelle structure. The formation of polymeric micelles in aqueous solution occurs at a temperature called the critical micelle temperature (CMT). The CMC and CMT are two interdependent terms which can be varied by change in composition of the hydrophilic and hydrophobic blocks. Generally, A-B-A triblock copolymer with A-hydrophilic segment, and B-hydrophobic segments can show a CMC/CMT based sol-gel transition e.g. poly[(ethylene oxide)-*b*-(propylene oxide)-*b*-(ethylene oxide)] (PEG-PPG-PEG)[49].

At low temperatures or concentrations, PEO-PPO-PEO copolymers dissolve in water as individual monomers. Temperature dependent micellization and gel formation are the most remarkable properties of aqueous A-B-A triblock polymer solution[50,51]. The micellization of block copolymers with a PPO core and a corona are dominated by hydrated PEO segments (hydrophilic group) in aqueous solution, and it is initiated at a given concentration by increasing the temperature up to its CMT. However, there is no information about whether the degree of rolling up is a function of temperature or concentration. There are discrepancies in CMC data simply due to impurities and different molecular weight distributions presented in these commercial products[52–54].

However ABA type block copolymers are only one of the example of CMC based hydrogels in recent studies, PEG based diblock copolymers, which has an hydrophilic segment (PEG) and a hydrophobic segment (lipid or short aliphatic hydrocarbon chains or hydrophobic polymer) were also studied as a CMC based hydrogel systems[55,56]. In addition, ABC type copolymers, grafted systems of hydrophilic/hydrophobic polymers also showed a micelle driven gel formation[57–59]. Moreover, by coupling two different homopolymers (PEG and PPG) or ABA triblock copolymers (PEG-PPG-PEG) via an degradable linkage to have multiblock copolymers, they showed much higher mechanical properties compared to pure ABA triblock copolymers or homo-polymers when heated near body temperature with same concentration[60–62].

Therefore, it was possible to get different size and structures of micelles (spherical, cylindrical, lamellar etc.) to show a gelation based on CMC. But, it is not necessary that every CMC based system should show a thermally induced gelation[63,64].

However, if the system gets more complicated, it is more difficult to evaluate the micelle formation. The CMC of polymer is frequently determined with fluorescent probes. Pyrene, a nonpolar polyaromatic molecule, preferentially partition from a hydrophilic to more hydrophobic environment (e.g. the core of the polymeric micelles) with a concurrent change in its fluorescent properties such as a red shift in the excitation spectrum and vibrational structure changes in the emission spectrum. The CMC of polymeric micelles can be determined as the onset of these spectral changes as a function of the polymer concentration. The advantages of the CMT gels over LSCT gels comprise low volume change (shrinking or swelling) during gel formation (Figure 2) and wide range of switching temperatures (by varying either the molecular weight or the composition of the polymer).

1.5 Thermosensitive architecture hydrogels

3D architectured hydrogels with interconnected pores could provide reasonable structural, morphological, physical and biological support which is necessary to act as temporary substitutes or mimic the extracellular matrix. These porous materials also provide control over its functions such as mechanical properties. Recent development in such materials was focused on designing biodegradable materials which can interact with and facilitate the regeneration of native tissue during their stay in the body. A general approach was to utilize 3D architectured hydrogels which provide sufficient structural and functional support during the regeneration process. The degradation process of such material should also be controlled in a way that it resembles the rate of regeneration. To accomplish such a system with controlled mechanical properties and degradability, a combination of synthetic and biopolymers seem to be the ultimate choice. The system derived from such combinations could provide desire structural support for the biomaterials to promote and maintain biological environment (due to presence of biopolymers) which enables cellular growth, adhesion, and differentiation which could simulate the process of regeneration as similar as extracellular matrix[34,65–69]. Very few studies have been made in the area of thermosensitive architectured hydrogels because it was difficult to have a combination of rigidity (mechanical properties) in the system as well as tunable functionality, specifically a thermosensitivity[70]. Various methods have been used to form porous hydrogel network such as, salt leaching, electrospinning fibres, different molds (to direct the pores), and foaming. However, the degradability is an additional factor playing an important role in terms of stability of these hydrogels, which mainly depends upon the amount of water in the system. So, it

would be a potential point of interest, if the water content could be regulated in the system depending upon the temperature.

Some recent approaches to thermosensitive scaffolds are based on *N*-isopropylacrylamide (NIPAAm), PEG-PCL-PEG (triblock copolymer), and poly(DL-lactic acid) (PDLLA) in conjugation with dextran or collagen[71–74]. These scaffolds have several disadvantages such as, large volume change (shrinking-swelling), dramatic decrease in water uptake capability near body temperature (37 °C), fast degradation rate (1 week) or small pore size (50-70 µm). This may restrict the use of such scaffolds in cell and nutrition transport and less stability in *vitro* which may be an important requirement for their use in biomedical applications.

Hence, taking all the challenges in to account, a 3D porous hydrogel system having a combination of biopolymer (biofunctionality and biodegradability) and synthetic polymer (thermosensitivity, and tunable mechanical properties) would be of potential interest.

1.6 The vitreous body and vitreous body substitutes

The vitreous body is a highly hydrated polymer matrix which behaves like a gel. It consists of almost 98% of water and the remaining 2% is a physical mixture of hyaluronic acid and collagen[75]. Although it contains only small amounts of biopolymers, their physical interactions within the vitreous body results in sufficient mechanical strength and elasticity to function as a gel, which simultaneously display a very high optical transparency. Main functions of the vitreous body are to provide support to retina, protect surrounding ocular tissues, allows light to reach to the sensory part at the back of eye, and also permits the circulation of metabolic solutes and nutrients[76–78]. Thus the vitreous body is playing an important role in maintaining

the function of an eye. There are some crucial situations where it becomes necessary to repair or replace the vitreous body with an artificial substitute[79,80]. Foremost, in many cases the vitreous itself get dysfunctional due to liquefaction, opacification or by physical collapse, which mainly results in poor vision or blindness. The main causes of dysfunctional vitreous are inflammation due to infection or injury or retinal diseases, systemic diseases like diabetes, and degenerative process due to aging. In all of these situations, replacement of damaged vitreous became necessary with biomaterial which is transparent, biocompatible, and similar mechanical properties like natural vitreous. The main purpose of replacement of vitreous is either to retain the original structure of eye prior to surgery or to replace the damaged vitreous in total. Until now many materials ranging from gases to liquids and polymers to oils have been applied. Although there were many synthetic materials tested as a vitreous substitute, only few of them such as perfluorocarbon gases, silicon oil, perfluoro carbon liquids, hyaluronic acid-collagen mixture, methylated collagen, poly(1-vinyl-2-pyrrolidinone), polyvinyl alcohol, etc. have been tested clinically or experimentally[75,77].

Since 1962, silicon oil and silicon oil derivatives have been proposed and investigated as vitreous substitute, due to suitable physical properties like transparency, stability, and high interfacial surface energy with aqueous humor and retina. However, most of recent studies have reported that due to hydrophobic nature of silicon oil, it leads to poor contact with retina and surrounding aqueous fluids. Potential emulsification within the eye due to the infiltration of humor aqueous into the vitreous cavity can lead to of silicon oil as vitreous substitute. It also prevents the passage of solutes and electrolytes, triggering metabolic changes in the cornea that

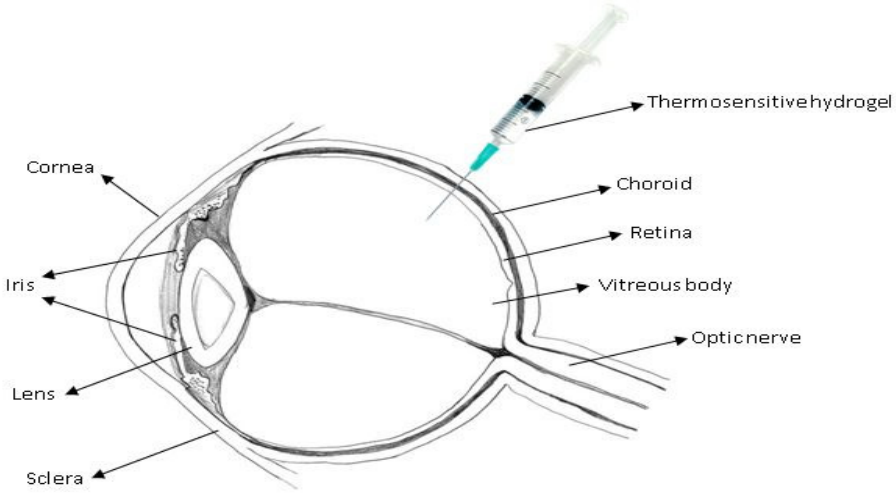

Figure 3**.** An eye model with an injectable themosensitive hydrogel

lead to the precipitation of calcium salts. Long term presence (6 months) of silicon oil leads to complicated situations such as keratopathy, cataract, glaucoma, and corneal decompensation which necessitate its removal. Unfortunately, it is very difficult to remove silicon oil completely. Thus to overcome these challenges, hydrogels are introduced as a vitreous substitutes. In this category many biopolymers, synthetic polymers and semisynthetic polymers have been tested[80,81]. Especially high molecular weight water soluble polymers like, sodium hyaluronate, dextran, alginic acid, chondroitin sulfate, guar gum, methylcellulose, carboxymethylcellulose, and hyroxypropylmethylcellulose, were studied as vitreous substitutes[75]. However, due to short time of residence in vitreous body and biodegradation of these polymers made them inconvenient for long term use a vitreous substitute. Thus, it is challenging and necessary to overcome certain critical material properties to develop a synthetic substitute for vitreous humor (Figure 3). In this regard, there is enduring demand to develop a hydrogel which could behave as a temporary substitute, which may be achieved by combination of biopolymers and synthetic, biocompatible/biodegradable polymers which can produce hydrogel mimicking structure or properties of vitreous body.

2. Aim of the Thesis

The aim of this thesis was to develop thermosensitive hydrogel systems with tunable thermo-mechanical properties, which exhibit higher elastic moduli (G′) and viscosities as well as a lower T_{sw} compared to typical ABA triblockcopolymers at the same concentration. Furthermore, other than ABA triblockcopolymers, the systems should not be destabilized upon the addition of water, but should rather show a Gel-Sol transition on demand, even without change of temperature. Similar to ABA triblockcopoylmers, no or only a small volume change upon switching should be observed.

It is hypothesized that such hydrogels can be prepared through a combination of a synthetic thermosensitive polymer forming micelles upon temperature increase and an additional macromolecular component providing additional netpoints to the system by crosslinking the formed micelles. The macromolecular component should be enzymatically degradable to provide dissolution of the systems on demand.

This hypothesis is tested in three different approaches.

1. Physical mixing of the two components, which can interact through electrostatic interactions, e.g. a thermosensitive polymer with positively charged end-groups, while the additional macromolecular component contains negatively charged groups. Such systems should display a thermoreversible sol-gel-transition, which might be exploitable for applications such as substituting the vitreous body of the eye.
2. Covalent coupling of the two components, which can result in systems showing a sol-gel or gel-gel transition with enhancement of the mechanical

properties (such as elastic modulus (G′) and viscosity) upon heating and could undergo on-demand solubilisation upon enzymatic degradation.

3. Transfer of the concept to functionalized architectured hydrogels, in which a three dimensionally structured, porous system under swollen condition could display an increase in mechanical properties upon heating and thus showing a control on the mechanical properties by temperature.

3. Strategies and Concepts

The three approaches to the thermosensitive systems detailed in the aims section require proper selection of materials and methods. As thermosensitive component, a polymer showing a CMC will be the right choice, as these systems typically do not show (large) volume change during the gelation. A typical and well investigated representative is poly(ethylene glycol)-*b*-poly(propylene glycol)-*b*-poly(ethylene glycol) (PEPE). These compounds furthermore offer the possibility of end group functionalization with amino groups to enable electrostatic interactions with a second component bearing carboxylic acid groups as well as easy covalent coupling to such groups. An additional advantage can in the longer run be the known applicability of PEPEs *in vivo*.

As a macromolecular component, polysaccharides will be a smart choice. Many polysaccharides bear carboxylic acid groups in their repeating units, which are required for the electrostatic or covalent coupling to the aminated PEPEs. Furthermore, these polysaccharides often form gels and are biodegradable through hydrolysis and especially by enzymatic action. To enable an efficient crosslinking of micelles by the second macromolecular component, high molecular weights of the biopolymer component will be beneficial. Therefore, HA will be the first candidate. In a following step, the results can be compared to other polysaccharide components with lower molecular weight, such as CS or pectin to evaluate the effect of type of biopolymer and molecular weight of biopolymer on thermo-mechanical properties of the resulting hydrogels.

The physical mixing of amine terminated PEPE will be performed with HA as a biopolymer, with different ratios of the two component to yield tailorable physico-

chemical properties such as T_{sw} and elastic/viscous modulus. Furthermore, it will be investigated, whether differences between systems based on mono-amine PEPE (mono-PEPE) or di-amine PEPE (di-PEPE) will be observed (figure 4). The systems are planned to show a sol-gel transition. A possible application of such a system are injectable systems solidifying at body temperature. If transparent, they might be applicable as vitreous body substitutes, so optical transparency, biocompatibility, and refractive index of these systems will be investigated in view of this potential application.

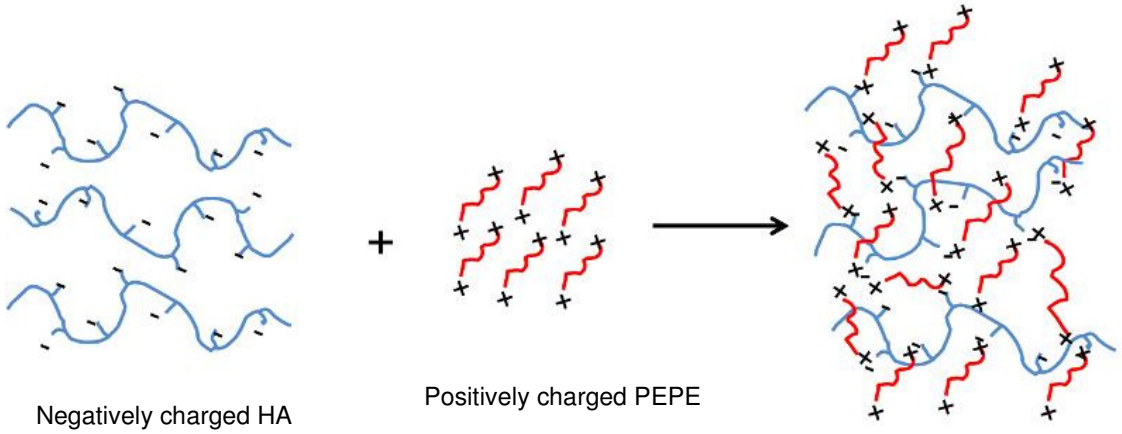

Figure 4. Potential electrostatic interactions resulting after physically mixing bi-functional PEPE with polysaccharide (HA)

Though the described systems might show a better stability towards dilution in water than the PEPE alone, covalent coupling of the components should show a better performance in this respect. Thus efficient chemical coupling of synthetic and natural polymers via an amide bond formation between carboxylic groups of the biopolymer and amine functionalized PEPE could be achieved e.g. by using 1-ethyl-3-(3-dimethylaminopropyl) carbodiimide (EDC) or 4-(4,6-Dimethoxy-1,3,5-triazin-2-yl)-4-methylmorpholinium chloride (DMTMM) as coupling agents. The mono-PEPE and di-PEPE will be selectively coupled to different biopolymers via carbodiimide chemistry

(figure 5). For removing unreacted PEPE, dialysis as well as ultrafiltration will be investigated.

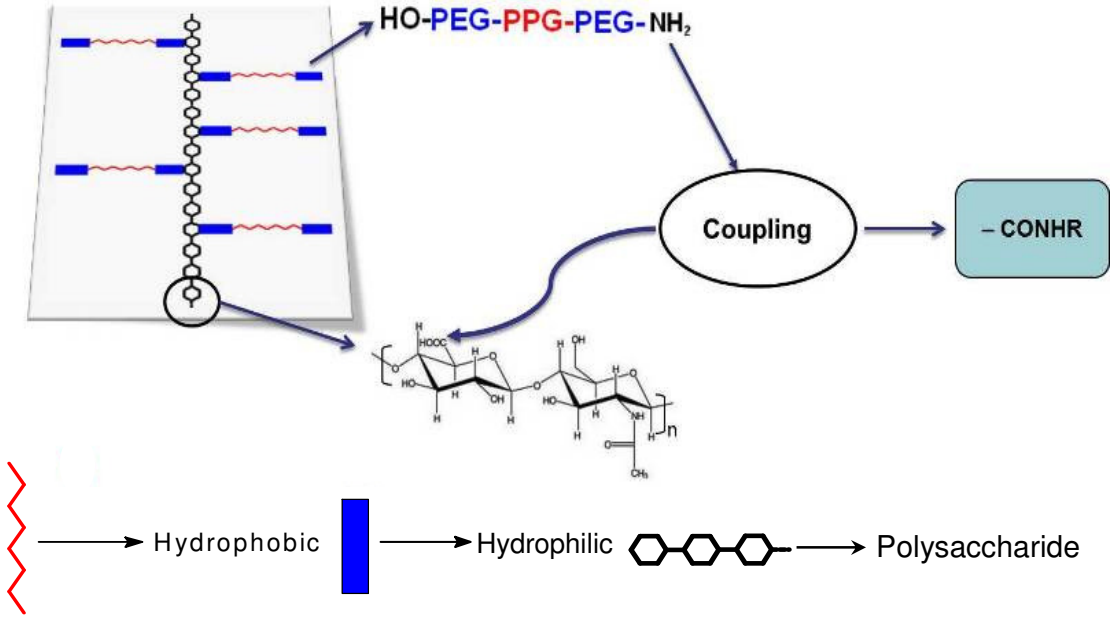

Figure 5. Synthesis of thermosensitive hydrogel by coupling PEPE to the polysaccharide

Again, it was planned to vary the ratio between the two components to yield tailorable switching temperatures and viscoelastic properties of the systems. In the recent studies, such systems with covalent coupling of polysaccharides and thermosensitive polymers have been described, but the characterization were not done in a way to understand the gelation mechanism, tailorable gelation temperature and mechanical properties, and more importantly to determine whether these two components are actually coupled (by means of covalent bonding). Therefore to understand these challenging and missing concepts, it was necessary to characterized these system in depth. Hence, a strategy to elucidate the molecular structure of these hydrogels could be the key to evaluate the mechanism of gelation and the viscoelastic properties, which could be determined by CMC/CMT determination of micelles or rheological measurements. The structure or micelles arrangement could be evaluated by using small angle x-ray scattering analysis and the Cryo-TEM analysis

will be used for the direct visualization of micelles and the thermal properties will be determined by DSC and TGA analysis. These characterization methods will allow to understand the gelation mechanism as well as thermo-mechanical properties of these thermosensitive hydrogels.

The biopolymer component of the system potentially enables an enzyme responsiveness of the materials, e.g. dissolution on demand by a stimulus other than temperature. This will be investigated by incubating the materials with an enzyme selectively hydrolysing the biopolymer component (e.g. hyaluronidase in the HA containing compounds) and observing the macroscopic properties of gels as well as measure the rheological properties of the systems as a function of time of degradation. Furthermore, the concept of thermosensitivity will be transferred to a more complex system, such as 3D architecture hydrogels (ArcGel). As previously studied, a well-defined ArcGel was derived from crosslinking gelatin by LDI having tailorable properties, shown biocompatibility, and *in vivo* regenerative properties. In addition to these known properties, thermosensitivity in such well-defined system might add another tailorable concept. This would show enhancement in mechanical properties upon heating near body temperature, which might be very useful in stem cells culturing to guide stem cells differentiation.

Such a ArcGel having thermosensitivity was planned to be synthesized by grafting PEPE to amino groups of gelatin, to achieve gelatin-*g*-PEPE thermosensitive architectured hydrogels (figure 6). The amount of grafting will be determined by TNBS assay and the remaining amino groups of gelatin will be utilized in crosslinking by lysine diisocyanate as a crosslinker. Before crosslinking, the effect of grafting PEPE to gelatin helix formation will be analysed by WAXS measurements, and further thermo-mechanical properties will be analysed by TGA, DSC, and most interestingly, the rheological properties will be evaluated to evaluate the effect of

grafting PEPE on T_{sw} of the hydrogels. The crosslinking will be performed by LDI, with the PEPE itself acting as a surfactant in the crosslinking process. These ArcGel will be more difficult to be characterized, but, as a first step, thermal stability, and helix content will be determined by TGA and WAXS measurements to see the effect of crosslinking on thermal stability and helical content in the resulting ArcGel. Furthermore, in order to check the effect of PEPE micellization on water uptake and degradation to the T-ArcGels, the water uptake water uptake at 25 ℃ and 37 ℃ will be determined. Finally, the most interesting thermo-mechanical analysis will be performed by rheology (bulk properties), aiming at an enhancement of the viscoelastic properties upon heating. The T_{sw} in such system could be adjusted by changing the grafting density of PEPE to gelatin. Further, by using AFM, local mechanical properties will be measured at temperature above T_{sw} and below T_{sw} of the T- ArcGel system.

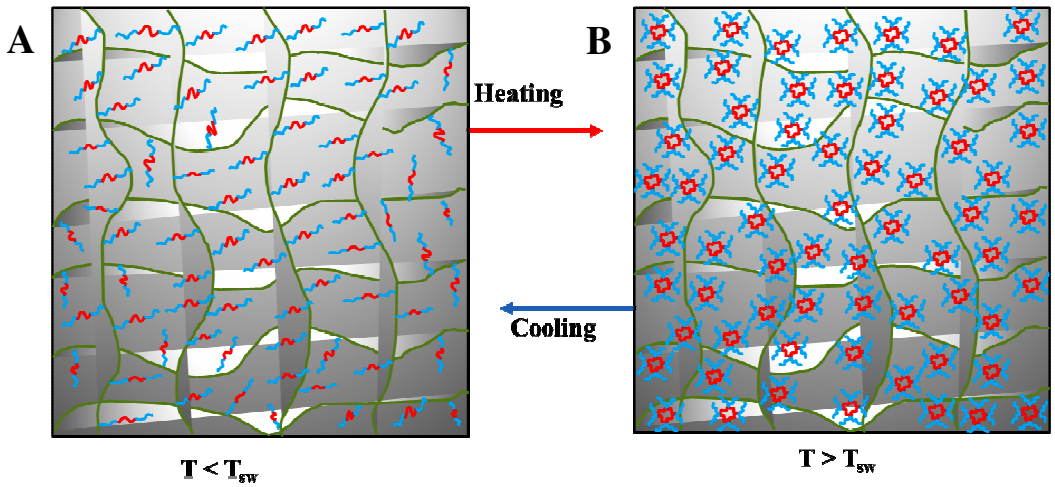

Figure 6. The CMC based micelle formation in GA-*g*-PEPE architectured hydrogel (-ArcGel). **A**. The -ArcGel system of GA-*g*-PEPE at swollen state in water below T_{sw} (25 ℃), B. T-ArcGel system of GA-*g*-PEPE at swollen state in water above $T_{sw,}$ at which micelles are formed and enhance the viscoelastic properties of system.

4. Synthesis of Hyaluronic Acid based Thermosensitive Hydrogels with Tailorable Properties

In this chapter, synthesis and characterization of HA based thermosensitive hydrogels prepared via physical crosslinking with amine terminated PEPE are discussed. The hydrogels are characterized by rheology, MALDI-TOF, CMC/CMT analysis, DSC, TGA, Cryo-TEM, and cytotoxicity test.

4.1 Synthesis of amine terminated PEPE

The amino groups were introduced by activation of the hydroxyl end groups of PEPE (by 4-nitrophenyl chloroformate) and followed by the addition of diaminopropane in the next step (scheme 1)[82]. As, there are two hydroxyl groups available on each chain of PEPE, the degree of functionalization to yield predominantly mono-aminated PEPE (mono-PEPE) or di-aminated PEPE (di-PEPE) was controlled by the molar ratios of the reactants. However, the synthesized compounds (mono-PEPE and di-PEPE) will likely be a mixture of unreacted PEPE and mono or di-PEPE. The amount of amino groups after the functionalization were determined with the Trinitrobenzenesulfonic acid (TNBS) assay and was about 80-95 mol% in both cases, based on either one (mono-PEPE) or two (di-PEPE) reactive groups.

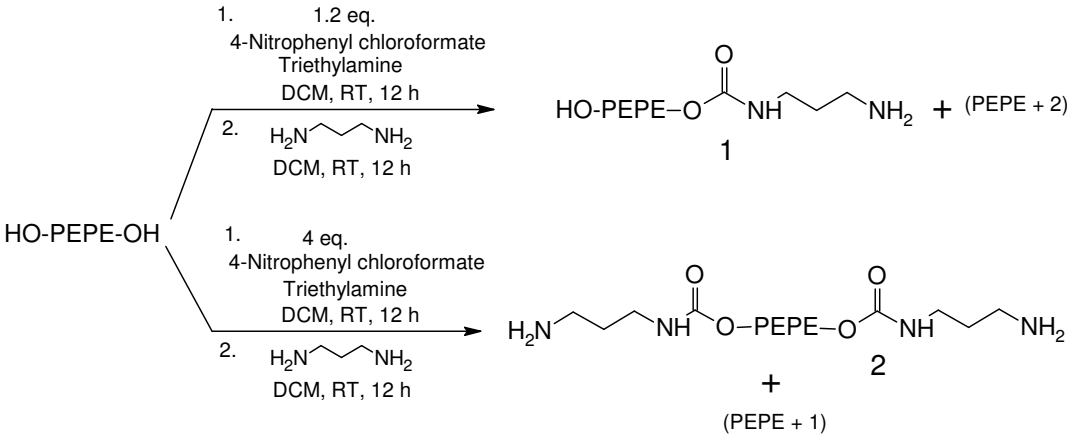

Scheme 1: Synthesis of mono-PEPE and di-PEPE

ATR-FTIR spectroscopy was used to evaluate the newly formed peaks by functionalization of PEPE with an amine group (Figure 7). The IR spectra clearly indicate the appearance of new bond at 1735 cm^{-1} (C=O stretch) corresponding to the carbamate linkage between PEPE and 1,3-propanediamine. The intensity of this band in the spectrum of di-PEPE is enhanced compared to mono-PEPE as expected.

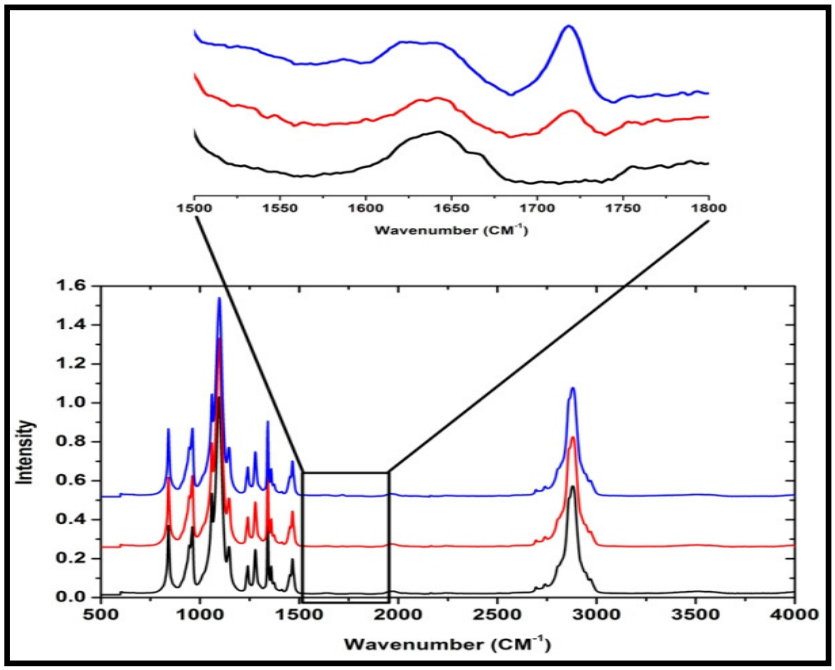

Figure 7 ATR-FTIR spectroscopy of PEPE and amine functionalized PEPE show a new peak at 1735 cm^{-1} (C=O stretch) referred to coupling of propane di-amine to PEPE via carbamate linkage. Where, PEPE (—), mono-PEPE (—), and di-PEPE (—).

In the ^{1}H-NMR spectra two new peaks for amine terminated PEPE appeared, δ= 9.76 (m,O=C-NH-) and 2.55 (m,-CH_2- of di-amine) ppm. Further, the molecular weight of PEPE, mono and di-PEPE was determined by MALDI-TOF-MS. The desired molecular weight of mono-PEPE was expected to show an increase of 150 g·mol^{-1} and di-amine with 300 g·mol^{-1} compared to non-functionalized PEPE. The non-functionalized PEPE gave a peak average molecular weight (M_p) of 16,175 g·mol^{-1}. The spectrum showed high polydispersity with no individual masses identifiable, as is typical for PEPE. As shown in figure 8, an increased M_p of around 200 g·mol^{-1} in mono-PEPE (16,378 g·mol^{-1}) and 300 g·mol^{-1} in di-amine PEPE (16,460 g·mol^{-1}). Though the spectra of the functionalized PEPE showed the expected increase in the final molecular weight, because of the broad distribution of molecular weight of starting polymer (PEPE) and presence of mixture of PEPE, mono, and di-PEPE in amine functionalized PEPE, the spectra do not give a clear results due to presence of small amounts of the unreacted PEPE and aminated PEPE in it. The incorporation of amino groups to PEPE led to change its physical and thermo-mechanical properties compared to non-functionalized PEPE.

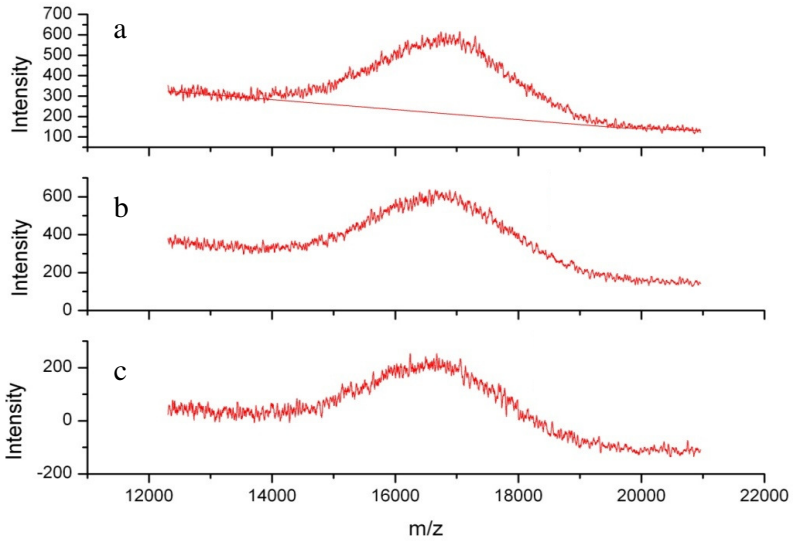

Figure 8. MALDI-TOF spectra of di-PEPE (a), mono-PEPE (b), and PEPE (c).

4.1.1 Thermal properties of amine functionalized PEPE

To evaluate the influence of functionalization of PEPE on the thermal properties such as melting temperature (T_m) and thermal degradation, amine functionalized and non-functionalized PEPE are analysed by DSC and TGA. As PEPE is semi-crystalline, it shows a T_m, which is around 62 °C for non-functionalized PEPE. After mono and di-amine functionalization, a decrease of T_m was observed as mono-PEPE has a T_m around 60 °C and di-PEPE of 58 °C (Figure 9 A) this corresponds to a decrease in crystallite size. Furthermore, a decrease of ΔH_m in the aminated compounds corresponds to pure PEPE was observed, which is related to the overall crystallinity of the sample.

A thermo gravimetric analysis (TGA) was performed to analyse the thermal stability of PEPE before and after functionalization (Figure 9 B). The major mass loss for PEPE started at around 285 °C and further at around 410 °C the remaining mass was close to zero. The initial mass loss for amine terminated PEPE seems to be shifted slightly to higher temperature which is 314 °C for mono-PEPE and 327 °C for di-PEPE as shown in figure 9 B. Moreover, both amine functionalized PEPEs have shown a similar trend of thermal degradation as of PEPE with slight shift in the starting point of the thermal degradation.

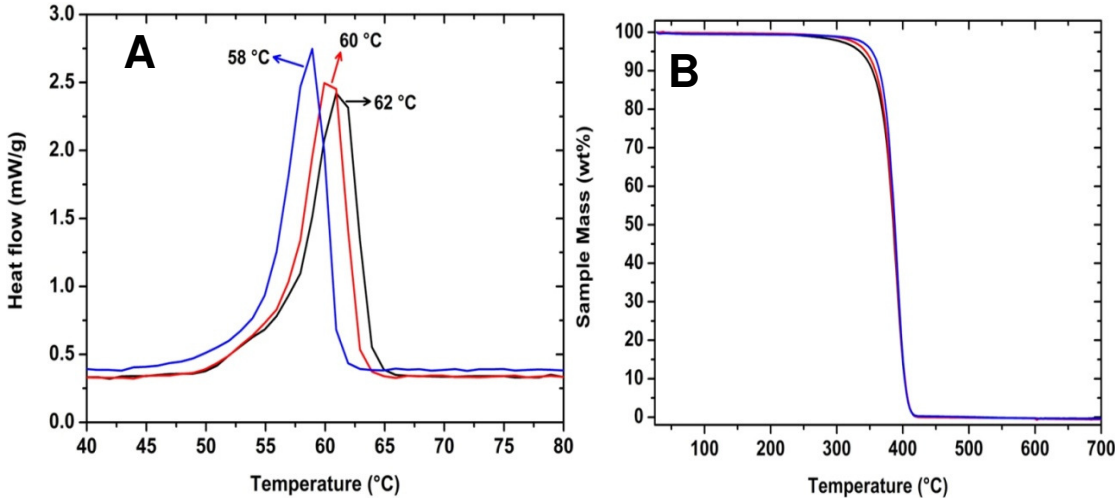

Figure 9. Thermal analysis of PEPE (—), mono-PEPE (—) and di-PEPE (—) **A**: DSC measurement and **B**: TGA measurement.

4.1.2 Rheological investigation of amine functionalized PEPE

The thermo-mechanical properties of PEPE and amine terminated PEPE were determined by dynamic shear oscillation measurements to specifically evaluate viscoelastic properties. The gel formation in the PEPE is driven by the formation of micelles and further packing of micelles at higher temperature to form a gel. This temperature induced gelation and changes in mechanical properties during the gelation process could be determined by rheological analysis. The micelle formation depended on the critical micelle concentration (CMC); the concentration required to form micelles and critical micelle temperature (CMT); the temperature required to form micelles. The gelation temperature (T_{gel}) of PEPE and functionalized PEPE solutions (16.8 wt%, prepared in phosphate buffer pH 7.4) were determined by thermo-mechanical observation of elastic (G′) and viscous modulus (G″) as a function of temperature. For the measurements, solutions were placed between rheometer plates and heated at the rate of 0.5 °C·min^{-1} from 15 to 45 °C under constant stress

of 1 Pa and frequency of 0.65 Hz for each sample. Before running the temperature ramp, each solution was equilibrated at 15 °C.

The temperature ramp of these solutions show that after a certain degree of temperature (30 °C), the elastic modulus (G′) and viscous modulus (G″) shows a sharp increase in the magnitude within a small temperature interval (Figure 10). The temperature at which both moduli increased rapidly is stated as a gelation temperature (T_{gel}). Interestingly, the sol-gel transition of amine functionalized PEPE was shifted compared to PEPE (34 °C), particularly showing a higher T_{gel} of mono-PEPE (37 °C) and showing a lower T_{gel} (31 °C) of di-PEPE. This shift in T_{gel} may be related to the change in the end groups of PEPE, which influences the (ionic) physical interactions between PEPE chains in solution. Additionally, the PEPE chains with similar functional group (either -OH or -NH_2) have higher mechanical properties (PEPE: G′ at T>T_{gel} = 16460 Pa (±3%) and di-PEPE: G′ at T>T_{gel} =16110 Pa (±3%)) compared to mono-PEPE which shows a value of G′ at T>T_{gel} = 11750 Pa (±3%). Moreover, the hydrogels with higher elastic modules (G′) showed low viscous modules (G″), meaning, due to higher elasticity, the mobility of polymer chains/micelles or viscosity decreased in such hydrogels. This analysis was very well supported by the values of viscous modulus as, PEPE: G″ at T>T_{gel} = 2072 Pa (±3%), di-PEPE: G″ at T>T_{gel} = 987 Pa (±3%), and mono-PEPE: G″ at T>T_{gel} = 2318 Pa (±3%). Hence the rheological analysis of PEPE and amine functionalized PEPE demonstrate a reversible sol-gel transition with a slight shift in $T_{gel.}$ Moreover during the cooling of samples the dissolution occurred at temperature lower then T_{gel} (observed around 8 °C lower than T_{gel}), because of strong physical interactions, the disintegration of micelles takes place at lower temperature.

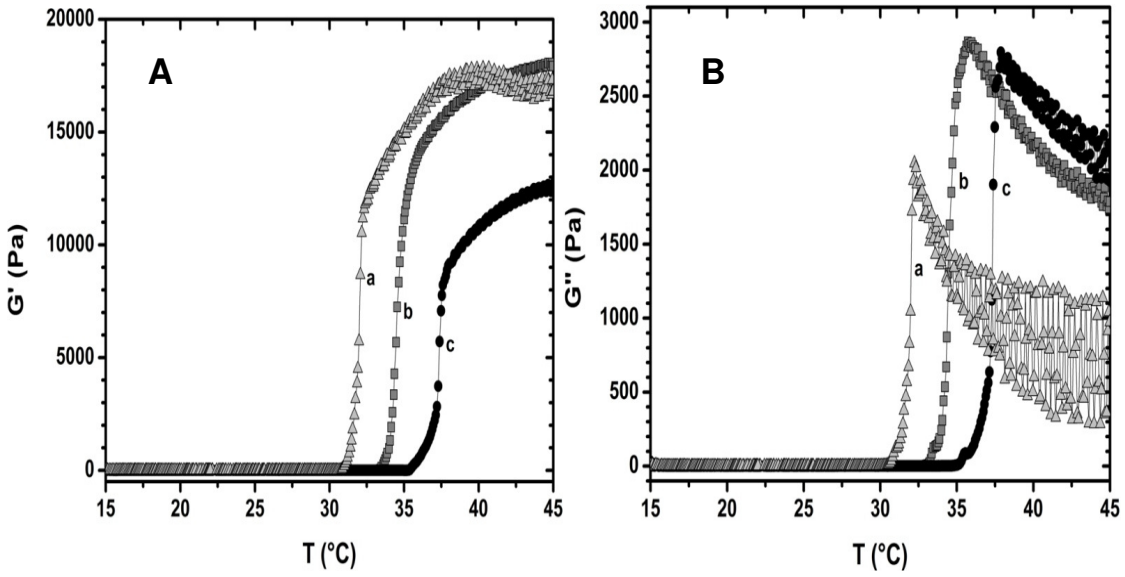

Figure 10. Evaluation of effect of functionalization on T_{gel} and mechanical properties of PEPE, determined by rheology as a function of temperature (**A**: G′ Vs T and **B**: G″ Vs T). Where, di-PEPE (▲), PEPE (■), and mono-PEPE (●)

4.2 Thermosensitive hydrogels from blends of hyaluronic acid and mono-PEPE

The hydrogels prepared by physical mixing HA and amine terminated PEPE (HA·mono-PEPE) are listed in the table 1 with their thermo-mechanical properties such as elastic modulus (G′), viscous modulus (G″), and gelation temperature were determined from the rheological experiments. In addition, the temperature interval between the switching of sol to gel (T_{gel} interval); the hysteresis in T_{gel} between heating and cooling cycle was also measured from temperature ramp measurements by rheology.

Table 1. Thermo-mechanical properties of HA·mono-PEPE hydrogels

M_n (HA) [MDa]	HA: PEPE [wt.-%]		T_{gel} - [°C]	T_{gel} Interval [°C]	Hys. [°C]	G′[a] [Pa]	G″ [a] [Pa]	|η*| [a] [kPas]	G′[b] [Pa]	G″[b] [Pa]	|η*|[b] [kPas]	Conc. [wt.-%]
3	2.8	97.2	36	5	n.d.	0.722	0.824	0.291	9594	675	2551	16.8
3	3.5	96.5	37	4	n.d.	1,13	0.408	0.319	7641	1551	2068	16.8
2.33	2.6	97.4	26	3	7	0.755	1.27	0.336	15600	812	3824	20
2.33	3.7	96.3	27	3	8	0.931	1.63	0.46	15570	716	3816	20
2.33	5.1	94.9	29	4	10	1.268	1.265	0.439	12440	1370	3063	20
2.33	8.2	91.8	29	4	12	1.61	1.844	0.599	9297	565	2281	20
1.6	4.6	95.4	31	3	n.d.	1.39	0.915	0.441	12330	584	3275	20
1.6	3.4	96.4	31	3	n.d.	1.054	0.851	0,359	13370	642	3552	20
1.13	2.7	97.3	31	5	n.d.	0.856	0.869	0.323	10920	701	2903	16.8
1.13	3.4	96.6	30	4	n.d.	1.2	0.935	0.406	15490	2678	4169	16.8
1.13	4.4	95.6	37	7	n.d.	0.849	0.53	0.265	10630	851	2830	16.8
0.9	2.6	97.4	33	3	n.d.	1.192	0.785	0.379	10250	285	2720	16.8
0.9	5.7	94.3	30	3	n.d.	0.57	1.106	0.33	11440	1430	3059	16.8
0.9	4.4	95.6	31	4	n.d.	0.863	1.184	0.389	12130	589	3221	16.8
2.6*	5.1	94.9	32	3	4	33.61	26.06	10.41	10640	1033	2619	20

Where, a: below T_{gel}, b:above T_{gel}, n.d. not determined, *: HO-PEPE-OH, Hys: hysteresis in T_{gel} (error for G′, G″ and |η*|= ±3 % and for T_{gel}=± 1.5 °C)

4.2.1 Investigation of thermo-mechanical properties of HA·mono-PEPE hydrogels

In case of temperature responsive hydrogels, the change in their physical state of polymer below and above the transition temperature is due to organization of chains in a stable physical state. Generally, they are in solution state below the gelation temperature and form a gel at higher temperature. This transition temperature is often called as an gelation temperature (T_{gel}). Here, the phase transition of HA·mono-PEPE solution is from sol to gel is mainly driven by micelle formation by PEPE

segment and additional mechanical strength is given by the high molecular weight HA chains. Thus, hydrogels with enhanced mechanical properties were prepared by the combination of natural and synthetic polymers.

As the concentration of PEPE in the composition decreases, the T_{gel} was found to be decreased by 4-6 ℃ (Table 1). Moreover, during the gelation process the elastic modulus (G′) increased dramatically after the T_{gel} but, the viscous modulus (G″) decreased. This may be due to the potential reason that, at lower temperature PEPE is in straight chain form and after the T_{gel} it starts to form micelle and further packing of micelles which restrict the mobility of system and hence results in higher elastic moduli (G′) and lower viscous moduli (G″). As shown in Table 1, various combinations of HA and aminated PEPE were prepared, specifically by varying the amount of PEPE (91.8- 97.2 wt%), varying the molecular weight of HA (0.9- 3 MDa), and changing the concentration of final solution. However, HA contributes to the mechanical properties of the gel via strong physical interaction with another Ha molecule or with PEPE (micelles), There was no significant difference was observed by changing the molecular weight of HA on the overall mechanical properties of the hydrogel (above T_{gel}). But, the mount of PEPE in the composition as well as the concentration of the polymer solution showed a strong influence on the mechancail properties as well as T_{gel} of the system. By decreasing the PEPE content and by changing the concentration from 20-16.8 wt%, the T_{gel} was increased from 29-36 ℃. Thus indicating the strong influence of PEPE content in the composition.

In addition, an effective decrease in the mechanical properties was observed due to decrease in PEPE content (Figure 11). As PEPE content decreases from 97.4-91.8 wt%, the elastic modulus was observed to be decreased from 15600 to 9297 Pa (±3%). This clearly indicates the contribution of PEPE in enhancing the mechanical properties of overall hydrogel. Moreover, the physical mixture with same composition

of PEPE as, HA·mono-PEPE have G′ 15600 Pa and Physical mixture of HA·non-functionalized PEPE have G′ 10640 Pa (measure above the T_{gel}). Thus, the slight increase in the elastic moduli (G′) may have influenced by ionic interactions between amino groups of PEPE and carboxylic groups of HA.

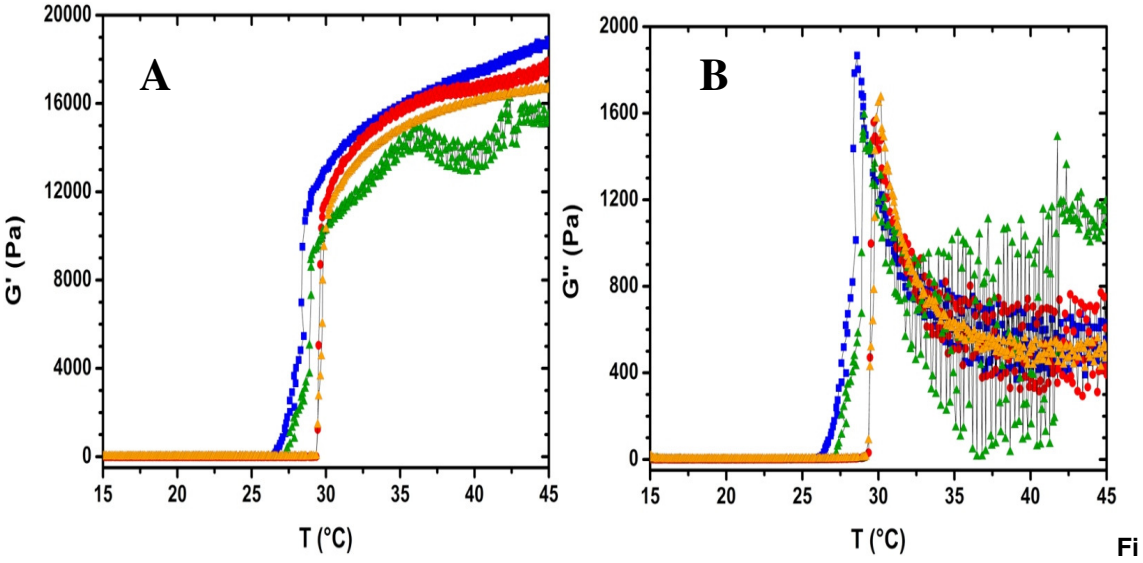

Fi gure 11. A temperature ramp measurement of HA·mono-PEPE hydrogel with different wt% of PEPE in composition. A: G′ vs Temperature and B: G″ vs Temperature. {HA:mono-PEPE composition, 2.6:97.4 (■), 3.7:96.3 (●), 5.1:94.9 (▲), and 8.2:91.8 (▲)}.

The thermal properties of the PEPE, mono-PEPE and physically mixed HA·mono-PEPE hydrogels were determined by using DSC and TGA to investigate the influence of physical mixing of semi-crystalline PEPE on T_m and thermal degradation in dry state and on micelle formation in solution state.

In the dry state, the melting temperatures (T_m) were analysed from the second heating scan (Figure 12 A). There was no T_m observed in HA. There was no significant effect on T_m of mono-PEPE was observed by addition of 2.7 wt% of HA compared to T_m of mono-PEPE. Due to addition of non-crystalline HA, a small shift in T_m of mono-PEPE observed which may be due to the decrease in the crystal size. Due to addition of high molecular weight HA (2.6 MDa), the molecular structure of

composition and simultaneously the crystallization of mono-PEPE got hampered, resulting in to broadening of crystallization peak of mono-PEPE

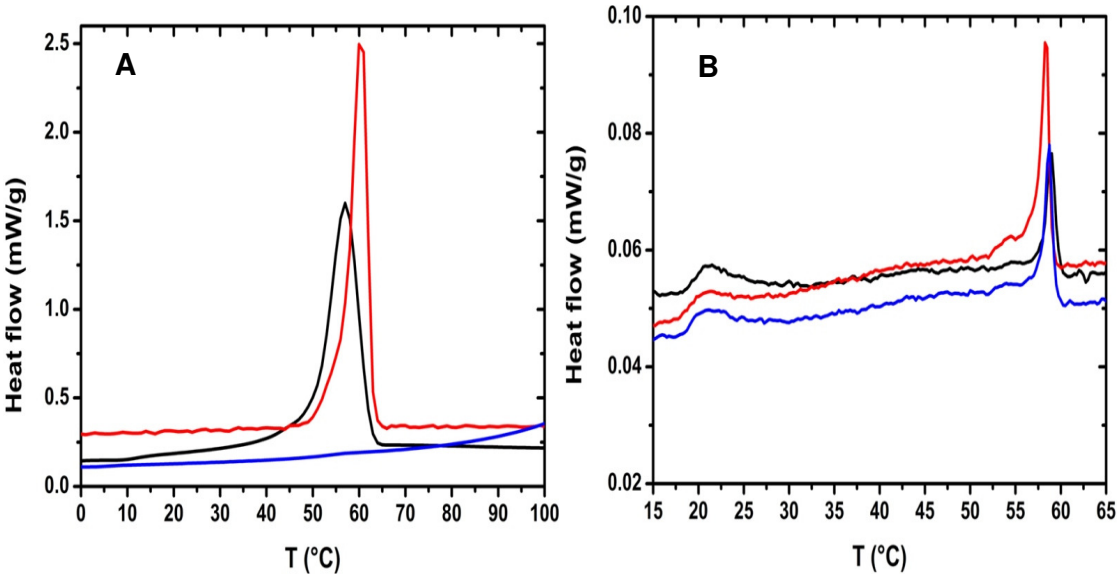

Figure 12. Second heating scans of, A. HA (—), mono-PEPE (—), and HA·mono-PEPE (—), B. DSC in solution state of PEPE (—), mono-PEPE (—), and HA·PEPE (—) (sample conc. 20 wt%).

In DSC measurements, an interesting point of evaluation was determination of micelles. As shown in figure 12B, PEPE, mono-PEPE, and HA·mono-PEPE shows a small transition at around 21 ℃, this transition is due to the change in the arrangements of PEPE chains into micelles, showing an endothermic transition in the DSC measurement[83]. In addition, the endothermic peak referring to the micellization process, may contribute from the change in the enthalpy of the polymer solution. Overall, there was no significant difference in the micelle formation temperature due to the amine functionalization or addition of HA was observed by DSC measurements.

TGA was performed in a N_2 atmosphere to determine the thermal stability potentially ascribed by physical crosslinking between HA and mono-PEPE (figure 13). A TGA plot of pure HA show a two-step degradation process which starts at around 70 ℃ with loss of moisture in the sample, and further at 250 ℃ due to thermal degradation

with nearly 60 wt% mass loss and finally combustion of remaining mass between 250 and 500 ℃. While the mono-PEPE is quite thermally stable and show only one major transition at around 400 ℃ with major mass loss of around 95 wt% within further 50 ℃. Interestingly, the physical mixture of HA and mono-PEPE has shown a two-step thermal transition, in which the first transition at 250 ℃ with around 10 wt% mass loss can be attributed to the HA degradation with the second transition with major mass loss of 85 wt% at around 380 ℃ was due to the degradation of mono-PEPE.

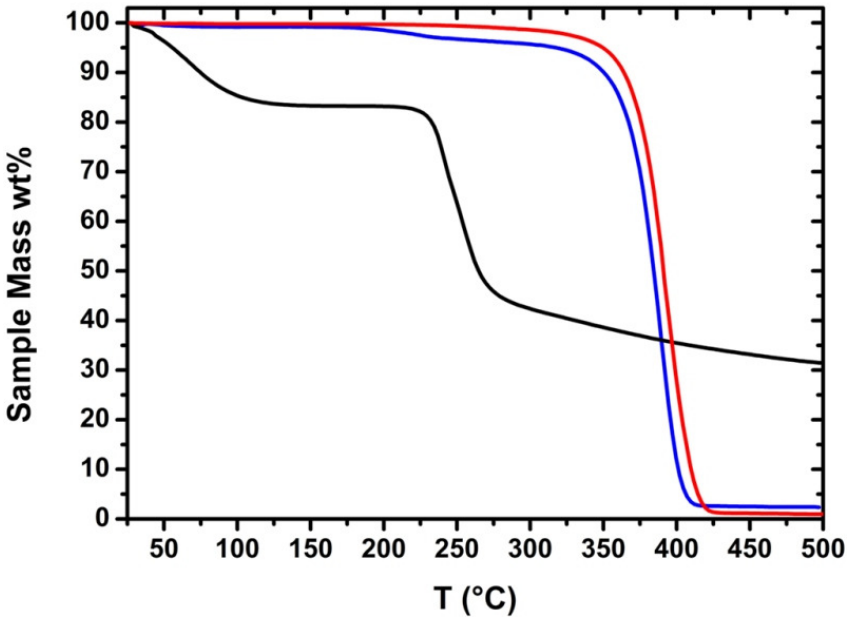

Figure 13. TGA of HA (–), mono-PEPE (–), and HA·mono-PEPE (–) samples in dry state

4.2.2 Determination of CMC and CMT

The concentration of polymer at and above which micelles are formed is known as critical micellization concentration for that polymer solution. The determination of micellization of amphiphilic block copolymers is more complex compared to small molecules or surfactants. Here, CMC and CMT values of physical mixtures of HA and mono-PEPE were determined by using Diphenyl hexatriene (DHP)[49]. DHP gives fluorescence only in a hydrophobic environment (such as core of a micelle) providing

a sensitive method of formation of micelles. The PEPE solution with concentration above CMC and temperature above CMT forms micelles having a hydrophobic core and a hydrophilic corona. So when the micelles are formed in the solution, the dye will give fluorescence and can be detected by UV spectroscopy by determining the absorbance at 356 nm.

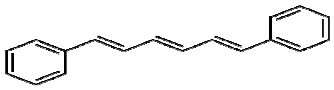

Trans-trans-trans-1,6-Diphenyl-1,3,5-hexatriene **(DPH)**

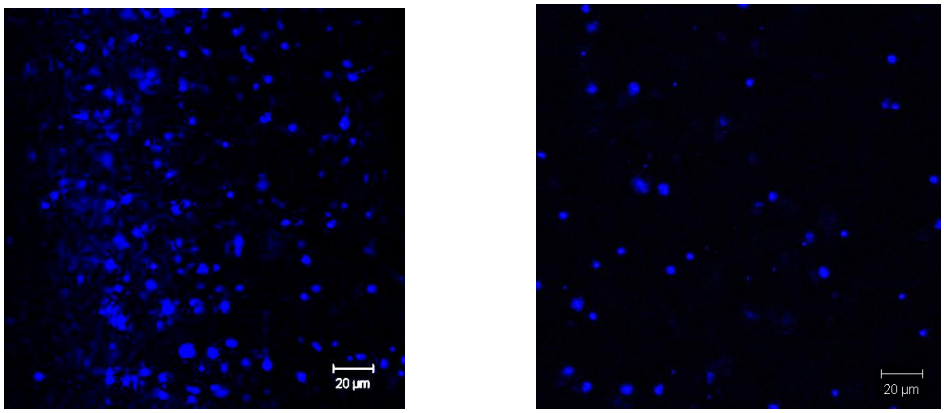

Figure 14. CLSM images of HA·mono-PEPE (sr. no.1 in table 2) micelles aggregates

Generally, with increasing concentration of the polymer in sample, the CMC value was observed at lower temperature and *vice versa* (Figure 15). The micelles were also visualised under confocal light scanning microscope (CLSM) in the form of small aggregates as shown in figure 14.

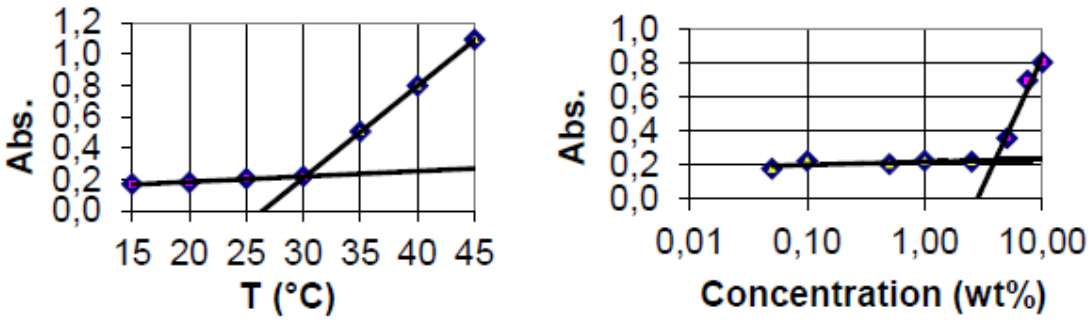

Figure 15. Determination of CMT and CMC of HA·mono-PEPE (4.4:95.6) sample

Table 2. The CMC values of HA·mono-PEPE

Sr. no.	Weight composition of HA: mono-PEPE	Molecular weight of HA (MDa)	Temp. 30℃	35 ℃	40 ℃	45 ℃
			Critical Micelle Concentration (% w/v)			
1	2.7:97.3	1.13	3.89	0.93	0.53	0.21
2	3.4:96.5	1.13	3.97	1.2	0.38	0.24
3	4.4:95.6	1.13	4.44	1.23	0.34	0.16
4	2.6:97.4	0.9	5.34	1.79	0.84	0.53
5	5.8:94.2	0.9	3.8	1.09	0.51	0.26
6	4.4:95.6	0.9	4.23	1.25	0.35	0.16
7	2.8:97.2	3	1.97	1.31	0.23	0.18

(error for all CMC values = ±5%)

The CMC and CMT values depend on temperature and concentration respectively. As the amount of PEPE was increased in the composition, lower concentration was required to show CMC and CMT (table 2 and Table 3). There was an absolute difference observed between CMT and T_{gel} as, the CMT is the temperature at which the micelle formation process starts and the T_{gel} is the process at which the micelles (at certain concentration) comes together to form a gel (two-step process). The formation of micelles does not lead to formation of gel as to form a gel it requires a certain amount of micelles to be present nearby to interact.

Moreover, the CMT values obtained from UV measurements were compared to the CMT values obtained by rheology as shown in Table 4.

Table 3. The CMT values of HA·mono-PEPE

Sr. no.	Weight composition of HA: PEPE	Molecular weight of HA (MDa)	Conc.0.1 %-w/v	0.5	1	2.5	5	7.5	10	20
			Critical Micelle Temperature (℃)							
1	2.7:97.3	1.13	40	35	33	29	28	25	24	23
2	3.4:96.5	1.13	-	35	33	29	37	25	24	23
3	4.4:95.6	1.13	39	36	35	30	29	25	24	22
4	2.6:97.4	0.9	39	36	35	33	32	26	25	24
5	5.8:94.2	0.9	41	35	33	31	29	27	25	24
6	4.4:95.6	0.9	-	36	35	31	30	25	24	22
7	2.8:97.2	3	42	36	34	31	28	24	23	22

(error for all CMT values = ±5%)

Table 4. Comparison of CMT values by UV and Rheology

Sr. no.	Weight composition of HA: PEPE	Molecular weight of HA (MDa)	CMT (℃) by UV	CMT (℃) by Rheology	T_{gel} (℃)
1	0:100	0	21	22	30
2	2.8:97.2	3	22	23	33
3	2.7:97.3	1.13	23	23	31
4	3.4:96.5	1.13	23	23	30
5	4.4:95.6	1.13	22	22	32
6	2.6:97.4	0.9	24	23	32
7	5.8:94.2	0.9	24	24	31
8	4.4:95.6	0.9	22	22	31

(error for all CMT values = ±5%)

The CMT values for all measured samples was determined from the temperature ramp. The temperature above which the elastic modulus (G′) starts to increase constantly, the temperature was taken as CMT. Because, as the temperature reaches to CMT for the polymer solution, the viscosity decreases due to, micelle formation and packing of micelles at higher temperature. This study was quite interesting as it was showing the values of CMT close to the values obtained by UV measurements.

4.2.3 Micelle formation by ^{1}H-NMR analysis

During the micelle formation in PEPE, the hydrophobic segment i.e. polypropylene glycol (PPG) will form the core while the hydrophilic segment i.e. polyethylene glycol (PEG) will form the corona, which is likely to happen due to the hydrophilic interactions of PEG segment with water molecules. Such a micelle with hydrophobic core and hydrophilic corona may hinder the interaction of PPG segment with surrounding water molecules. This could be observed by line broadening of the peak corresponding to the CH_3- group of PPG in temperature dependent ^{1}H-NMR measurements[84] (Figure 16). Thus, an experiment was performed in D_2O at temperature range of 25-40 ℃ with interval of 5 ℃. The sample concentration of 4

wt% was used in this experiment. As expected, with increasing temperature, the intensity of CH_3- protons decreased and the peak show a broadening effect. The result of this study support the micelle formation of the materials corresponding to the results from rheology and CMC/CMT analysis.

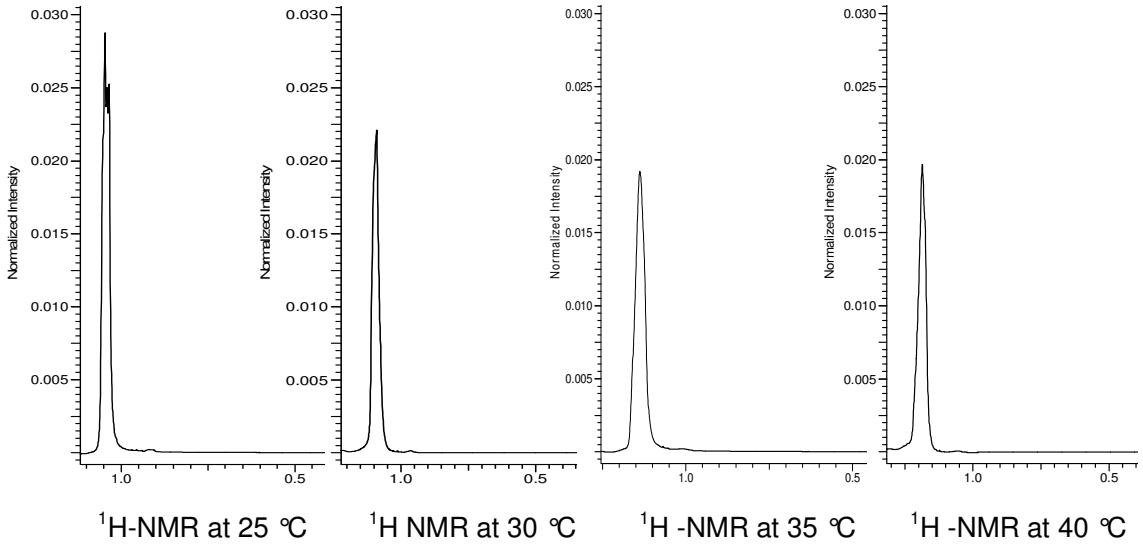

Figure 16. ^{1}H-NMR spectra of HA·mono-PEPE (4 wt% solution in D_2O) showing decrease in the intensity of methylene proton of PPG with increase in temperature.

4.2.4 Cryo-TEM measurements to determine the superstructure formed by micelles

The micellization of PEPE and HA·mono-PEPE (HA molecular weight = 1.13MDa, 2.6:97.4 wt%) was investigated by determination of CMC, CMT, and SAXS measurements (sees section 4.2.2 and 4.2.5) but, in these methods direct visualization of micelles is not possible. Hence, to determine the size, structure, morphology of the formed micelles, Cryo-TEM analysis were performed[85] (The experiments were performed at Free University of Berlin by Dr. Christoph Boettcher). In short, a solution of HA·mono-PEPE (2.7:97.3, concentration 15 wt%) was placed

on a TEM grid which was kept under humid conditions at 37 ℃ ($T > T_{gel}$) in a closed chamber for 20 mins. allowing the formation of micelles. Then, the sample was suddenly immersed in a liquid ethane (-190 ℃) to freeze the micelles.

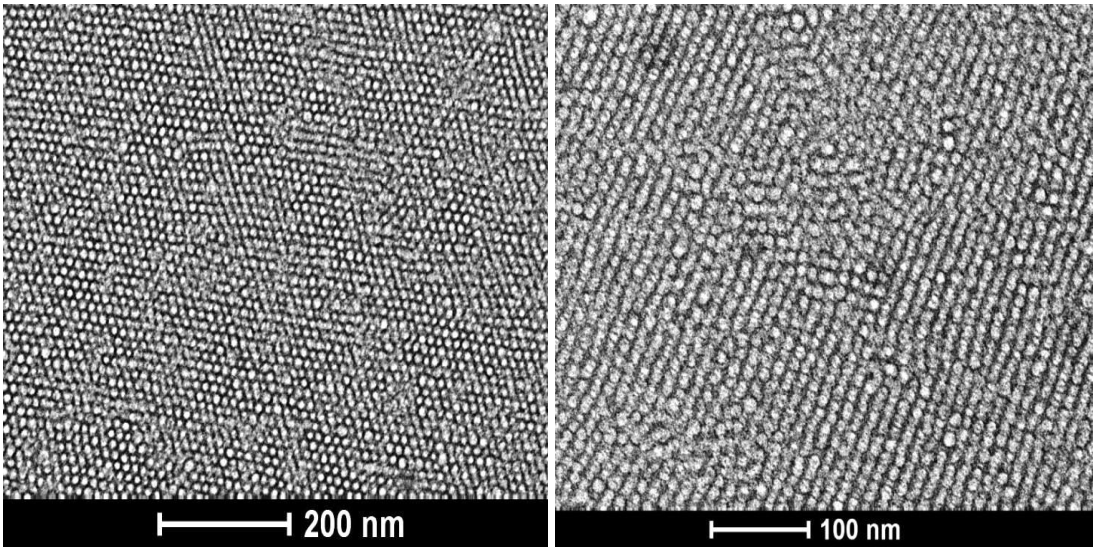

Figure 17. Cryo-TEM analysis of HA·mono-PEPE (2.7:97.3) solution at two level of magnifications, indicating the micelles and superstructure formed due to packing of micelles above T_{gel}.

As shown in figure 17, the average size of micelle around 20-30 nm. The alignment of micelles in the superstructure is non-uniform and can be supported by the Fourier transformation image, which indicates two different types of packing of micelles as,

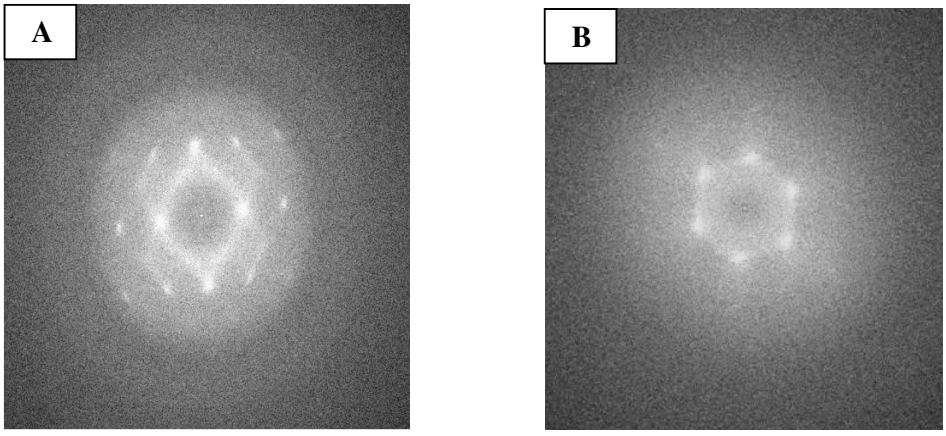

Figure 18. Fourier Transformation of Cryo-TEM images showing packing of micelles, **A.** Body centred cubic (BCC) packing of micelles and **B.** Hexagonal packing of micelles.

BCC and hexagonal packing (Figure 18). However, the Cryo-TEM analysis clearly showed the formation of micelles and different types packing of micelles upon heating near body temperature.

4.2.5 Small angle x-ray scattering measurement for determination of micelles

The small angle measurements were performed to investigate the influence of HA on micelles formation and its arrangements in the gel state. The small angle x-ray scattering measurements were performed at 20 °C (below T_{gel}) and 45 °C (above T_{gel}). As shown in figure 19, in all samples there was no micelle formation at 20 °C and hence showing an amorphous circle. But, when heated at 45 °C, the micelles were formed and got packed together to form a gel. At this situation, the ordering of micelles was appeared as a ring around the amorphous region and further rings are appeared as micelles were got packed in to second and third order of structure. The intensity of amorphous region decreased more micelle were arranged to form highly ordered structure[86]. The micelle formation was slightly hindered by the addition of HA, which can be seen from the intensity of amorphous region in the physical mixtures and the appearance of rings was not clear especially in physical mixture of HA and di-PEPE (HA·di-PEPE) as compared to PEPE.

Moreover, the appearance of crystalline peaks due to packing and ordering of micelles were also detected by small angle x-ray scattering measurements (Figure 20). The PEPE resulted in sharp and narrow peaks than physical mixture of HA and amine terminated PEE which might happen due to the increase in amorphous HA.

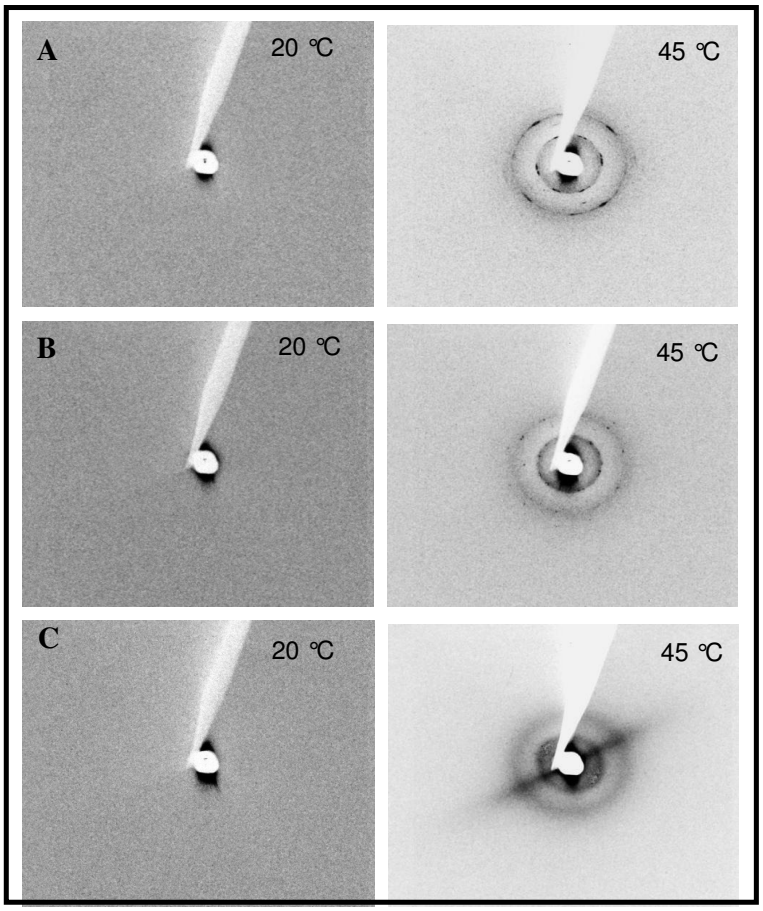

Figure 19. Small angle scattering measurements of PEPE (**A**)and HA·mono-PEPE (**B**), and HA·di-PEPE (**C**) shows packing of micelles upon heating above CMC/CMT indicated by formation of rings at 45 ℃

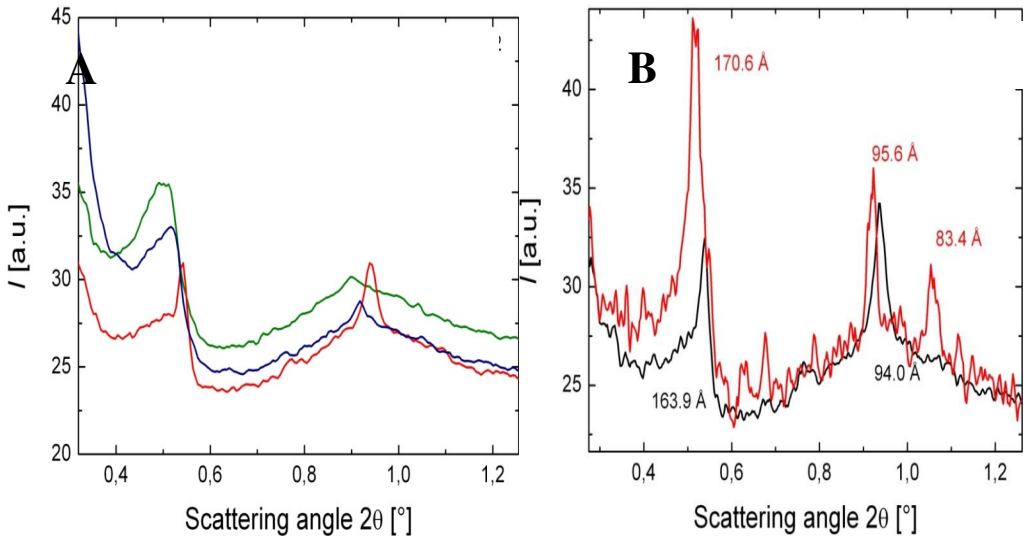

Figure 20. Comparison of the small-angle X-ray scattering signal obtained from, A. PEPE (—), HA·mono-PEPE (—), and HA·di-PEPE (—) hydrogel (concentration 20 wt%) and B. A closer look at PEPE and HA·mono-PEPE samples.

4.2.6 Change of mechanical properties during enzymatic degradation of HA·mono-PEPE hydrogels.

As the HA component contributes to the mechanical properties of the gel, the enzymatic degradation of HA may influence the mechanical properties of these hydrogels. Although there was no chemical crosslinking between HA and mono-PEPE (as it was seen in the rheological analysis) the enzymatic degradation study was performed to evaluate the changes in mechanical properties and T_{gel} during the degradation process. To study the degradation of physical mixtures of HA with different composition of mono-PEPE, the hydrogels prepared are reported in Table 1. For this study HA (2.33 MDa) with different composition of mono-PEPE were selected. During the degradation of the hydrogel, the hyaluronidase will randomly cleave β-*N*-acetylhexosamine-[1→4] glycosidic bonds in HA[87]. However, it is known that the physical and mechanical properties of hydrogels are strongly dependent on polymer chain length and polymer backbone and chain-chain interactions. Thus, by the degradation of long chain HA may influence the mechanical properties of hydrogel. Moreover, due to the interactions of small fragments of HA with PEPE the gelation process was also delayed, resulting in shift of T_{gel} to higher temperature as degradation progresses (Figure 21). The T_{gel} of initial composition was 26 °C, which was shifted to 29 °C after 48 h. of degradation time and clearly indicating the influence of HA degradation on gelation mechanism of PEPE. A similar kind of behavior was observed in all other hydrogels of HA·mono-PEPE composition.

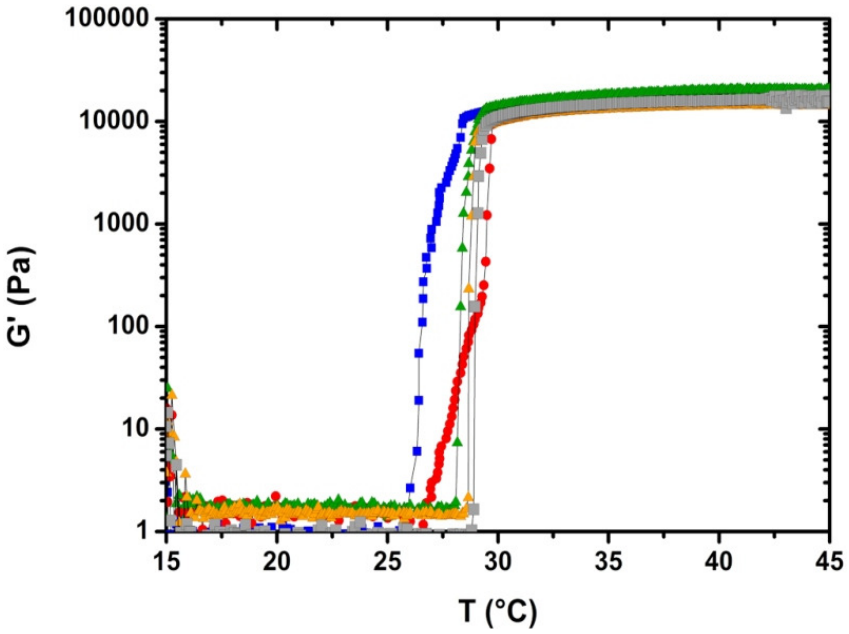

Figure 21. Temperature ramp of HA·mono-PEPE (2.6:97.4 wt%) hydrogels during degradation at different time points.{ 0h (■), 4h (●), 8h (▲), 10h (▲), and 48h (■)}.

The frequency sweep test at 37 ℃ (T>T_{gel}) was performed in order to investigate to detect the changes in the mechanical properties during the degradation process. As shown in Figure 22, the initial elastic modulus (G′) of hydrogel was around 18000 Pa, which was decreased to 15000 Pa after 1h degradation time. Further it decreased down to 12500 Pa within 4h of degradation time. This clearly indicate that the degradation of high molecular weight HA into small fragments with which it loses the chain entanglement and intra molecular chain interactions, resulted in decrease in the mechanical properties of hydrogel. Nevertheless, the hydrogel does not lose the ability to show a thermal gelation but, was shifted to higher temperature. Thus, the study clearly indicate that the HA does contribute to the mechanical properties of hydrogel and further degradation shows decrease in mechanical properties with time of degradation, even the final wt% composition oh HA is too low compare to PEPE

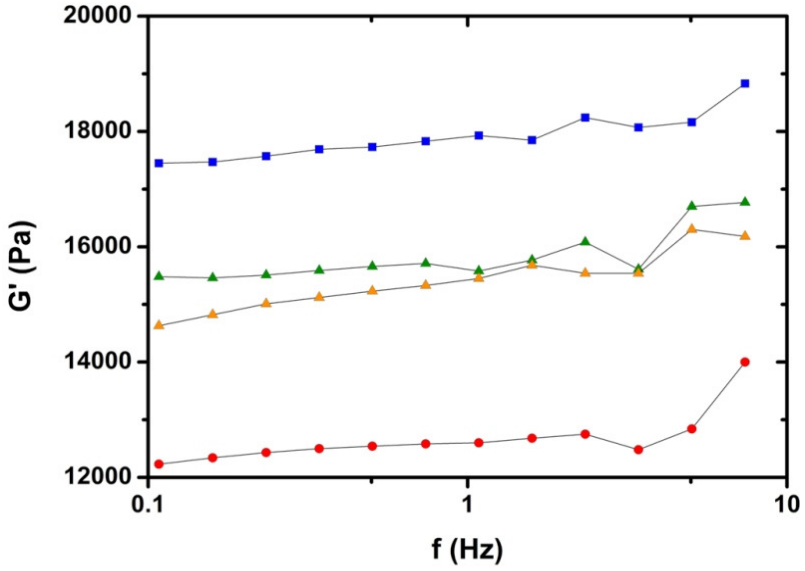

Figure 22. Frequency sweep test of HA·mono-PEPE (2.6:97.4 wt%) hydrogels at different time points. {0h (■), 1h (▲), 2h (▲), and 4h (●)}.

4.3 Thermosensitive hydrogels derived from di-PEPE and hyaluronic acid

In this section, the development of cytocompatible thermosensitive hydrogels is presented. The mechanical properties, endotoxin test, cytotoxicity test, and direct cell test of hyaluronic acid based hydrogels are discussed. (Cooperation project funded by BMBF: Biocompatible and thermosensitive polymers as vitreous replacement).

4.3.1 Synthesis of thermosensitive hydrogels

Regarding the background outlined above, here it is necessary not to have an absolute replacement but possibly mimic the viscoelastic properties and structure of as vitreous body substitute. A vitreous substitute is defined as the treatment agent, which helps to incorporate the functional characteristics of the glass body while exerting an additional stabilizing effect in the diseased eye, and to be treated. This

general consideration suggests that there will not be an ideal vitreous replacement, but a temporary vitreous replacement prevent the dysfunction of eye. The goal of this research study was to develop a polymer system as a vitreous replacement or as vitreous humor tamponade by using biocompatible polymer system, which basically derived from combination of biopolymers and synthetic polymers with thermosensitive properties resulting an injectable hydrogel which can form a gel at body temperature.

As reported in section 4.2, the ionic interaction of mono-PEPE and HA leads to form a thermosensitive hydrogel and it was also observed that, the ionic interactions of mono-PEPE was stronger than ionic interactions of non-functionalized PEPE with HA which was proved from rheological investigations. In this study, initially combination of mono-PEPE and HA was used to be evaluated as an artificial vitreous but, due to lack of sufficient mechanical properties, stability of hydrogel, and osmolarity, the combination of di-PEPE and HA (HA·di-PEPE) was chosen as it seems more promising material combination. The hydrogel was prepared by using different molecular weight of HA and different composition of di-PEPE as shown in the Table 5. Preparation of hydrogels was performed in clean room environment using endotoxin free materials.

Table 5. Composition, T_{gel}, and viscoelastic properties of thermosensitive hydrogels of HA·di-PEPE

M_n (HA) [MDa]	HA:	PEPE	T_{gel} [°C]	T_{gel} Interval [°C]	Hys. [°C]	G′[a] [Pa]	G″[a] [Pa]	|η*|[a] [kPas]	G′[b] [Pa]	G″[b] [Pa]	|η*|[b] [kPas]	Conc. [wt%]
2.33	4.5	95.5	34	2	7	2.395	0.507	0.599	15580	1176	3825	17
2.33	4.5	95.5	37	5	8	2.082	1.062	0.572	1648	243	407	13
1.2	5.5	94.5	29	3	8	1.202	0.997	0.382	21280	940	5216	20
1.2	5.5	94.5	32	3	7	1.189	1.065	0.391	15560	1376	3824	17
1.2	5.5	94.5	39	5	5	1,732	0.737	0.461	2972	590	741	13

Where, a: below T_{gel}, b:above T_{gel} (error for G′, G″ and |η*|= ±3%, for T_{gel} and T_{gel} (interval) = ± 1.5 °C)

4.3.2 Thermo-mechanical properties

The Thermo-mechanical properties and effect of additional ionic interaction (due to amino groups) on mechanical properties was investigated by rheological temperature ramp shown in Figure 23. The enhancement in the elastic modulus (G′) from 16330 Pa to 22450 Pa (±3%,) and decrease in the T_{gel} from 29 to 26 ℃ indicates the strong interaction between HA·di-PEPE is stronger compare to HA·mono-PEPE. The reason for enhancement in mechanical properties could be the increase in number of amino groups on PEPE, which then has more effective ionic interactions with carboxylic group of HA. Moreover, the mechanical properties and T_{gel} could be controlled by changing the concentration of polymer. Interestingly, the combination of high molecular weight HA and strong ionic interaction (due to di-PEPE) shows a thermosensitive gelation even at 13 wt% concentration.

The transition tended to be a little sharper, and the transition was also observed at lower concentrations compared to HA·mono-PEPE. Furthermore, the systems studied here showed a higher stability against dilution experiments. The material with the composition of HA (2.33 MDa) + di-PEPE (4.5:95.5 wt%) showed all the physical parameters that were set to start as specifications of target application.

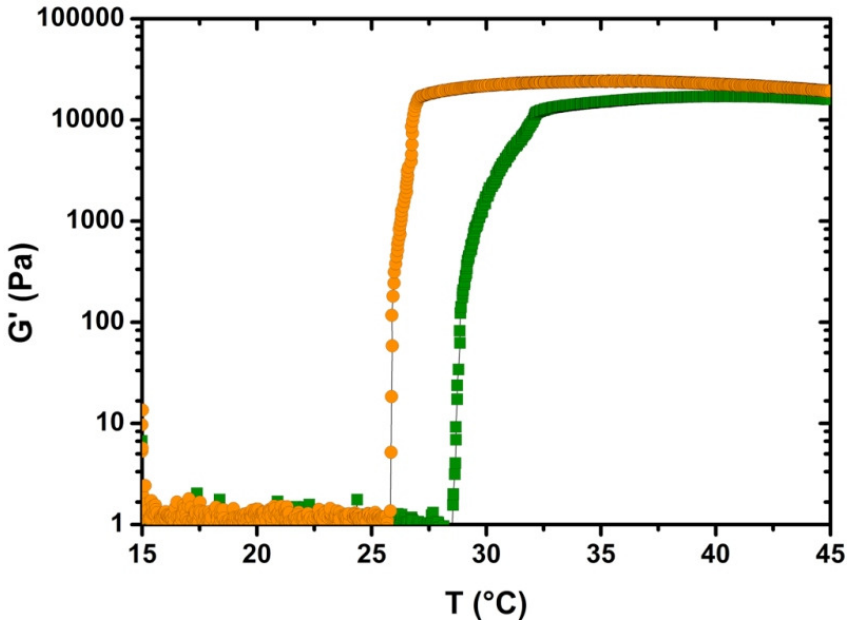

Figure 23. Rheological temperature ramp of HA·mono-PEPE (■), T_{gel} = 29 ℃ and HA·di-PEPE (●), T_{gel}= 26 ℃. (Concentration = 20 wt%)

4.3.3 Stability of hydrogels at 37 °C

Stability test was performed by using 20 wt% solution of HA·di-PEPE hydrogel and Tryptan blue (30 %) dye in water at 37 ℃ (Figure 24). The study shows an interesting behavior of hydrogels as the dye was did not diffuse into the gel (even after 2 weeks); a very important factor considering a hydrogel as a vitreous substitute that should not allow other solvent to dilute it which will destroy the structure and also the function of the system. The reason could be explain by the strong micelle packing through ionic interactions in BCC and hexagonal packing structure (already shown in Cryo-TEM analysis in Figure 18 and SAXS analysis Figure 19).

Figure 24. Stability test of HA·di-PEPE at 37 ℃

The second important point was that, after 2 weeks of time the hydrogel was intact and interestingly by slow diffusion of hydrogel into the dye solution, the whole system became a gel while maintaining the transparency as of initial hydrogel. Thus as explained before, the HA·di-PEPE combination have capability to form a thermosensitive hydrogel at low concentration (13 wt%) is also verified.

In addition to these properties, the refractive index of hydrogel was investigated. Ideally it should be similar at sol and gel state (e.g. refractive index of silicon oil= 1.404). The refractive index of HA·di-PEPE hydrogel provided a value of 1.358 at below T_{gel} (25 ℃) and above T_{gel} (37 ℃). Meaning there was no change in the refractive index during the gel formation of these hydrogels.

Further, it is very important for an material to be used as a vitreous body mimic, the optical transparency. Ideally the material should have 100% transmission. In our study, HA·di-PEPE hydrogel was tested by UV transmission (Thermo Scientific, Genesys 10 UV scanning) measurement between the wavelength 470-800 nm and the hydrogel was observed to be >90% transparent.

4.3.4 Degradation study of HA·di-PEPE hydrogels

The enzymatic degradation of HA·di-PEPE was performed in order to investigate the mass loss of hydrogel using different solutions. Degradation studies were performed to evaluate the long-term behavior of the materials. There are two important aspects to be considered. On the one hand, the mass loss, which gives information about whether soluble fragments are formed, this can no longer contribute to the functionality of the material. On the other hand, material properties may change on a weight loss and material composition. These changes are, therefore very essential to be determined during the degradation processes. However, are also important for the functionality of the materials during application. As shown in figure 25, significant initial mass loss occurred within the first week in all the samples but, afterwards the gel was stable for many weeks. Moreover it was observed that there was no significant difference in behavior of the materials in different mediums used.

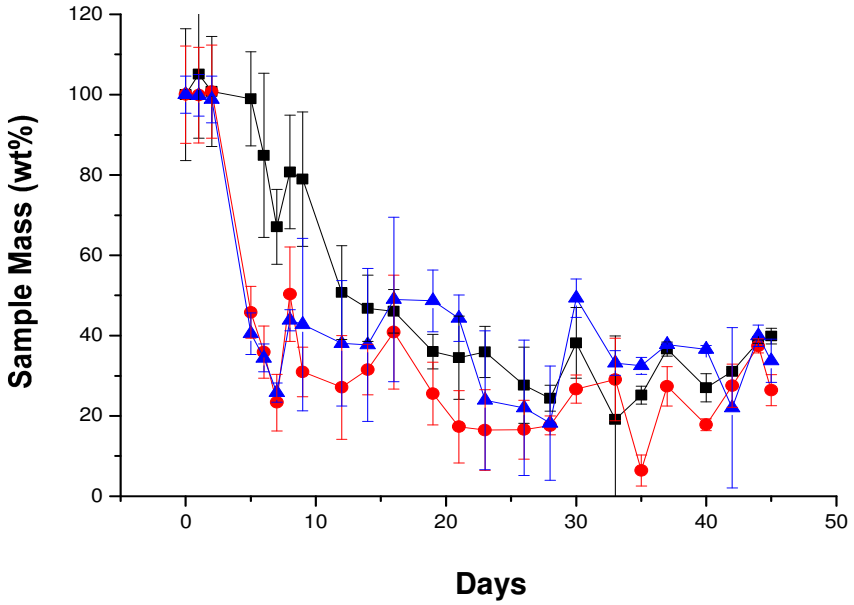

Figure 25. Enzymatic degradation of HA·di-PEPE showing the remaining mass of the sample {Performed in, Intraocular solution (●), vitreous extract (▲), and hyaluronidase (■)}

4.3.5 Biological evaluation of hydrogel

In order to evaluate the biological properties of first the materials have been tested by the endotoxin test and cytotoxicity test (These test were performed by Dr. Toralf Roch). The material bound microbial products were analysed by a cell based assay called Quanti-Blue assay as shown in Figure 26. LPS 10 ng·ml^{-1} was used as a positive control and elutes were prepared according to ISO10993-12.

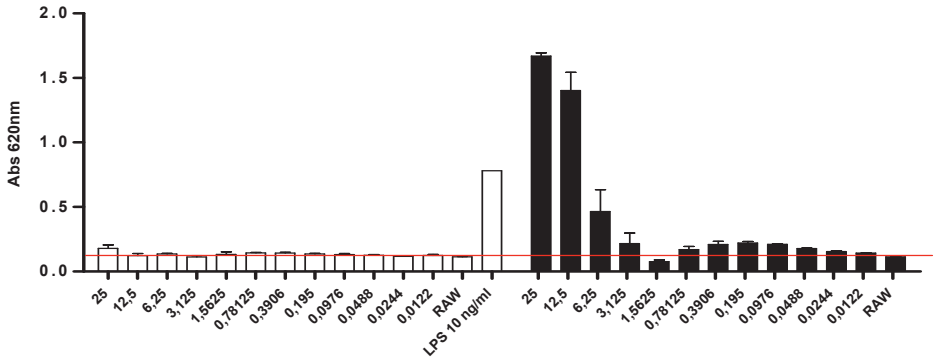

Figure 26. Endotoxin test of di-PEPE (□) and HA·di-PEPE (■)

There was some cell activated by HA·di-PEPE which indicate presence of some endotoxin in the material. In order to evaluate the cell behavior when coming in contact with these hydrogels a cell test with direct contact of hydrogel was performed (This test were performed by Dr. K. Kobuch) and variable results were obtained during the cell tests, change of pH and osmolarity was detected during the tests.

4.4 Summary

Thermosensitive hydrogels prepared via physical mixing of aminated PEPE and HA showed enhancement in the mechanical properties, especially elastic modulus (G′) and also decreased the gelation temperature. This effect was observed due to strong electrostatic interactions of carboxylic group of HA and amino groups of PEPE. In addition, it was also observed that with increase in number of amino group (mono-

PEPE to di-PEPE) these physical interactions became stronger and resulted in further increase in mechanical properties and decrease in T_{gel}. Further, it was possible to control the T_{gel} by varying the PEPE content in the composition. But, overall no effect was observed by varying the molecular weight of HA on the viscoelastic properties of these hydrogels.

Thermosensitive hydrogel system, which shows an alternative concept and provides better biocompatibility and could be used as a potential artificial vitreous substitute. The hydrogel was prepared via physical mixing of hyaluronic acid with amine terminated thermosensitive poly(ethylene glycol-*b*-propylene glycol-*b*-ethylene glycol)s (PEPEs). The hydrogel exhibits enhancement of shear viscosity and also form a transparent gel near body temperature. The ionic interaction between amino groups of PEPE (especially di-amino PEPE) and carboxylic group of HA show an increase in mechanical properties and lower gelation temperature compare to the mono-amine PEPE and non-functionalized PEPE samples with same concentration. In addition the hydrogel was able to closely fit the required properties such as, pH (7.1-7.3), optical transparency of >90% at 37 ℃ (in gel state) and at wavelength of 430-800 nm, a refractive index of 1.358, injectability through a 27G needle, steam sterilizability, which was close to the properties required by an synthetic vitreous substitute. The in vitro studies with mouse fibroblast cells show a promising biocompatibility of the hydrogel. Histological examination of the gel shows that all layers of retina were intact and no loss of tissues was evident.

5. Synthesis of Covalently Coupled Polysaccharide and PEPE Hydrogels with Tunable Properties

The data and part of the text presented in this chapter which is related to Pectin-*g*-PEPE hydrogels have been published as: Thermal Gelation and Stability of Pectin grafted with PEPE, Harshal D. Santan, Axel T. Neffe, Stefan Kamlage, and Andreas Lendlein, *Mater. Res. Soc. Symp. Proc.* / Volume 1403 / mrsf11-1403-v17-05 2012.

In addition, the data presented related to covalent coupling of HA formed the basis for a manuscript with the title, Thermosensitive Hydrogels Derived From Covalently Coupled HA and PEPE With Tunable Thermo-Mechanical Properties, Harshal D. Santan, Axel T. Neffe, Karola Luetzow, Ulrich Noechel, and Andreas Lendlein.

In this chapter, pectin, chondroitin sulphate, and hyaluronic acid based covalently coupled thermosensitive hydrogels with tunable properties were synthesized via EDC or DMTMM mediated coupling. The resulting hydrogels properties were characterized by IR, NMR, rheology, DSC, TGA, gel electrophoresis, and enzymatic degradation.

5.1 Synthesis of Pectin and Chondroitin sulphate grafted PEPE hydrogels using EDC as a coupling agent.

The hydrogels were synthesized via EDC mediated coupling of carboxylic group of polysaccharides with amino group of PEPE. The grafting of a thermosensitive PEPE onto pectin with different grafting ratios was achieved in two steps. PEPE was

aminated[88] by adding sub-equivalent amount of 4-Nitrophenyl chloroformate, followed by addition of 1,3-diaminopropane in the next step (Scheme 1). Subsequently, the free carboxylic groups of pectin were activated with EDC and the aminated PEPE was added to give the Pectin-*g*-PEPE (PGP). An analogues synthesis route was used for the synthesis of chondroitin sulphate-*g*-PEPE (CGP) hydrogels (Table 6). The synthesized hydrogels were characterized by IR showing the formation of new amide bond by appearance of new peaks at 1672 cm^{-1} (amide I) and 1595 cm^{-1} (amide II) hence, giving the first proof of coupling.

The grafting yield was calculated using equation 1:

$$\text{Grafting yield} = \frac{W_{PSGP} - W_{PS}}{W_{MAP}} \qquad \text{(eq. 5.1)},$$

where, W_{PSGP} is the weight of the freeze-dried grafted copolymer, and W_{PS} and W_{MAP} are the weights of pectin and aminated PEPEs in the feed, respectively.

Further, The number of free carboxylic acid groups in the pectin was determined with equation 2:

$$\text{Free carboxylic acid groups (Pectin)} = \frac{(W_{Pec} * 0.95)}{176.93 \frac{g}{mol}} \qquad \text{(eq. 5.2)}$$

For pectin, the galacturonic acid content (74 wt%) and degree of methylation (6.7 mol%) in the pectin. The grafting density, i.e. the percentage of free carboxylic acid groups of pectin and chondroitin sulfate functionalized with PEPE, was calculated with equation 3:

$$\text{Grafting density} = \frac{\left(\frac{W_{PSGP} * C_{PEPE}}{M_n(PEPE)} \right)}{W_{PS}} \qquad \text{(eq. 5.3)}$$

with C_{PEPE} = PEPE weight content in the PGP.

Table 6: Composition and grafting density (determined by eq.5.3) of the PGP and CGP

Sample ID	Composition of polysaccharide : PEPE (wt%)	Experimental yield[a] (wt%)	Grafting density (mol%)[b]
PGP 40	3.9 : 96.1	93	40
PGP 28	5.4 : 94.6	94	28
PGP 20	7.5 : 92.5	93	20
PGP 12	12 : 88	91	12
CGP 39	3: 97	91	39
CGP 28	4.2 : 95.8	93	28
CGP 20	5.6 : 94.4	94	20
CGP 11	9.3 : 90.7	92	11

a: determined from final weight of product after dialysis, b: from eq. 5.3

5.2 Characterization of hydrogels

5.2.1 Thermogravimetric Analysis of CGP and PGP Hydrogels

The thermogravimetric analysis is often a useful method for determining the composition of graft polymers. The thermograms of pectin, PEPE, and the PGP 40 are shown in Figure 27. Weight loss of pectin starts in the range of 60–75 °C, which is likely to be associated with loss of absorbed moisture in the sample. Decomposition was observed between 110–135 °C. In the next step between 225–250 °C, the sample rapidly lost around 55 wt%. Weight loss of PEPE starts at 250 °C, with a rapid mass loss between 350 °C and 380 °C. The expected curve of the grafted system would be the mathematical combination of the curves described above, and this is what is observed for physical mixtures of the two components (data not shown). However, interestingly the onset and major part of the mass loss of the grafted systems was observed at higher temperatures, i.e. the grafting process increased the thermal stability of the system. This observation might be explained by

a degradation mechanism of the polysaccharide in which the free carboxylic acid groups play an important role. These are now (at least partially) carboxamides, and hydrogen bonds between the two components are formed, which increased the thermal stability of the grafted system.

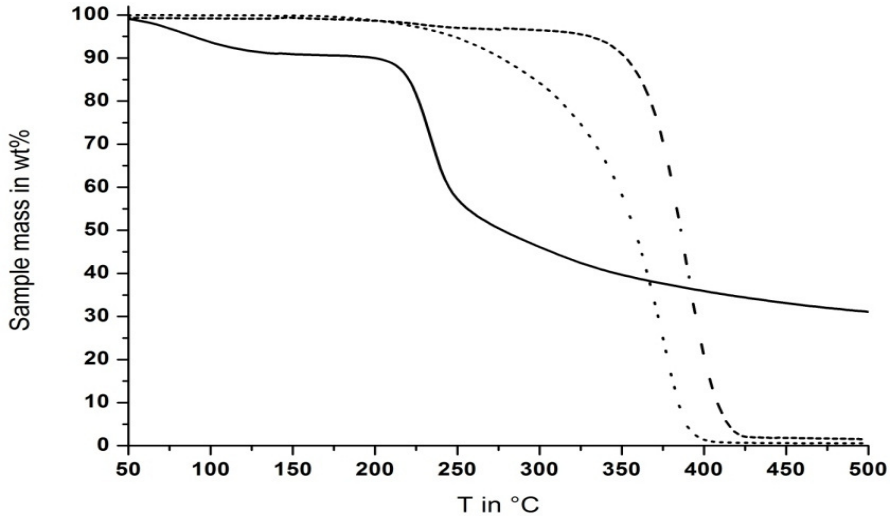

Figure 27. Thermo gravimetric analysis of pectin, PEPE, and PGP 40 in an N_2 atmosphere (solid line: pectin, dot line: PEPE, and dash line: PGP 40)

5.2.2 Determination thermo-mechanical properties of hydrogels

The rheological properties of pectin, chondroitin sulfate, PEPE, and the grafted hydrogels at different temperatures for Pectin (Figure 28 A.) and chondroitin sulphate (Figure 28 B) were observed to be non-thermosensitive in the given temperature range. The 20 wt% solution of PEPE has shown sol-gel transitions (T_{gel}) at around 34 °C, while after grafting to pectin (20 wt% solution) the T_{gel} was observed near 30 °C (Figure 29). This clearly shows the effect of grafting, which allows to form gels at lower temperature. By variation of the grafting density of the PEPE on the pectin, the T_{gel} of the system could be adjusted from 25 °C to 33 °C, whereby increasing the

grafting resulted in a decreasing T_{gel} (Figure 30). However, also the temperature interval for the transition is larger for systems with lower T_{gel}. Interestingly, the elastic moduli G′, the viscous moduli G″ and the viscosities of the systems were found to be similar and in all cases G′ and the viscosity increased during the gelation by four orders of magnitude.

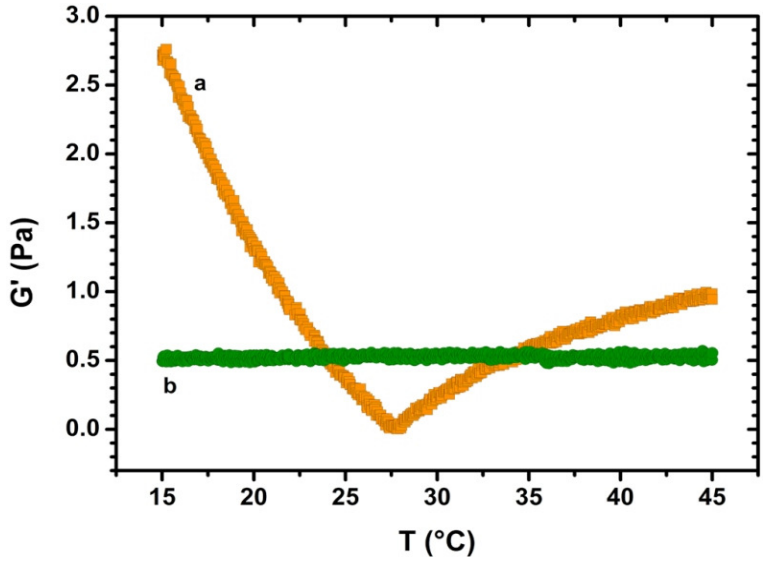

Figure 28. Rheological temperature ramp of, **a**. Pectin and **b**. Chondroitin sulfate showing a non-thermosensitive behavior (sample conc. 5 wt%)

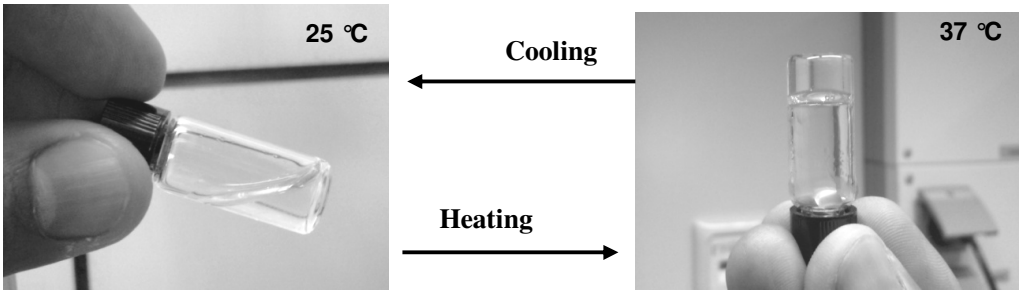

Figure 29. A reversible sol-gel transition of PGP40 sample at 20 wt% concentration

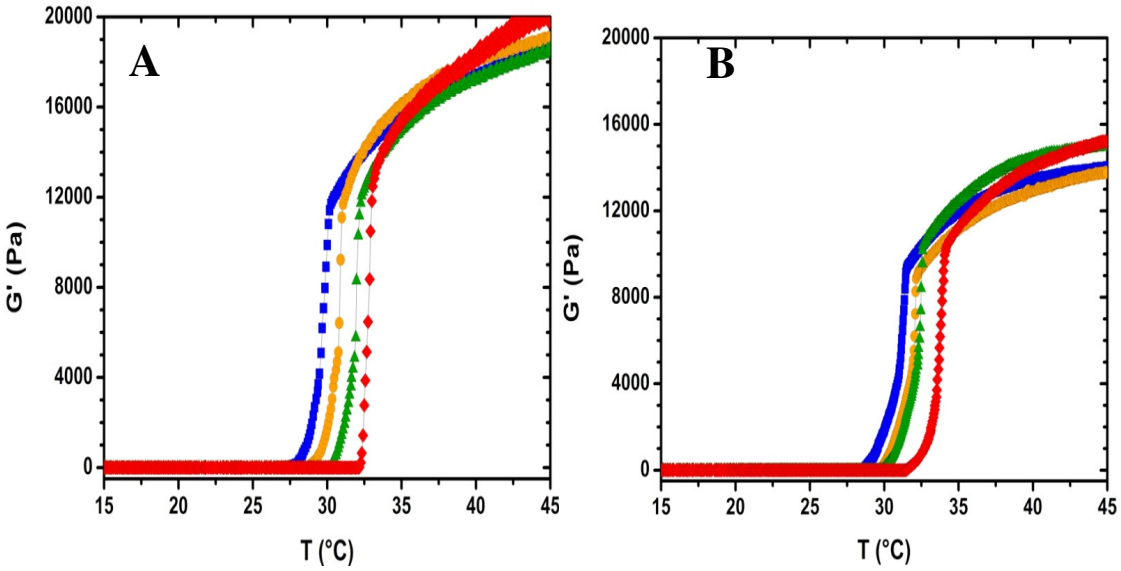

Figure 30. Tunable T_{gel} (from 25 – 34 °C) of PGP and CGP hydrogels influenced by the grafting ratio of PEPE. **A**. Pectin-*g*-PEPE (■:PGP40, ●: PGP 28, ▲: PGP20, and ■: PGP12) and **B**. Chondroitin sulfate-*g*-PEPE hydrogels (where, ■: CGP 39, ●: CGP28, ▲: CGP20, and ■: CGP11) (conc. for all sample = 20 wt% solutions).

5.2.3 Determination of CMC and CMT properties

The micelle formation in the pectin-*g*-PEPE (PGP) system was investigated by the determination of CMC and CMT. The UV-visible spectra of aqueous solutions of PGPs from 0.05 to 20 wt% concentrations containing DPH were measured at 5 °C temperature intervals over the range of 15-45 °C. For all samples, UV absorption was measured in the range of 300 – 400 nm. To calculate the CMC and CMT values, the intensity of absorption at 356 nm, which is the characteristic peak of DPH, was determined (data not shown). The CMC value for PGP 40 at 30 °C was found to be 3.5 wt% (0.8 wt% for PEPE) and the CMT for a 10 wt% solution was observed at 23 °C (21 °C for PEPE). By increasing the polymer concentration, the CMT decreased, while with increasing temperature the CMC decreased. The CMT values are lower than the observed T_{gel}, which corresponds to the two-step gelation

mechanism (first, formation of micelles, second, gelation due to micelle-micelle interactions).

5.2.4 Determination of molecular weight by gel electrophoresis

The determination of the molecular weight of the polysaccharide-*g*-PEPE systems is important to i) confirm the covalent attachment of the PEPEs, b) estimate the degree of grafting and c) investigate, if actually crosslinking took place. On the other hand, because of the extreme high molecular weight and self-ordering behavior of the systems in aqueous solution, it is also a challenging task.

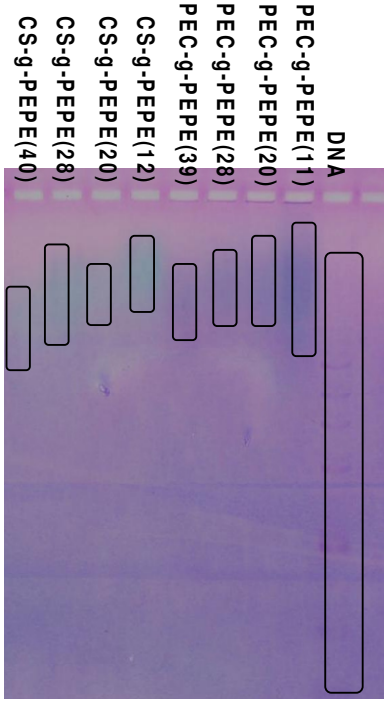

Figure 31. Electrophoresis of CS-*g*-PEPE and PEC-*g*-PEPE on 0.5% agarose (for each sample the concentration was 3 mg/ml)

As standard, DNA fragments of known molecular weights were used, as these were the only available standards in a suitable weight range (Figure 31). In the table 7, the

observed R_f values of Hyaluronic acid, CS-*g*-PEPE, and PEC-*g*-PEPE sample are given in table 7.

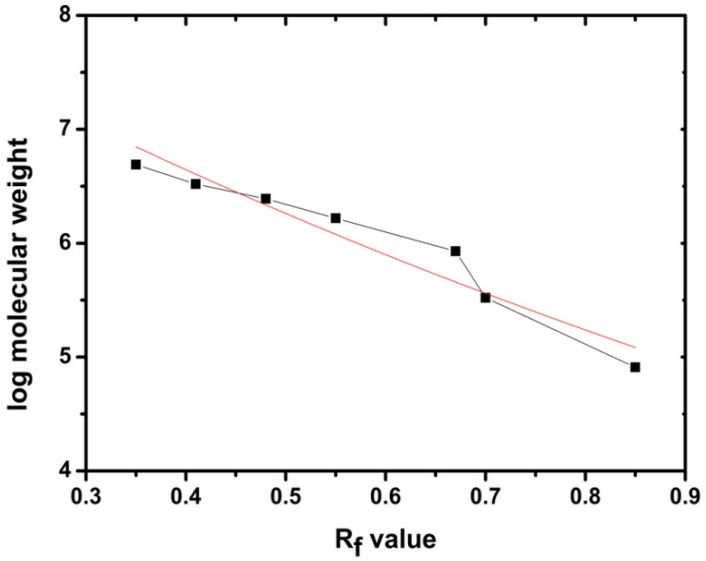

Figure 32 R_f values of DNA ladder and corresponding molecular weight.

Table 7. The R_f values and corresponding molecular weights of CS-*g*-PEPE and PEC-*g*-PEPE hydrogels

Sr. no	Sample name	R_f values	Molecular weight by gel electrophoresis (MDa)
1	Hyaluronic acid 1.6 MDa	0.29- 0.58	10 – 1
2	PEC*-*g*-PEPE (12)	0.11 - 0.26	42.39 – 12.83
3	PEC*-*g*-PEPE (20)	0.13 - 0.22	36.14 – 17.64
4	PEC*-*g*-PEPE (28)	0.13 - 0.23	36.14 – 16.29
5	PEC*-*g*-PEPE (40)	0.14 - 0.23	33.37 – 16.29
6	CS-*g*-PEPE (11)	0.11 – 0.21	42.19 – 19.11
7	CS-*g*-PEPE (20)	0.14 – 0.23	33.37 – 16.29
8	CS-*g*-PEPE (28)	0.14 – 0.26	33.37 – 12.83
9	CS-*g*-PEPE (39)	0.17 – 0.29	26-28 – 10.11

* The molecular weight of Pectin is = 60,000 to 90,000 g/mol. (error R_f values= 0.02)

The calculated values of the PEC and CS-based systems can be estimates only, as the values are outside the linear range of the standards. However, the calculations indicate that the molecular weight of these samples is higher, or, at least, that the

mobility of the samples in the gels was lower. This suggest that the EDC mediated coupling of PEC/CS with mono-amine terminated PEPE was carried out successfully. Moreover, the amount of PEPE grafting to PEC/CS was not affected by the feed amount of PEPE during the reaction or the molecular size slows the movement of the grafted molecules through the gel and hence appearing at lower side of the gel, therefore indicating higher molecular weight of the corresponding sample.

5.2.5 Effect of Enzymatic Degradation on Thermo-mechanical Properties of Hydrogels

The enzymatic degradation was performed in order to evaluate the changes in the mechanical properties and T_{gel} of the hydrogels. The hydrogels were taken out at selected time point and the thermo-mechanical properties were measured by temperature ramp and frequency sweep (Figure 33).

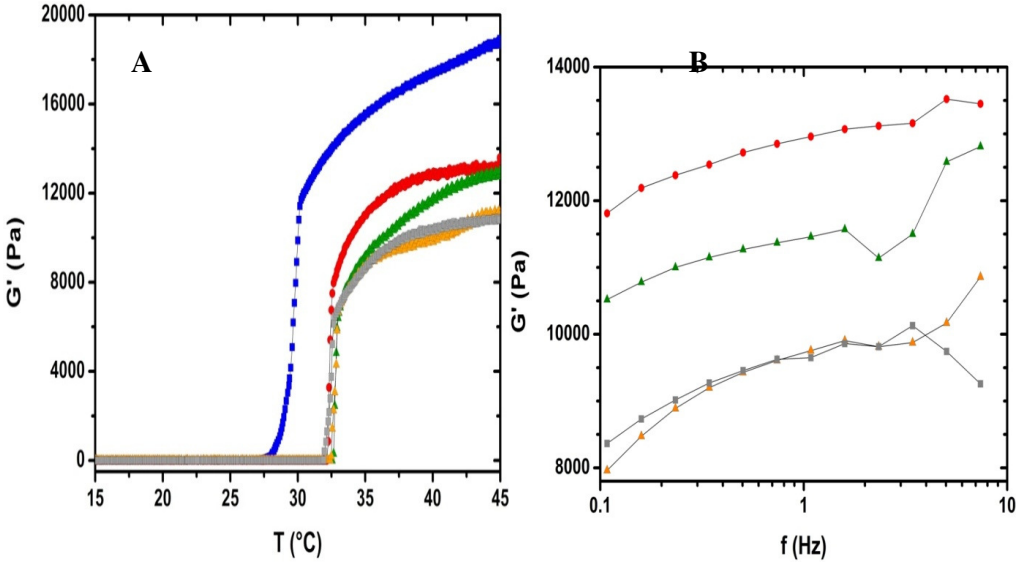

Figure 33. Thermo-mechanical properties of PEC-*g*-PEPE40 hydrogels during degradation at different time points. **A.** Temperature ramp and **B.** Frequency sweep at 37 ℃ {0h (■), 1h (●), 2h (▲), 4h (▲), and 6h (■)}.

As shown in figure 33 A, during the degradation of pectin-*g*-PEPE hydrogels, the T_{gel} was slightly shifted from (28- 33 ℃) within 6h of time, due to enzymatic degradation of α-1,4-glycoside bonds between galacturonic acid. Moreover, the G′ of the hydrogel was decreased from around 17500-9000 Pa (±3%) during the degradation process. This effect in decrease in G′ was also clearly shown in frequency sweep test at 37 ℃. The fragments formed due to degradation of pectin could interfere on the micellelization process of PEPE, thus delaying the process of gelation after degradation. The degradation process not only affected the gelation process but also the mechanical properties. As shown in figure 33 B, due to the degradation of pectin chain, it loses the chain entanglement and intra molecular chain interactions, resulted in decrease in the mechanical properties of overall hydrogel. Overall it should be noted that due to the random cleavage of Pectin during the enzymatic degradation process could results in slight different mechanical properties e.g. elastic modulus (G′) and T_{gel}. The similar effect of decrease in mechanical properties with decrease in T_{gel} was observed in all other composition of pectin-*g*-PEPE hydrogel, one example of temperature ramp of pectin-*g*-PEPE11 is shown in Figure 34.

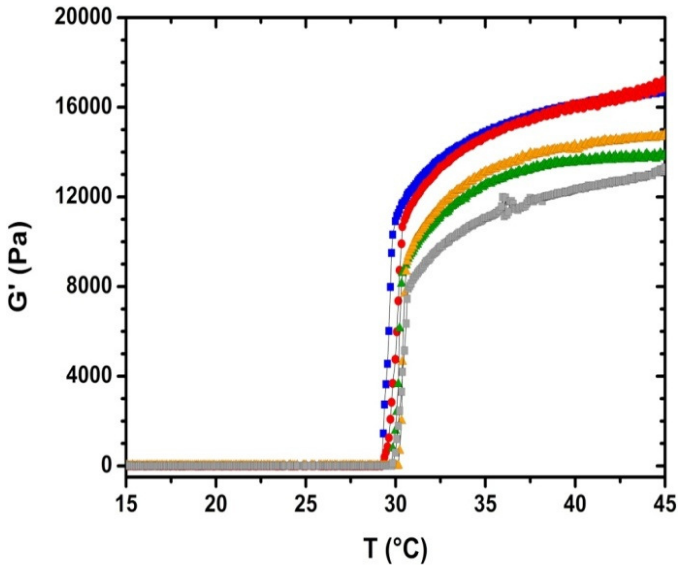

Figure 34. Temperature ramp of Pec-*g*-PEPE11 hydrogel during degradation. {0h (■), 1h (●), 2h (▲), 4h (▲), and 6h (■)}.

5.3 Summary

The polysaccharides pectin and chondroitin sulfate were functionalized with thermosensitive PEPE to have a thermosensitive, degradable hydrogel. Grafting of amine terminated PEPE to pectin and chondroitin sulfate was performed in order to investigate if tailoring of the sol-gel-transition temperature can be achieved by adjusting the grafting ratio. The sol-gel transition of the pectin, chondroitin sulphate, PEPE, and the grafted system (PGP and CGP) was investigated by rheology, where it was clearly shown that pectin and chondroitin sulfate was unable to show thermosensitive gelation. The gelation temperature (T_{gel}) of the system could be adjusted by varying the grafting density of PEPE onto pectin and chondroitin sulfate as well as by the concentration of the thermosensitive polymer in aqueous solution. A concentration of 15 – 20 wt% of the grafted system in water led to gelation temperatures in the range of 25 – 33 °C and the critical micelle concentration (CMC) and critical micelle temperature (CMT) of the Pec-*g*-PEPE systems were determined by UV spectroscopy. The viscosity and the G′ increased by four orders of magnitudes at T_{gel}, which is comparable to PEPEs alone, but could be reached at lower PEPE concentrations.

Moreover, the enzymatic degradation of Pec-*g*-PEPE hydrogels show that the viscoelastic properties (G′ and G″) of hydrogel was decreased by degradation of pectin and the gelation of hydrogel was shifted to higher temperature. However, the hydrogel still hold the ability to show a sol-gel transition after the degradation of its biopolymer backbone, such property of these hydrogel could be very useful in different biomedical application, e.g. drug delivery where a long term presence of the implant is necessary.

5.4 Synthesis of HA covalently coupled with PEPE using DMTMM.

5.4.1 Synthesis of hydrogels

The hydrogels were synthesized via amide bond formation between carboxylic group of HA and amine terminated PEPE using DMTMM as a coupling agent. This coupling method was found to be efficient over the EDC mediated coupling method due to, a. it does not required a specific pH (4.5 - 4.7) to carry out the coupling and b. the by-products of this reaction are easily removable by washing with water. Moreover, the ultrafiltration (filtration using a membrane with pore size 0.025 µm) provided a reliable removal of unreacted PEPE from the reaction mixture to give pure covalently coupled product.

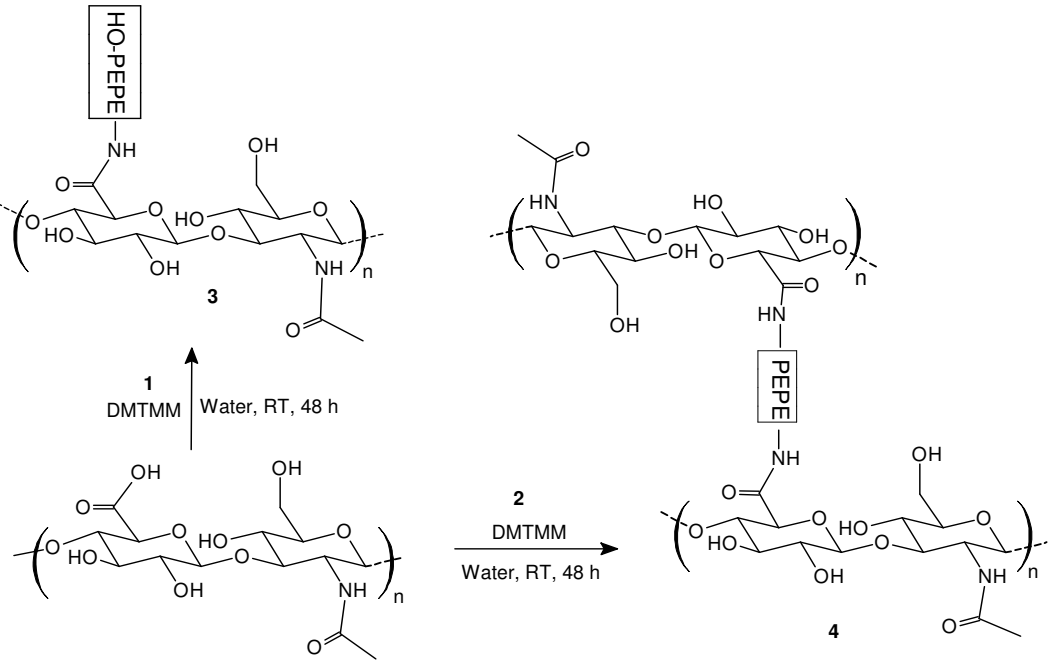

Scheme 2. Synthesis route of HA-*g*-PEPE (HGP), and HA-*x*-PEPE (HXP) by using DMTMM in water at room temperature

By coupling mono-PEPE and di-PEPE to HA, the hydrogels with two different architecture (grafted and partially crosslinking) was expected which, could show a distinguishable variance in there thermo-mechanical properties due to the type of covalent bonding (Scheme 2). Thus, the hydrogel was synthesized and purified by systematic methods, and further characterized by different methods to evaluate the thermo-mechanical properties depending upon either concentration or temperature. The covalent coupling between HA and amine terminated PEPE was confirm by ATR-FTIR, the degree of functionalization and expected molecular weight of hydrogels was calculated as,

Free –COOH groups in HA (M_{COOH})= $\left[\frac{(W_{HA})}{383\frac{g}{mol}}\right]$ (eq. 5.4)

Degree of functionalization (D. F.) = $\left[\frac{M_{PEPE}}{M_{HA}}\right]\times 100$ (eq. 5.5)

$M_x = \frac{wt\%_x}{MW(x)}$

Molecular weight of HGP or HXP = $\left[((MW_{HA} * D.F.) * M_{PEPE}) * W_{PEPE} + MW_{HA}\right]$ (eq. 5.6)

Where, $\mathbf{M_{COOH}}$ = mols of free carboxylic groups in HA, $\mathbf{W_{HA}}$ = amount of HA, $\mathbf{M_{PEPE}}$ = mols of PEPE in HGP or HXP, $\mathbf{M_{HA}}$ = mols of HA in HGP or HXP, $\mathbf{MW_{HA}}$ = Molecular weight of HA, **x** = HA or PEPE, **MW** = 383 g·mol^{-1} (HA) or 14500 g·mol^{-1} (M_n of PEPE).

The hydrogels obtained by this method are listed below in table 8.

Table 8. Nomenclature and composition of HA:PEPE in HXP and HGP systems synthesized in MES buffer (6.5 pH) or water

Sample ID*	Determined by weighing			Determined by TGA		
	HA:PEPE (wt%)	D. F. (mol%)	Molecular weight calculated (MDa)	HA:PEPE (wt%)	D. F. (mol%)	Molecular weight calculated (MDa)
HXP93	27:73	7	9.3	7:93	36	37.1
HXP88#	21:79	11	13.2	12:88	20	21.8
HXP83	25:75	8	10.3	17:83	13	15.1
HGP88	28:72	6	8.3	12:88	19	21.4
HGP73	32:68	6	8.3	27:73	7	9.3
HGP58#	52:48	3	5.47	42:58	4	6.4

D. F.: Degree of functionalization, *: Nomenclature according to composition determined by TGA, #: In MES buffer (6.5 pH)

5.4.2 ATR-FTIR spectroscopy

The successful coupling between HA and PEPE could be demonstrated by new bands in the IR spectroscopy corresponding to amide bonds which indicates the formation of new functional group within the molecules (Figure 35). The amide bond formation between HA and mono-PEPE or di-PEPE was confirmed with ATR-FTIR by the fairly strong increase of the absorption peaks at 1660 cm^{-1} (C=O stretching) and 1555 cm^{-1} (N-H bending, Amide II) . The additional peak at 1740 cm^{-1} (compared to HA) due to the urethane bond, which is present in the aminated PEPE (C=O stretching) as shown in figure 7. In addition, the presence of PEPE was investigated by the strong absorption peak at 2883 cm^{-1} which shows C-H stretching vibrations and a peak at 1097 cm^{-1} which was attributed to the characteristic C-O-C stretching vibration from PEPE segment.

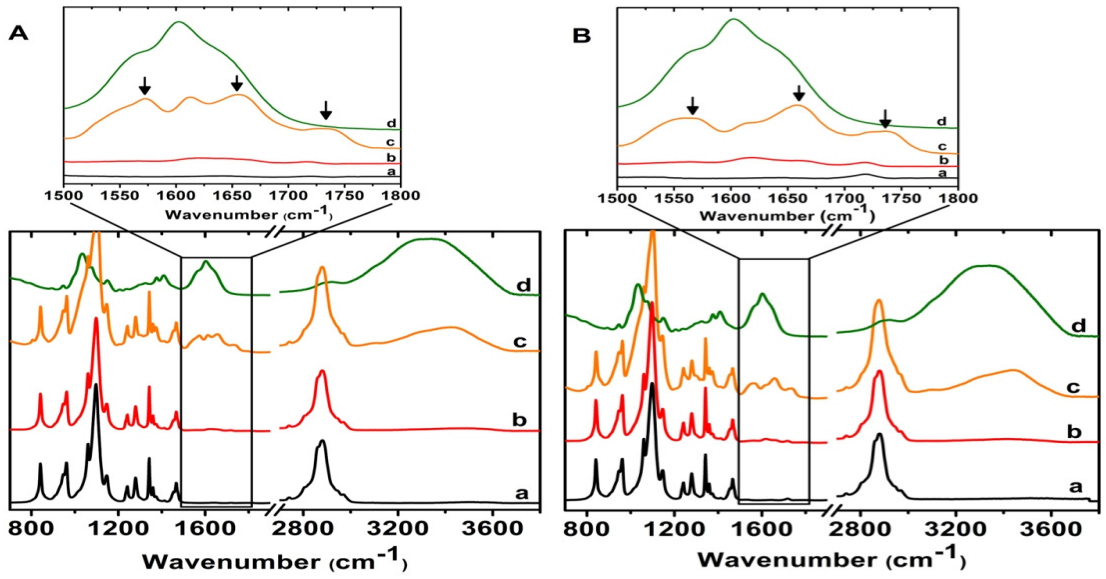

Figure 35. ATR-FTIR spectra: **A**. mono-PEPE (a), physical mixture HA·mono-PEPE (b), HGP88 (c) and HA (d). **B**. di-PEPE (a), physical mixture HA·di-PEPE (b), HXP93 (c), and HA (d). The amide bond formation in HGP88 (A(c)) or HXP93 (B(c)) can be seen by the absorption peak at 1740 cm^{-1} (C=O stretching), 1660 cm^{-1} (N-H bending), and 1555 cm^{-1} (N-H bending) which are well separated from amide peak of HA (1550 cm^{-1} and 1600 cm^{-1}).

5.4.3 Thermal properties and determination of composition of hydrogels

The thermal properties of HGP and HXP copolymers were investigated by DSC and TGA. The DSC thermograms show a T_m for the PEPE educts **1** and **2** of 55 °C and 53 °C while HA showed no T_m. While the physical mixtures of HA and **1** or HA and **2** showed a similar T_m as the corresponding aminated PEPE, the HGP and HXP copolymers showed lower melting temperatures (T_m) (Figure 36 A) than the corresponding PEPEs **1** or **2**. The lowest T_m of 42 °C was found for the grafted hydrogel HGP58, which also has the lowest PEPE content, while the partially crosslinked hydrogel with the lowest T_m content was HXP88 with a T_m of 45 °C (Figure 36 B). In both cases, the increase in PEPE content led to a rise in T_m revealing the resulting higher crystal size with increase of PEPE content in the

corresponding HGP and HXP gels. The increase in crystallinity was also seen in x-ray scattering investigations of the partially crosslinked gels (data not shown).

The exact HA:PEPE ratio of the synthesized hydrogels was calculated from the TGA measurements which was based on the TGA analysis of the educts HA and the aminated PEPE **1** or **2**. In case of HA, the thermal weight loss started at 70-90 °C with an initial mass loss of 15-18 wt%, which includes loss of moisture. A major mass loss of around 40 wt% was observed at 240 °C. The mass loss of the aminated PEPE started at a much higher temperature. In case of the mono-amino PEPE **1**, the major mass loss started at around 352 °C and after another 50 ° (at 405 °C) 95 wt% of the initial mass was lost. In HGP and HXP hydrogels, the peak at 237 °C indicates the first step of thermal degradation presumably due to the HA segment which is

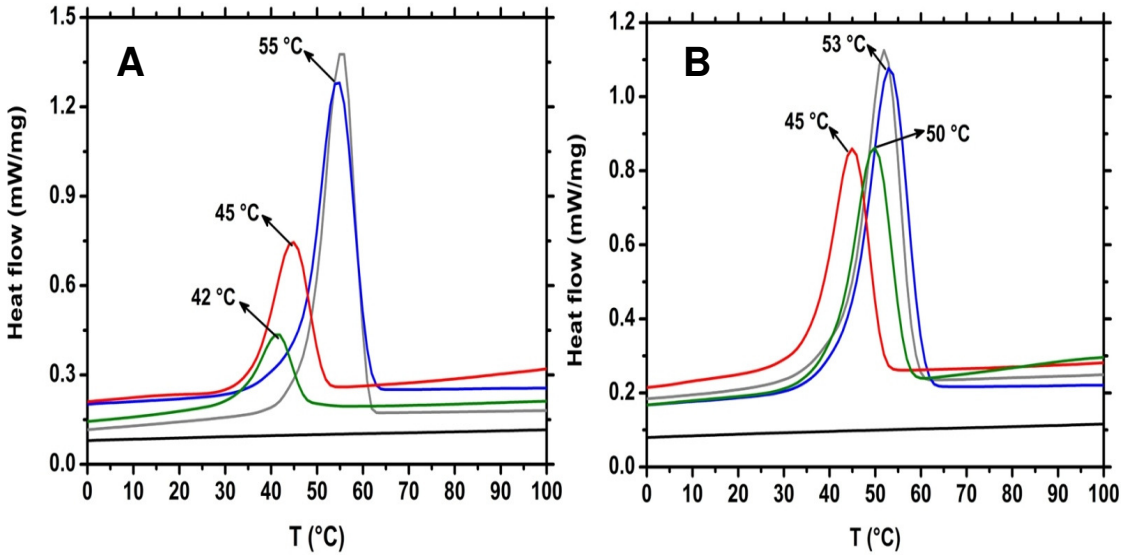

Figure 36. Thermograms from Differential Scanning Calorimetry (DSC): **A.** Grafted hydrogels HGP73 (—) and HGP58 (—) compared with HA (—), PEPE **1** (—), and physical mixture HA·PEPE1 (—). **B.** Partially crosslinked hydrogels HXP93 (—) and HXP88 (—) compared with HA (—), PEPE **2** (—), and physical mixture HA·PEPE2 (—). The melting temperature (T_m) and ΔH increased with degree of functionalization, likely because of the increase in crystallinity and crystal size.

around 5-10 wt% and another peak observed at 345 °C with mass loss of 80 wt%, which is presumably due to the PEPE segment (Figure 37 A and B). However, in case of HGP and HXP systems, the mass loss at 405 °C was only approximately 85 wt% and thus lower, which is expected to be due to the covalent coupling of HA and amino PEPE. Thus, it was possible to estimate the amount of HA and PEPE incorporated in HGP and HXP copolymer system from TGA analysis. The quantitative amount (in wt%) of each segment was calculated by plotting a line with a quantitative combination of HA and the corresponding amino PEPE, which was fitted to the HGP or HXP line obtained by TGA (Table 8). By calculating the amount of amino PEPE coupled to HA in HGP and HXP hydrogels, it was possible to calculate the estimated molecular weight of copolymers by using eq. 5.6.

However, in case of physical mixtures no significant difference was observed in comparison to the corresponding amino PEPE, which is assumed to be due to absence of covalent bonding between HA and amino PEPE. Thus, this study demonstrates that the covalent coupling and degree of functionalization in HGP and HXP copolymer system have a strong effect on the thermal properties. The results from the TGA were compared to the final weight of the synthesized hydrogel. However, it showed that the calculations based on the weight difference between the quantity of the HA used for the reaction and the weight of the final hydrogel is too un-exact to draw any further conclusions presumably because of weight loss during the work-up.

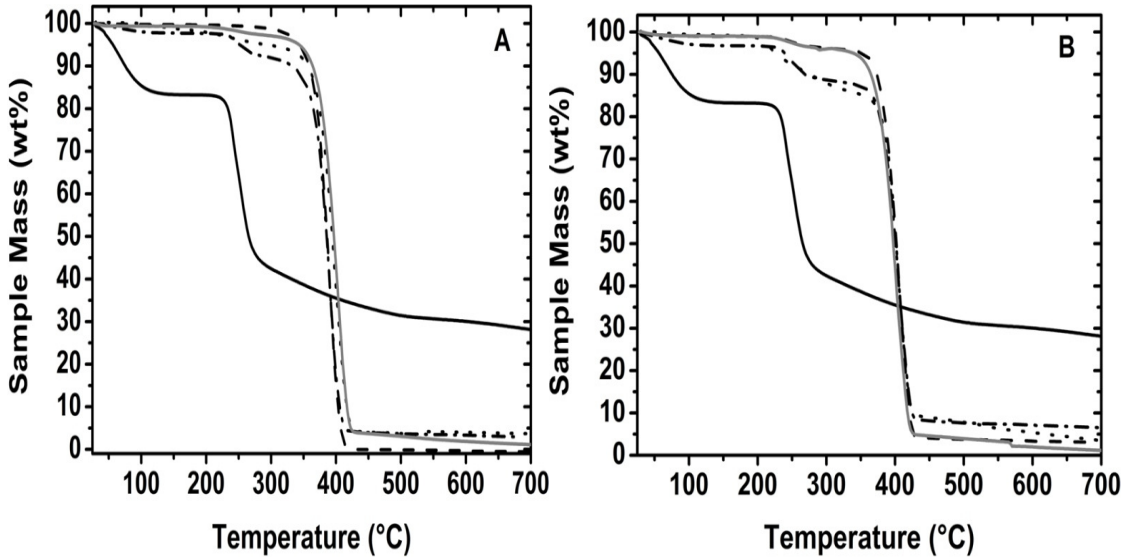

Figure 37. Thermogravimetric analysis (TGA): **A.** Grafted hydrogel HGP88 (···) compared with its educts (HA (—), PEPE **1** (---) and the physical mixture HA·PEPE1 (—) and the mathematical fit of HGP88 (**-·-**). **B.** Crosslinked hydrogel HXP93 (···) compared with its educts (HA (—), PEPE **2** (---), and physical mixture HA·PEPE2 (—) and the mathematical fit of HXP93 (**-·-**).

5.4.4 Determination of Thermo-Mechanical Properties Induced by Temperature and Concentration of Hydrogels

In order to better understand and evaluate the influence of covalent linkage on the mechanical properties during the gelation process, a rheological analysis was performed. The elastic modulus (G′) and viscous modulus (G″) were monitored as a function of temperature and frequency. Gel formation of PEPE is triggered by micelle formation and takes place above CMC and CMT at a concentration of >16 wt% which is reversible upon cooling. In case of HA, no thermosensitive behavior is observed, but it has a very high viscosity at low concentration (1-3 wt%). The physical mixture of the HA and the aminated PEPE **1** or **2** respectively (weight ratio 5:95) show a T_{sw} of 28 °C or 25 °C respectively (close to the T_{sw} of PEPE **1** and PEPE **2** using the same concentration) and an enhancement in elastic modulus from 0.892 Pa to 14660 Pa upon heating HA·mono-PEPE at a concentration of 20 wt%, while no effects were

observed at a concentration of 10 wt%. Similar results were found for the physical mixture HA·diamino-PEPE95. The grafted and crosslinked hydrogels showed already at a concentration as low as 2.5 wt% an increase in thermo-mechanical properties, while previously studied systems required a polymer concentration of 18-25 wt% to show gelation near body temperature[88–91]. This gelation at a much lower concentration was possible by creating covalent net points by covalently coupling amino-PEPE to the HA backbone in addition to the physical netpoints, which are created by micelles of PEPE above CMC/CMT (Table 9).

In case of the grafted hydrogels, it could be observed that an increase in PEPE content of the hydrogel leads to an increase in the elastic modulus. However, no significant effect on T_{sw} in relation to PEPE content was observed which was at 32/33 °C. At T > $T_{sw,}$ the 5 wt% hydrogels prepared from HGP58, HGP73, and HGP73 88 showed an increase in elastic modulus G′ from 18 Pa to 703 Pa and finally to 1367 Pa. The difference between the mechanical properties below T_{sw} and above T_{sw} varied only by the factor 1.6 to 4.5, which is much lower than for the physical mixtures.

In case of the HXP copolymer systems, the thermo-mechanical properties varied in dependence of the hydrogel concentration (2.5 – 10 wt%) (Figure 38). The T_{sw} of 30 °C was also much higher than for the physical mixtures. In the temperature ramp of HXP93 above T_{sw}, the 2.5 wt% sample revealed a G′ of 1150 Pa which increased to 4326 Pa (±5%) at concentration of 5 wt % and up to 13080 Pa (±5%) at concentration of 10 wt%. It is also noticeable that, in case of HXP93 at 2.5 -10 wt% concentration the G′ after T_{sw} increased by factor 2.3-3 compared to G′ below T_{sw}.

Table 9. Rheological properties of physical mixtures of HA·aminated-PEPE, HGP, and HXP hydrogels.

Sample	Concentration (wt%)	T_{sw} (°C)	G′ before T_{sw} (Pa)	G′ after T_{sw} (Pa)	T_{int} (°C)	Factor (fold)
HA·PEPE1*	20	28	0.892	14660	3	$1.6 \cdot 10^4$
HA·PEPE1*	10	NO	0.956	0.972	NO	1
HA·PEPE2*	20	25	1.116	16670	3	$1.4 \cdot 10^4$
HA·PEPE2*	10	NO	1.245	1.342	NO	1.1
HXP93	2.5	30	514	1150	10	2.3
HXP93	5	30	1286	4326	10	3
HXP93	10	30	5000	13080	10	2.6
HGP88	5	33	1367	2416	12	1.7
HGP88	10	32	10810	19130	12	1.7
HGP73	2.5	32	250	400	12	1.6
HGP73	5	32	306	703	11	2.3
HGP58	5	33	4	18	12	4.5

T_{sw}: Switching temperature, T_{int}: Temperature interval, NO: Not observed. * HA:PEPE ratio 5:95 wt% (Error for G′ and G″ = ±5%, Error for T_{sw} and T_{int} = ±1.5 °C)

This study demonstrates that the covalent coupling of amino PEPE to HA leads to thermosensitive hydrogels which have a tunable T_{sw} and tunable mechanical properties. While earlier reports on physical mixtures required high concentrations of 18-27 wt%[15,23,92] of HA and the thermosensitive PEPE, the now presented approach results in hydrogels that have enhanced mechanical properties at physiological temperature using only 2.5 wt% of polymer concentration. The physical mixtures required a concentration of 25-27 wt% of HA and PEPE to demonstrate a T_{sw} of 33-37 °C at which G′ and G″ increased; the addition of only 1-2 wt% of HA to 25-27 wt% PEPE solution, which would be comparable concentration to the now reported HGP

or HXP hydrogels, does not have a significant influence on the gelation temperature of physical mixtures.

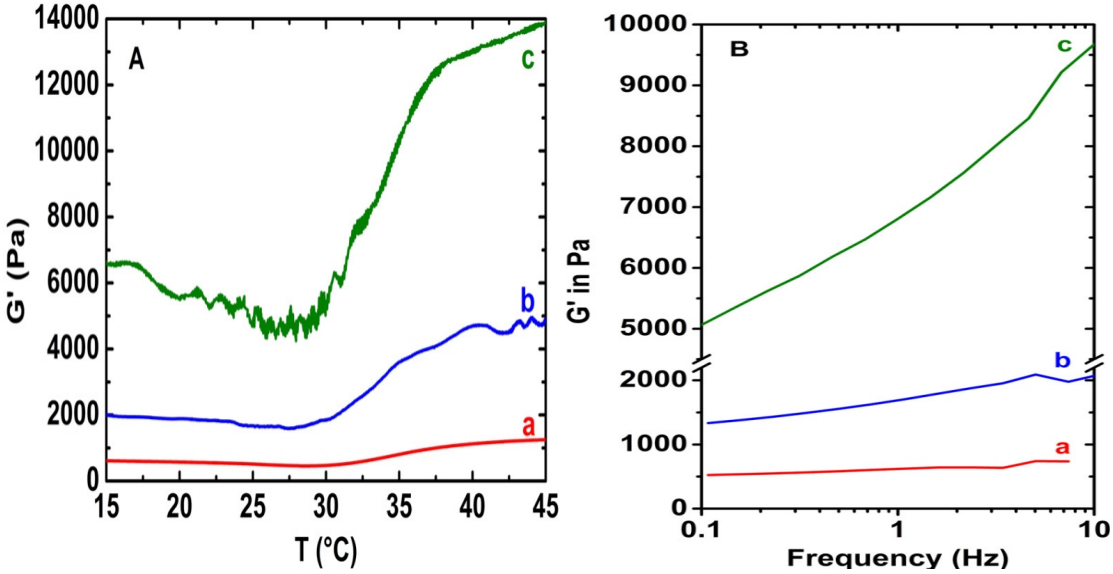

Figure 38. Increase in complex shear storage moduli (G′) of HXP93 hydrogel with different concentration measured as a function of temperature (**A**) and as a function of frequency (**B**) by rheology. (**a**: 2.5 wt% HXP93, **b:** 5 wt% HXP93, and **c**: 10 wt% HXP93).

The gelation in physical mixture results from the hydrophilic/hydrophobic association of polypropylene glycol (PPG) and polyethylene glycol (PEG) segments in the PEPE and occurs within a definite range of concentration as well as temperature. The gel formed by such mechanism, easily disintegrates to a solution by further reduction in concentration.

Hydrogels resulted from EDC mediated coupling and purified by dialysis, seem to have a large quantity of non-reacted educts[89,93–95]. The observation, that PEPE with a molecular weight of approximately 14.6 kDa does not pass during dialysis the membrane, and the described gelation and the corresponding mechanical properties lead to this assumption. The thermal gelation of these hydrogels required a concentration of 18-25 wt% gel in water to show a gelation temperature in the range of 26-34 °C. The reported minimal concentration for gelation of HA-*g*-PEPE was 18

wt%[94,95] Even in case of the highest grafting degree, no significant effect in shift of the gelation temperature due to grafting was observed. Thus, covalent grafting and cross-linking using DMTMM as a coupling mediator and the work-up using ultrafiltration to remove unreacted PEPE quantitatively, lead to hydrogels, which show a strong increase in the thermo-mechanical properties compared to the physical mixtures; an increase in the elastic modulus (G′) was observed already at a concentration as low as 2.5 wt% gel in water. The current results show that (1) varying the coupling strategy, i.e. choosing the grafting or the cross-linking approach and variation of coupling density, (2) varying the PEPE content in the copolymer, and (3) varying the dilution of the hydrogel in water, and (4) varying the applied temperature, i.e. working below or above T_{sw}, allows the final tuning of the mechanical properties.

5.5 Summary

This study shows that covalent coupling of the thermosensitive unit PEPE to HA leads to a phase transition at lower concentrations (2.5 -10 wt%) compared to the physical mixtures (16.8-20 wt%) of the same components, which was achieved by an efficient covalent coupling of amine terminated PEPE to HA to form a thermosensitive hybrid. DMTMM showed to be a much more effective coupling agent than EDC, and purification by ultrafiltration was necessary to remove unreacted PEPE quantitatively to obtain covalently coupled hydrogels. All synthesized compounds were in the gel state at low concentrations at room temperature, in contrast to physical mixtures of the same components. The covalent coupling of HA and amine terminated PEPE was shown by FT-IR, and TGA was a suitable method for the exact determination of the composition. The covalently coupled hydrogels showed enhanced elastic

modulus (G′) when heated near to body temperature. The viscoelastic properties were tailorable by the covalent coupling strategy, PEPE content, concentration of the hydrogel, and the degree of functionalization. Interestingly, the thermosensitive behavior could be demonstrated even at a very low concentration of these hydrogels in water (2.5-10 wt%), in contrast to physical mixtures of the same components, which need a concentration of more than 16 wt%. furthermore, when these hydrogels were treated with the enzyme hyaluronidase, it turned into a solution due to the degradation of HA chains and thereby showed an on-demand solubilization of these hydrogels. Moreover, the rheological experiment of these degraded hydrogels showed a sol-gel transition with slight shift in T_{sw} to 40 °C, indicating the presence of thermosensitivity even after degradation. Thus, unlike the CMC based hydrogels, these hydrogels were not solubilized after addition of excess solvent but, showed an on-demand solubilization by enzymatic degradation.

Thus, covalent coupling of amine terminated PEPE to HA with DMTMM provides a sufficiently high local concentration of PEPE segments, which show thermosensitivity near body temperature as well as tunable mechanical properties. Future study on these promising hydrogels concerning their hydrolytic and enzymatic degradation and the corresponding effect on the viscoelastic properties (G′, G″, and |η*|) and thermosensitivity of these hydrogels is needed to draw a conclusion concerning their application in Regenerative Medicine.

6. Synthesis of Gelatin-*g*-PEPE thermosensitive architectured hydrogels (T-ArcGel)

In this chapter, the synthesis and characterization of Gelatin-*g*-PEPE based architectured hydrogels were described. Further, the evaluation of swelling, water uptake, thermo-mechanical properties, and hydrolytic degradation of the hydrogels is discussed.

6.1 Synthesis of GA-*g*-PEPE hydrogels

The hydrogels of GA-*g*-PEPE were synthesized by covalent coupling of PEPE and amino groups of gelatin. First PEPE were reacted with 4-nitophenyl chloroformate and further reacted with amino groups of gelatin as shown in scheme 3.

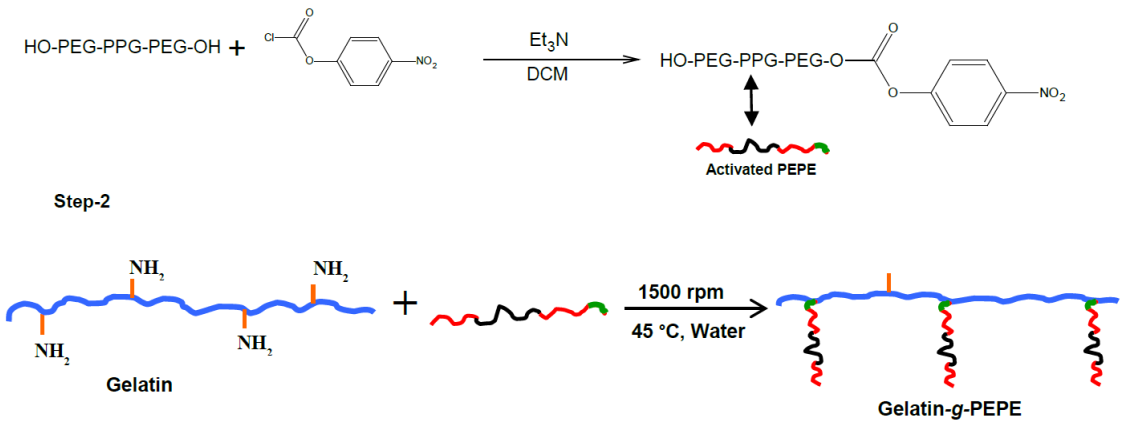

Scheme 3. Synthesis of GA-*g*-PEPE hydrogels

Further by controlling the initial amount of PEPE added during the reaction, the grafting density of PEPE in gelatin-*g*-PEPE was varied. The TNBS test revealed degrees of functionalization of 22 to 54 mol% of amino groups of gelatin by PEPE. Here, different amount of PEPE functionalization on different blooms of gelatin (see table 10) was studied. In this study gelatin with 300, 200, and 90-120 bloom was used. The strategy behind using different blooms of gelatin and different grafting density was to evaluate the effect on mechanical properties of the resulting hydrogel. The non-functionalized amino groups of gelatin were used for crosslinking in the next step of the synthesis

Table 10. Degree of grafting of PEPE to gelatin

Sample. no.	Gelatin bloom	Functionalization of -NH_2 groups of gelatin (mol%)
1	300	22
2	300	54
3	200	24
4	200	28
5	200	30
6	200	34
7	90-120	37
8	90-120	43

6.2 Characterization of GA-*g*-PEPE hydrogels

6.2.1 ATR-FTIR and ^{1}H-NMR analysis

The GA-*g*-PEPE hydrogels were characterized by ATR-FTIR and NMR spectroscopy to detect the changes in the peaks due to formation of new bonds by grafting PEPE to gelatin and hence identifying the product. As shown in figure 39, decrease in the intensity of -NH_2 (3400 cm^{-1}) group due to a chemical modification by PEPE was observed. Other peaks at 2950 cm^{-1} (C-H stretching) and 1020 cm^{-1} and 950 cm^{-1} (C-O-C, ether linkage in PEPE) reveal the presence of PEPE in the sample.

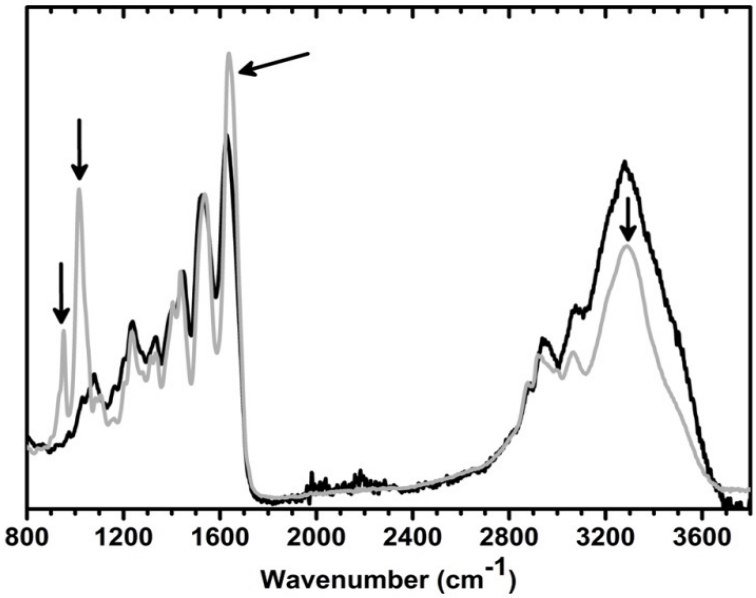

Figure 39. IR of GA200 bloom (—) and GA200-*g*-PEPE24 (—).

As gelatin is a natural polymer derived from collagen i.e. consist of amino acids, there are several signals appeared in the spectra the ^{1}H-NMR spectra and was complicated to understand. So, the proton signal of our particular interest was -NH_2 groups of lysine which were functionalized by PEPE. The list of different signals is given in Table 11. The NMR was measured at 45 ℃ for better resolution of proton signals (Figure 40).

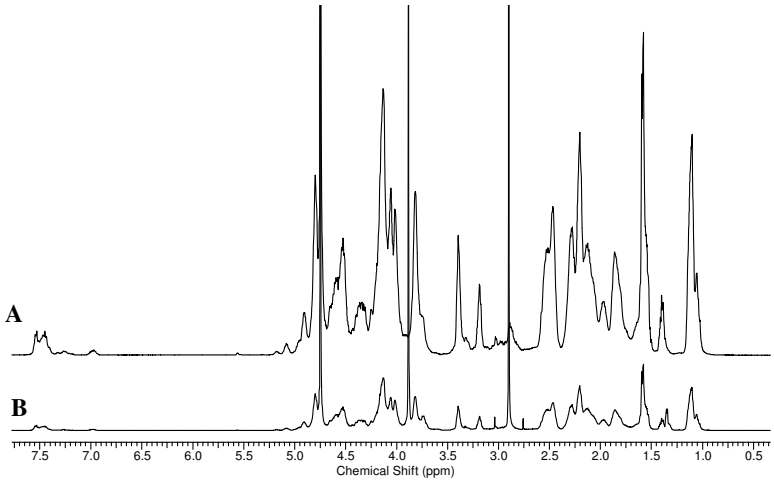

Figure 40. ^{1}H-NMR spectra of hydrogels in D_2O, **A:** pure Gelatin and **B:** GA200-*g*-PEPE34.

Table 11. Assignment of specific peaks in the ^{1}H-NMR spectrum of gelatin solution

Peak No.	Chemical Shift (ppm) of gelatin at 45 °C	Chemical Shift (ppm) of GA-*g*-PEPE at 45 °C	Assigned to different protons
1	1.06	1.04	Leucine, Valine, and Isoleucine
2	1.39	1.40	Threonine
3	--	1.34	-CH_3 of PPG
4	1.58	1.58	Alanine
5	1.86	1.86	Lysine and arginine
6	1.98	1.97	Lysine and arginine
7	2.89	2.90	Aspartic acid
8	3.18	3.19	Lysine
9	3.40	3.40	Arginine
10	--	3.74	-O-CH_2 of PEG
11	3.82	3.89	Proline
12	7.43-7.56 (m)	7.44-7.55 (m)	Tyrosine

Due to the chemical binding of PEPE:4NCP to –NH_2 group of lysine, mainly the protons of the carbon adjacent to amino group in lysine (-CH_2-NH_2) shows shift from 3.18 to 3.19 ppm. The appearance of peak at 1.34 ppm (-CH_3 of PPG), 3.74 ppm (-CH_2-O protons of PEG and PPG), and 3.82 ppm (-CH-O protons of PPG) indicate the presence of PEPE in the GA-*g*-PEPE hydrogel.

6.2.2 Thermo-mechanical properties

The GA-*g*-PEPE systems were characterized by DSC (TMDSC), TGA, and rheology to evaluate the thermo-mechanical properties. First, the DSC analysis was carried out in order to identify thermal transition in the GA-*g*-PEPE hydrogels in dry state (Figure 41). However, the PEPE is known to have a sharp T_m at around 58 °C, the thermal properties of gelatin were complicated. By using temperature modulated DSC (TMDSC) the glass transition of dry gelatin hydrogels was determined. The pure gelatin generally shows an endothermic peak mainly associated to helix-coil

transition, which mainly depend on the sample history (source, storage condition, etc.). For anhydrous solid gelatin the T_g = 217 ℃ and T_m = 230 ℃ and both values are strongly affected by the moisture content*. Here one main endothermic peak at 170-190 ℃ was observed which was seemed to be reduced due to moisture in the sample. But for GA-*g*-PEPE hydrogel samples, two peaks are observed, one peak at 50 ℃ is likely from the PEPE melting and another peak from 200 to 230 ℃ is mainly due to the melting of triple helices of gelatin.

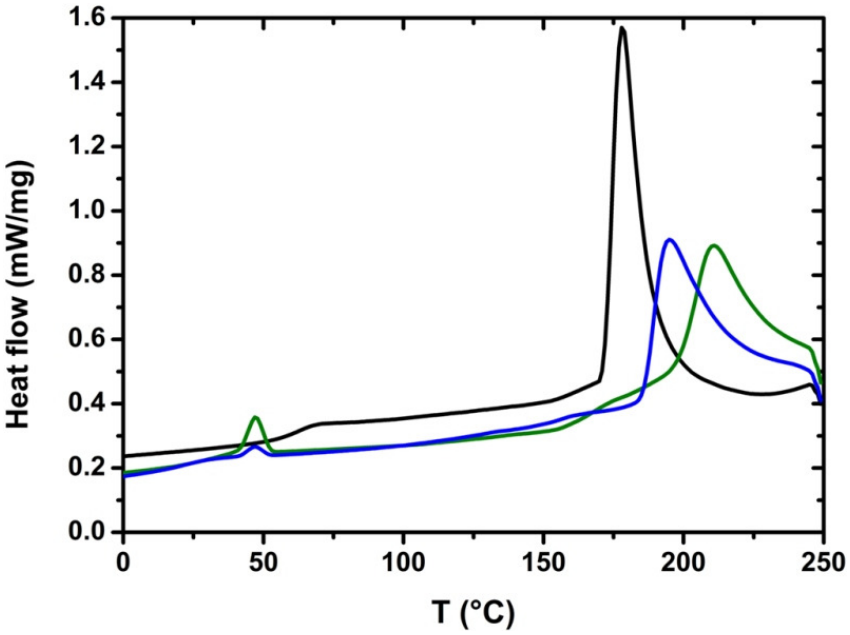

Figure 41. DSC spectra of GA200 (—), GA200-*g*-PEPE28 (—), and GA200-*g*-PEPE34 (—).

In addition, the TGA was performed on dry samples of GA-*g*-PEPE hydrogels in order to characterize the thermal properties of PEPE functionalized gelatin. TGA was performed in N_2 atmosphere (Figure 42). The TGA of pure gelatin shows three thermal degradation steps as, loss of moisture from 50-100 ℃, gelatin decomposition between 250-350 ℃, and finally combustion of remaining mass between 400-700 ℃. The GA-*g*-PEPE hydrogels also shows three step degradation at 80, 150-300, and 350-700 ℃. The former is attributed to moisture loss; mass loss at 150-300 ℃ can be related to the gelatin decomposition not as sharp as pure gelatin but, due to the

resistance created by grafted PEPE chains and the third mass loss from 350-700 ℃ is due to the combustion of gelatin and PEPE. In both GA-*g*-PEPE samples the degradation starts earlier then compare to pure gelatin, the reason could be the grafting of PEPE to gelatin restricts the gelatin chains to from triple helices and thus losing the strength of the network. Thus, it seems that GA-*g*-PEPE hydrogels required low energy to disintegrate the intermolecular and partial breaking of the molecular structure. From the figure 42, it seems that higher the PEPE content in the composition lower is the temperature required to show thermal degradation process. Hence, PEPE-grafting to gelatin reduced the formation of triple helices and therefore the thermal degradation of GA-*g*-PEPE hydrogels is occurred at low temperature (200 ℃) compared to pure gelatin (290 ℃).

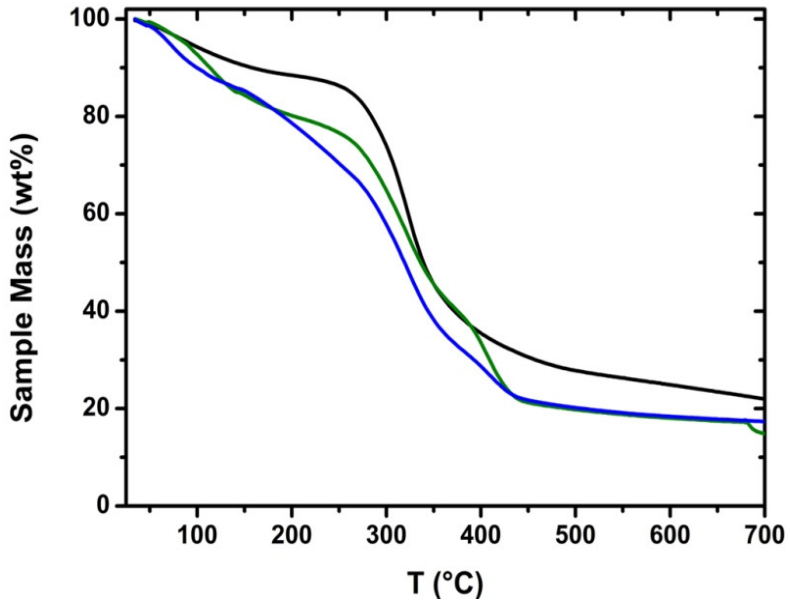

Figure 42. TGA spectra of GA200 (—), GA200-*g*-PEPE28 (—), and GA200-*g*-PEPE34 (—).

The WAXS analysis was carried out to elucidate the details of chain organization and inherent molecular organization of GA-*g*-PEPE hydrogels. Here, it was interesting to evaluate the effective suppression of formation of triple helices

which could change the physiochemical behavior of the system. As shown in figure 43 the WAXS spectra of three different gelatin bloom with grafted PEPE.

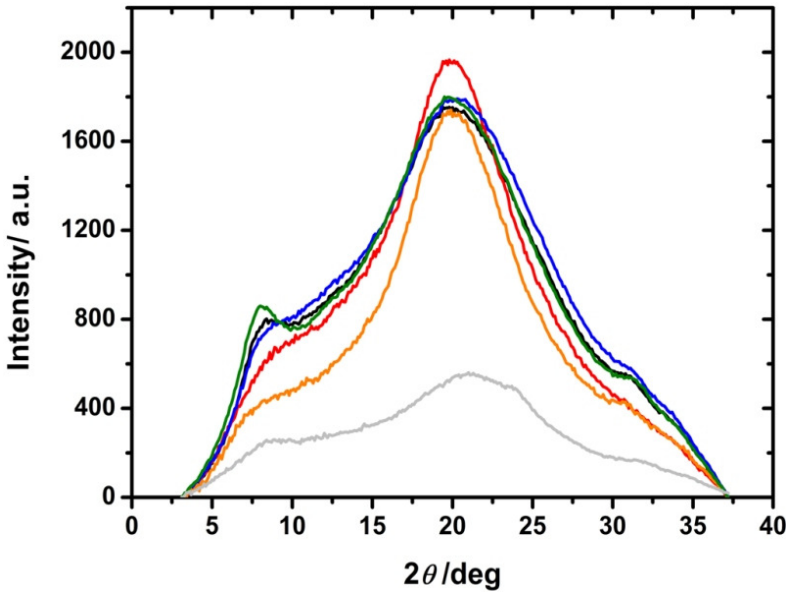

Figure 43. WAXS spectra of pure gelatin and GA-*g*-PEPE hydrogels. GA90 (—), GA90-*g*-PEPE (—), GA200 (—), GA200-*g*-PEPE (—), GA300 (—), and GA300-*g*-PEPE (—).

For all pure gelatin sample, the peak at 20° was related to the amorphous region was detected. The peak referring the triple helices (9°) and single helices (31°) show their strong presence in all pure gelatin samples. In case of GA-*g*-PEPE samples also have a strong amorphous peak at 20°, while the peak related to triple and single helices seem to be decreased compared to pure gelatin. It's likely that the grafted PEPE might be inhibiting the formation of triple helices as well as the helicalization of single strands. These results could support the investigation obtained from the TGA analysis that, the thermal degradation of GA-*g*-PEPE was started earlier than pure gelatin samples. Thus, the thermal analysis have shown not a significant effect on gelatin but allowed to change the behavior of thermal properties by grafting the PEPE segment.

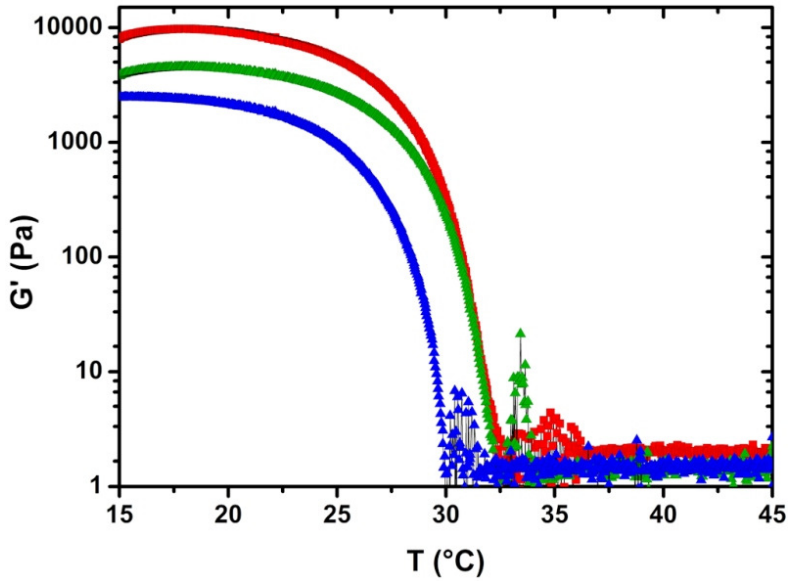

Figure 44. The temperature ramp of GA200 (■), GA200-*g*-PEPE30 (▲), and GA200-*g*-PEPE37 (▲). (concentration = 10 wt% each).

The thermo-mechanical properties of GA-*g*-PEPE hydrogels were investigated by the rheological measurements. The hydrogels were pre-dissolved in water and analysed by rheometer from 15-45 ℃ temperature ramp (figure 44). The hydrogels with different bloom of gelatin and different grafting density of PEPE have been analysed to see the effect of grafting PEPE on thermo-mechanical properties, especially the elastic modulus (G′). As shown in table 12, no significant difference was observed by changing the bloom value of gelatin on the gelation behavior except, gelatin with 300 bloom have shown higher T_{sw} compare to gelatin with 90 and 200 bloom. The interesting point here is, with increasing PEPE content in the gelatin hydrogels it seems that the mechanical properties of hydrogels (G′) found to be decreased. At 20 ℃ the elastic modulus (G′) of GA200 = 9270 Pa (±3%), which was reduced to 4338 Pa (±3%) by 30 mol% PEPE grafting which further brought down to 2145 Pa (±3%) by 37 mol% grafting of PEPE to gelatin. Moreover, the micelle formation by PEPE chains during the temperature ramp was not observed, which may be dominated by the gelatin chains. However, the PEPE show an influence on aggregation of gelatin

chains, which normally happened at lower temperature and causes the increase in mechanical properties. The switching temperature of the GA-g-PEEP hydrogels does not show a clear influence on the T_{sw} by varying the degree of functionalization of PEPE and bloom value of gelatin. This may happen due to the random functionalization of PEPE over the gelatin chains (as gelatin is in the random coil state in solution).

Table 12. Switching temperature of different GA-*g*-PEPE hydrogels

Sample. No.	Sample ID	D.F. of -NH_2 groups of Gelatin (mol%)	T_{sw} (℃)
1	GA(300)-*g*-PEPE	25	37
2	GA(200)-*g*-PEPE	24	31
3	GA(90-120)-*g*-PEPE	34	32

D.F = degree of functionalization

6.3 Synthesis of GA-*g*-PEPE T-ArcGel

The GA-*g*-PEPE T-ArcGels were synthesized by crosslinking the remaining -NH_2 groups of GA-*g*-PEPE hydrogel by ethyl ester of lysine diisocyanate (LDI) as a crosslinker. The LDI was chosen because it is known to results in a non-toxic lysine derivative degradation products[96]. The LDI is slightly soluble in water and PEPE itself act as a surfactant to incorporate the hydrophobic crosslinker. Thus, there was no need of an additional surfactant to formation and stabilization of foam. Generally, the GA-*g*-PEPE hydrogel was solubilized at 45 ℃ in water, after complete dissolution of hydrogel with the help of the mechanical stirrer the solution was stirred at high speed to obtain a stable foam (scheme 4). At last the LDI was added to crosslink the foam. After storing the foam at -20 ℃ overnight, it was washed water for 2 days by vigorously changing the surrounding water to remove the unreacted material and further lyophilized for 2 days. The dry foam were used to determine further properties.

Moreover, it is also important to know the reactivity of LDI as, it mainly reacts with nucleophilic groups of gelatin (mainly amino groups of lysine). However, it may reacts with other nucleophilic groups in gelatin such as, aromatic NH-groups (histidine), alcohols (serine, threonine and also in PEPE), phenols (tyrosine), thiols (cysteine), carboxylic acids and amide functional groups[97–99]. Generally, gelatin has approximately 3 mol % of amino groups[100] (lysine/hydroxylysine) which was also verified in the starting by using TNBS colorimetric assay. Generally, during the crosslinking, isocyanates group of LDI reacts with lysine ε-amino groups along two opposing gelatin chains. On the other hand, in aqueous condition, decarboxylation of ioscyanates may occur, which forms free amino groups that can react with other LDI molecules. Thus, the crosslinking reaction of LDI is quite complex and may have side reactions and may influence the properties of gelatin after crosslinking.

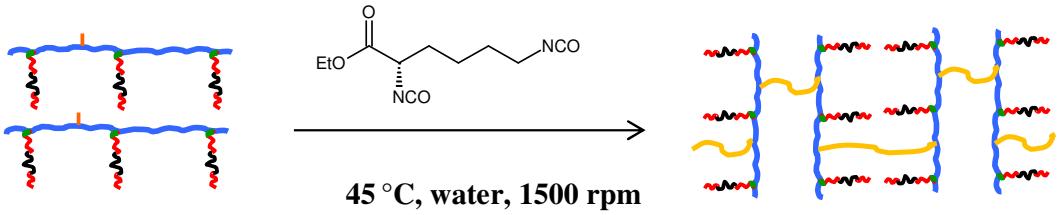

Scheme 4. Synthesis of GA-*g*-PEPE T-ArcGel

6.3.1 Investigation of water uptake by T-ArcGel

The GA-*g*-PEPE T-ArcGel of known weight were used to investigate the water uptake studies of these hydrogels. The incorporation of crosslinker with a rigid structure between gelatin chains may reduce the movements of individual chains and may results in a more rigid network with low degree of swelling. The water absorption capacity of these hydrogels was determined by gravimetrically and volumetrically by using following equation of water uptake (*H*),

$$H = \frac{W_s - W_d}{W_d} \qquad \text{(Equation 6.1)}$$

Generally in crosslinked hydrogels, with increasing crosslinking density have a tendency to show decreasing water uptake. But here, the influence of PEPE on water uptake capacity was investigated. The measurements were performed at two different temperatures as 25 ℃ to observe the effect of linear PEPE and at 37 ℃ to observe the effect of micellar PEPE on water uptake. As shown in figure 45, the water uptake of GA200-*g*-PEPE24 has lower water uptake at 37 ℃ and slightly higher water uptake at 25 ℃. At higher temperature (37 ℃), there may be micelle formation of PEPE and less mobility of gelatin chains (due to crosslinking) which could have reduced the capacity of hydrogel to absorb water.

Whereas, at lower temperature (25 ℃) PEPE do not have any micelles and thus the water uptake was slightly increased. But, when crosschecked with ArcGel without PEPE (grafted), the effect of temperature on water uptake was found to be similar. This may be due to the fact that, overall there are only 3 mol% amino groups (from lysine) and if out of that, 20-40 mol% are functionalized with PEPE, still the total amount of PEPE was very less compare to amount of gelatin in the T-ArcGel.

Thus, water uptake did not show a clear trend which could be influenced either by temperature or by grafting PEPE to gelatin. This may be due to the total amount of PEPE in the crosslinked system compare to amount of gelatin which may influence more on water uptake capacity of overall system.

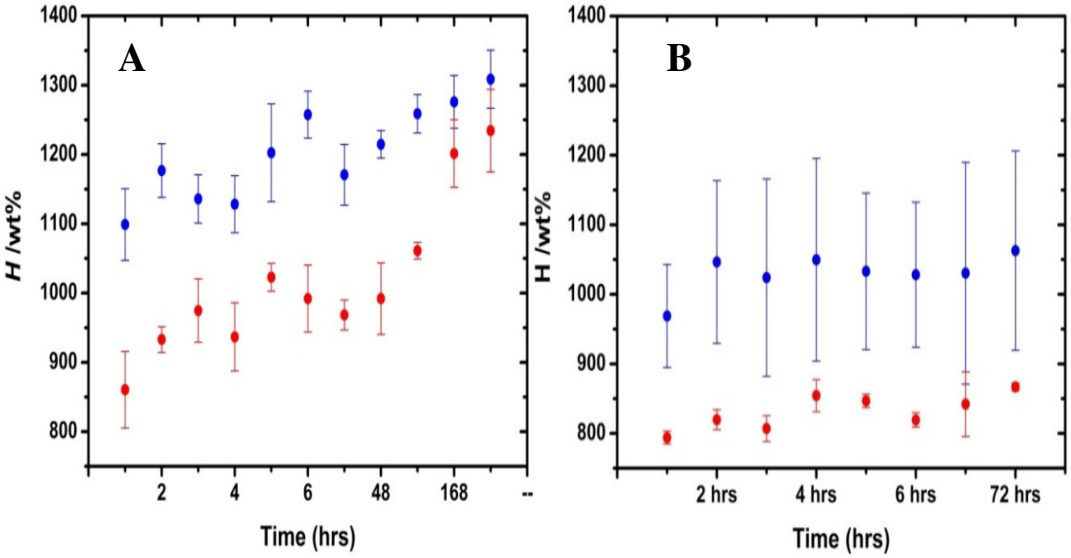

Figure 45. Water uptake (*H*) of, **A**. GA200-*g*-PEPE24 T-ArcGel and **B**. GA200 ArcGel at 25 and 37 ℃ (●: 25 ℃ and ●: 37 ℃).

6.3.2 Analysis of porous structure of GA-*g*-PEPE T-ArcGel

The porous structure was analysed by SEM and µCT measurements in the dry state, and gelatin of two different bloom (90-120 and 200) was used for the analysis. As shown in the figure 47, the SEM images at 50, 100, 500-fold magnification show the open porous structure of the T-ArcGel as well as the interconnectivity of the pores in the matrix which might be necessary for promoting cell proliferation and transport of nutrition. The pore size was calculated from both SEM and µCT measurements, the average pore size for GA200-*g*-PEPE24 T-ArcGel was 272 µm and 180 µm by µCT (Figure 46) and SEM analysis respectively (See Table 13). Generally, there was no effect of bloom on porosity of material was observed, but in case of the GA90-*g*-PEPE43 sample a large pore distribution was observed compared to GA200-*g*-PEPE24 sample. Moreover, the pore size remained unaffected by the PEPE grafting. Finally, the SEM and µCT analysis show a difference in the pore size, which might occurred due to the limitations of methods to analyse the pore distribution in the T-ArcGel.

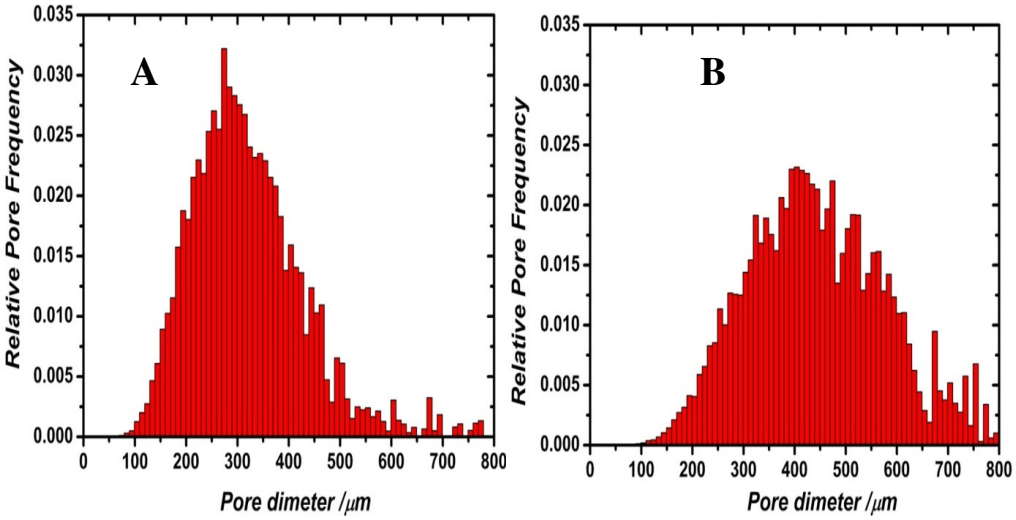

Figure 46. The µCT measurements of **A.** GA200-*g*-PEPE24 and **B.** GA90-*g*-PEPE43.

Table 13 The pore size for different T-ArcGel determined by µCT and SEM analysis

Sample name	Pore size (µm)	
	By µCT	By SEM
GA90-*g*-PEPE37	207 (± 5)	NC
GA200-*g*-PEPE24	272 (± 12)	180 (±71)
GA90-*g*-PEPE43	283 (± 10)	116 (±43)

NC: not calculated

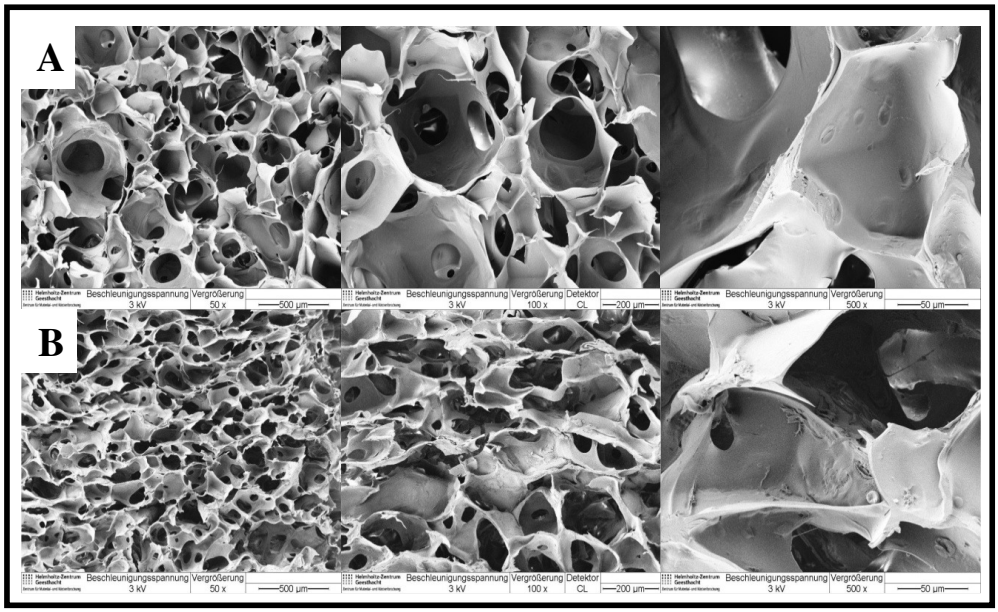

Figure 47. Porous morphology of T-ArcGel investigated by SEM. **A.** GA200-*g*-PEPE24 and **B.** GA90-*g*-PEPE43 at different magnification (at 50, 100, and 500x magnification levels)

6.3.3 Thermo-mechanical properties of T-ArcGel

DSC, TGA, rheology, and AFM analysis were performed on T-ArcGel in order to evaluate the thermo-mechanical properties. The DSC (TMDSC) and TGA were performed at dry state and rheology and AFM was performed in swollen state of the sample. As already discussed in section 6.2.2, the thermal properties of gelatin were complicated to evaluate and mainly depend upon the history of sample. Here, it was interesting to see the effect of crosslinking gelatin chains on thermo-mechanical properties of T-ArcGel.

The pure gelatin and GA-*g*-PEPE (figure 48 A and 48 B) shows a endothermic peak associated with the helix-coil transition in the temperature range of 180-230 ℃ and a peak at around 50 ℃ due to the melting of PEPE segment. But after crosslinking with LDI, the helix-coil transition disappeared, meaning the gelatin chains were majorly crosslinked by LDI and hence the mobility of the chains is blocked. However, in figure 48 A, peak at 50 ℃ indicate the melting of PEPE segment which is grafted to gelatin, which still have mobility to show the effect. There is decrease in the melting temperature of PEPE from 58 ℃ to 50 ℃, which is may be due to the crystal size and amount of PEPE in the system.

As previously explained in section 5.4.3, the T_m of PEPE was found to be decreased with decreasing PEPE content in the hydrogel. Moreover, TGA analysis of T-ArcGel was compare with pure gelatin and GA-*g*-PEPE hydrogel in a temperature range of 25-800 ℃ to evaluate the effect of crosslinking on the thermal stability of the system.

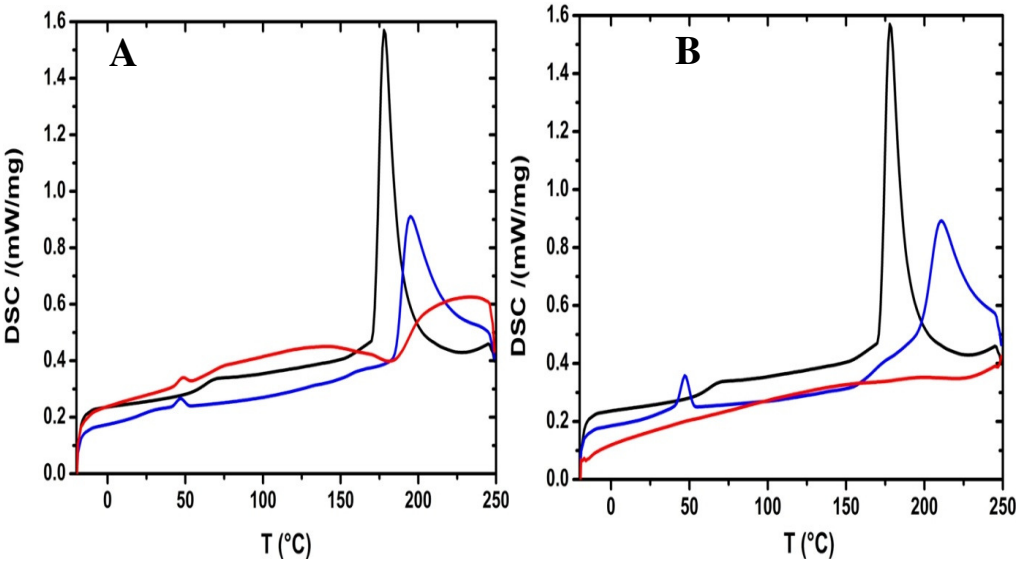

Figure 48. DSC spectra of, **A.** GA200 (—), GA200-*g*-PEPE34 (—), and GA200-*g*-PEPE34 ArcGel (—) and B. GA 00(—), GA200-*g*-PEPE28 (—), and GA200-*g*-PEPE28 T-ArcGel (—).

As discussed in section 6.2.2, the grafting reduces the formation of triple helix and the thermal degradation occurs at lower temperature compared to pure gelatin. But, further crosslinking of GA-*g*-PEPE hydrogel by LDI enhanced the thermal stability of hydrogel compared to the grafted system. As shown in figure 49, irrespective of the amount of PEPE in the hydrogel, the crosslinking has increased the rigidity in the hydrogel by fixing the gelatin chains which gave a similar trend as the triple helix formation in pure gelatin in case of thermal stability. Though the triple helices are formed due to physical crosslinking and the actual chemical crosslinking of GA-*g*-PEPE by LDI show similar behavior, which may be due to the grafted PEPE segment which creates soft segments in the system and showed dominance over gelatin chains after crosslinking by LDI.

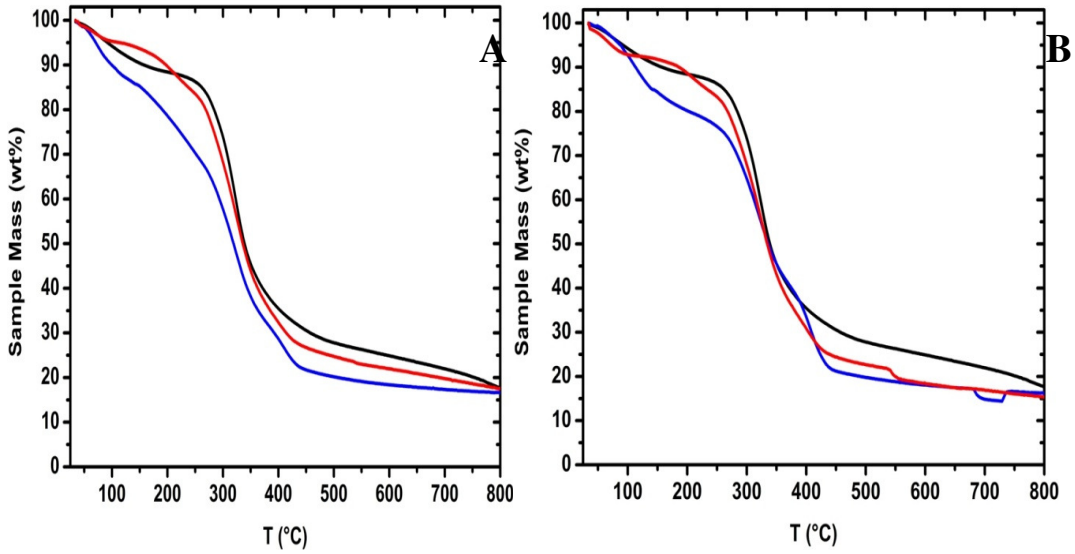

Figure 49. TGA analysis of, **A**. GA200 (—), GA200-*g*-PEPE34 (—), and GA200-*g*-PEPE34 ArcGel (—) and **B**. GA200 (—), GA200-*g*-PEPE28 (—), and GA200-*g*-PEPE28 T-ArcGel (—).

Thus, even chemically crosslinked GA-*g*-PEPE hydrogel have shown similar thermal behavior. The compression test of GA-*g*-PEPE T-ArcGel was performed in order to investigate the mechanical properties (compressive modulus (E_c) and compressive stress (σ_{max})) in dry and wet conditions. The initial shape of material was not recovered after 50% compression (Figure 50) due to compression of porous structure at dry state (and recovered the original shape after swelling in water). But, in dry state the mechanical properties of material was very high (Table 14). In case of wet compression, the material was equilibrated at 25 ℃ in water for 24 h before actual measurement. The shape of material was recovered even after 50% compression; the recovery of shape at 25 ℃ was possible due to the macroscopic elasticity of porous structure which may be related to the lowering in the T_g of gelatin in wet state which also reduced the mechanical properties in wet condition (Table 14).

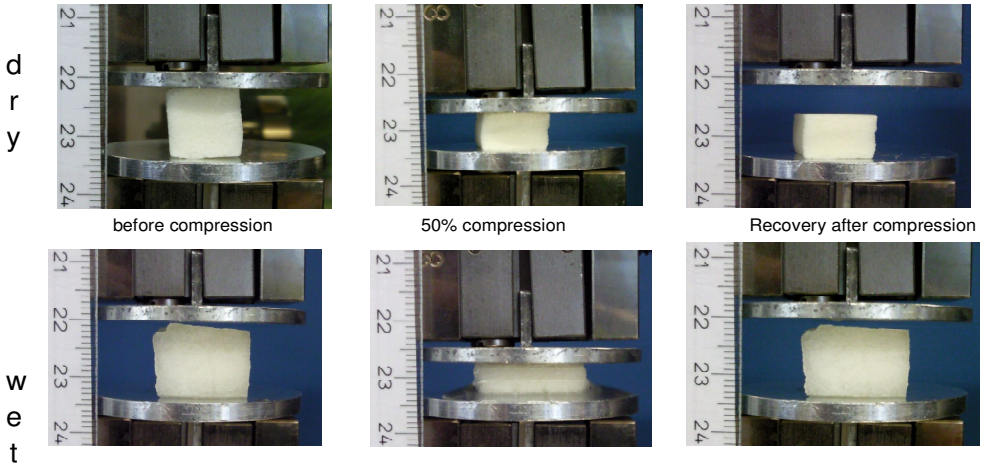

Figure 50. Compression of scaffold under dry and wet condition (at 25 ℃).

The thermo-mechanical properties of GA-*g*-PEPE T-ArcGel were determined by rheological measurements. The evaluation was performed under constant stress and temperature and frequency as a function for measuring changes in the elastic modulus (G′) and viscous modulus (G″). Gelatin ArcGel was used a control sample.

Table 14 The compression data for dry scaffold

Sample Name	Ec/kPa	σ_{max}/kPa
GA90-*g*-PEPE37	1440 (±110)	526 (±84)
GA200-*g*-PEPE24	1517 (±125)	381 (±28)
GA90-*g*-PEPE43	2323 (±139)	476 (±38)

Table 15 The compression data for wet scaffold at 25 ℃

Sample Name	Ec/kPa	σ_{max}/kPa
GA90-*g*-PEPE37	6 (±3)	4 (±2)
GA200-*g*-PEPE24	7 (±2)	4 (±2)
GA90-*g*-PEPE43	4 (±2)	3 (±2)

Where, K: compressive elastic modulus, σ_{max}: stress at 50% compression

As shown in figure 51, a 10wt% sample of pure gelatin was run through a temperature ramp measurement from 15 to 45 ℃. The G′ decreases from 25 to 45

℃ from 1100 to 850 Pa (±3%) and the G″ remains constant (100 Pa (±3%)) during the measurement, showing no thermosensitive effect.

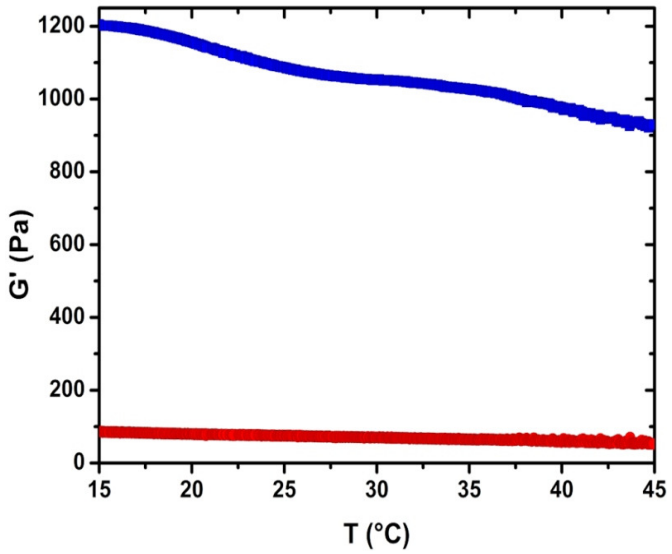

Figure 51. Mechanical properties of pure gelatin ArcGel as a function of temperature. G′ (■), G″ (●).

However, in GA-*g*-PEPE ArcGel, the T_{sw} was decreased from 37 to 32 ℃ due to grafting PEPE to gelatin; here the thermal gelation of PEPE was dominated by gelatin. So, here it was interesting to see the effect of fixing the mobility of gelatin chains (crosslinking with LDI) on thermo-mechanical properties of T-ArcGel.

Two samples of T-ArcGels with similar gelatin bloom (200) and different PEPE grafting density (28 and 34 mole %) were measured. As shown in the figure, the first interesting thing was these hydrogels have shown a reversible thermosensitive behavior i.e. increase in the mechanical properties upon heating and coming back to the initial mechanical properties upon cooling below T_{sw}, which strongly contradicts the normal gelatin behavior (gelatin chains in water form triple helix at room temperature which makes it solid and upon heating the solution above T_{sw}, from a solution due to disintegration of triple helix in to single helix). The fact here was, upon crosslinking the gelatin chain in solution state, it was possible to hinder the formation of triple helix upon and vice versa. So, by fixing the chain structure, it was possible to

suppress the gelatin behavior and thus allowing the grafted PEPE to demonstrate its effect of thermal gelation, which shows an enhancement in viscoelastic properties (G′, G″, and |η*|) upon heating above T_{sw}. The phenomenon could be explained by formation of micelles by grafted PEPE upon heating and deformation of micelles in chains upon cooling, thus having a reversible effect on viscoelastic properties. However the determination of micelle formation in such a system was a challenging task and may not be possible to detect due to the overall low concentration (28-34 mol%) of PEPE in the sample, which may limit the minimum concentration required to detect the micelle formation in the structured hydrogel. Nevertheless, it was shown before in the section 5.4.4 that, using lower concentration of PEPE (2.5-10 wt %) it show a thermo-sensitive behavior with enhancement in mechanical properties upon heating near body temperature (30-32 °C). However, for pure PEPE minimum concentration of 16 wt% is required to show the thermosensitve behavior.

Moreover, the amount of PEPE grafted to gelatin was having an influence on the mechanical properties as well as T_{sw} of T-ArcGel. As shown in figure 52, in the sample GA200-*g*-PEPE28 the observed T_{sw} was 42 °C with G′ above T_{sw} was in the range of 50,000-65,000 Pa (± 3%) and for the sample GA200-*g*-PEPE34 the observed T_{sw} was 37 °C with G′ above T_{sw} was in the range of 90,000-150,000 Pa (± 3%). This values gave an indication that may be due to increase in the PEPE content in the system, the number of micelle formation was increased which contributed in decreasing the T_{sw} and enhancing the mechanical properties of overall system. In addition, the viscous modulus (G″) was also increased from around 100-15,000 Pa (± 3%) in GA200-*g*-PEPE28 and from 50-30,000 Pa (± 3%) in GA200-*g*-PEPE34 respectively.

In addition, fully water swollen GA-*g*-PEPE T-ArcGel upon heating (up to 50 °C) or cooling (up to 5 °C) did not show any change in the physical structure, which was

contradictory to the previously stated polyNIPAM based crosslinked thermosensitive porous hydrogel, which have a large volume change (shrinking) when heated from 4 - 37 ℃ under swollen condition[71]. Moreover, the actual enhancement in the mechanical properties (elastic modulus G') was only 10 fold, whereas in the GA-*g*-PEPE it was 108 fold (GA200-*g*-PEPE28) and 170 fold (GA200-*g*-PEPE34) higher compare to initial values and thus providing a wide range of tunability in GA-*g*-PEPE T-ArcGel system. The swelling or shrinking of ArcGel may cause additional forces (during swelling) or may not fit properly in the defect (during shrinking) while using such materials as an implant. Thus, on demand changes in the mechanical properties without changing size of material could be an advantage.

These evaluation of GA-*g*-PEPE T-ArcGel shows a successful incorporation of thermosensitive functionality, which allow the rigid system to show an enhancement in the mechanical properties upon heating without any volume change, which was not shown by pure gelatin ArcGel under similar conditions.

In addition to the temperature dependent rheological measurements, temperature dependent force measurements were also performed to study the force applied by the material when deforming above the T_{sw}. For this study four T-ArcGel with 28 and 34 mole % PEPE content and two different crosslinking densities i.e. 3x and 8x of LDI were measured. As shown in figure 53A, GA200 crosslinked using 8X LDI was used as a control sample (without PEPE grafting) which show overall constant force during the given temperature range. This may be due to the fact that once the gelatin chains are crosslinked, the major deformation upon heating is blocked (i.e. triple helix ↔ single helix formation) and the mechanical properties of the material remains constant within the given range of temperature. These results also correlate with the rheological temperature ramp measurements which also show similar behavior. But, when the gelatin chains are grafted by PEPE (with different grafting densities) before

crosslinking with LDI, it has shown increasing mechanical properties upon heating the sample. Thus, it was interesting to crosscheck the property of the T-ArcGel by performing a compression test with temperature as a function. As shown in figure 53 B and 53 C, The T-ArcGel crosslinked by 3X and 8X LDI shown similar behavior as in temperature ramp. In addition, it was possible to detect the early stage of deformation changes and corresponding mechanical properties of the ArcGel. The T_{sw} show a slight shift to lower temperature range compare to the previous results by temperature ramp measurements. Moreover the T_{sw} was not affected by the amount of crosslinker (3x or 8x LDI) but, the amount of PEPE grafted to gelatin. Thus GA200-*g*-PEPE28_3x and GA200-*g*-PEPE28_8x showing a T_{sw} = 30 °C and GA200-*g*-PEPE34_3x and GA200-*g*-PEPE34_8x showing a T_{sw} = 27 °C approximately. Nevertheless, the sample crosslinked with 8x LDI show higher force of 0.28 - 0.45 N while sample crosslinked with 3x show 0.07- 0.3 N, indicating the initial strength of material depended on the amount of crosslinker used. Moreover, it was also seen that samples crosslinked with 3x LDI have wide range of deformation compared with highly crosslinked samples.

Thus, the compression measurement by rheology with temperature as function could also support the thermosensitive behavior of T-ArcGel by showing the increase in the value of force above the T_{sw}. The rheological measurements evaluated the bulk thermo-mechanical properties of GA-*g*-PEPE T-ArcGel, however it was also an interesting task to evaluate further the microscopic properties of such a system to demonstrate the thermally induced mechanical changes happening at micro level. Thus, a method which accurately characterize the local mechanical properties of porous material is required. Hence, atomic force microscopy (AFM) technique was used to evaluate the local mechanical properties of T-ArcGel.

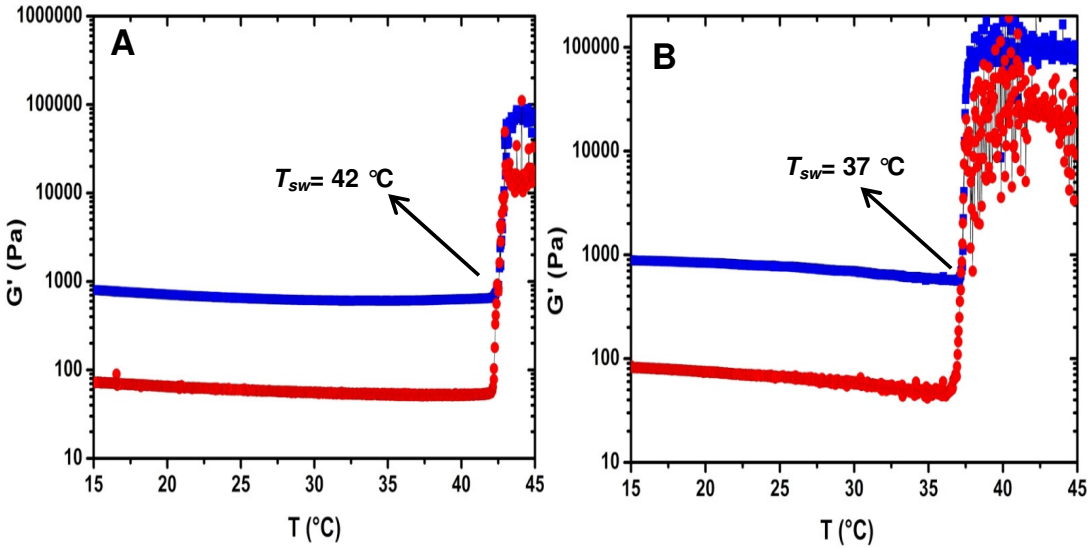

Figure 52. Mechanical properties of GA-*g*-PEPE T-ArcGel as a function of temperature, **A.** GA200-*g*-PEPE28 and **B.** GA200-*g*-PEPE34. Where, G′ (■),G″ (●).

As the mechanical properties of porous material mainly depends upon the bulk properties as well as geometry and porosity of the T-ArcGel, the evaluation of local mechanical properties of such complex system was not easy. The AFM measurements were mainly performed on the single pore walls of swollen T-ArcGel at two different temperatures (25 °C and 37 °C) one below the T_{sw} and other above the T_{sw} (The AFM measurements were performed by Oliver Frank). The isolation of single pore wall under swollen condition was a difficult job and previously measured (section 6.3.3, page 104) compression under swollen condition gave very low compressive moduli (E_c = 4-8 kPa) which make the AFM measurement extremely challenging.

The AFM results in the figure 54 and 55 show variation of data compared to the rheological measurements, which is probably due to the difference between areas of measurement and may be due to the technical limitation of the method. Taking this into account, the Young's moduli are compared between the samples with high and low crosslinker (LDI) and temperature (25 and 37 °C). The overall results show that

in the sample GA200-*g*-PEPE28_3x at both temperatures the local E moduli are in the same range. But, in case of GA200-*g*-PEPE28_8x sample the local E moduli at 25 °C was in the range of 5-10 kPa which further increased to 25-35 kPa at 37 °C. The reason to have increase in mechanical properties might be influenced by two factors, the higher concentration of crosslinker (8x LDI) and temperature. On the other hand, changing the PEPE grafting also demonstrate similar behavior for the T-ArcGel crosslinked by 3x and 8x LDI as, there was no significant difference in the *E* at 25 and 37 °C for GA200-*g*-PEPE34_3x samples whereas, in case of same composition with 8X LDI content show a dramatic increase in the *E* from 10 to 30 kPa (average values).

The results obtained from AFM measurements show that there might be an increase in Young's moduli (*E*) due to the amount of crosslinker or the PEPE content in the porous material. But, the values of *E* for all sample containing 3x LDI (irrespective of amount of PEPE) remained unchanged even after at higher temperature. Nevertheless, the *E* values for all sample with 8X LDI was shifted to higher values upon heating to 37 °C.

The overall results obtained by AFM for the local mechanical properties of T-ArcGel showed a change in the mechanical properties however, may not be as convincing as the bulk mechanical properties obtained from rheology hence, defining local mechanical properties of a porous material was crucial compare to the bulk mechanical properties.

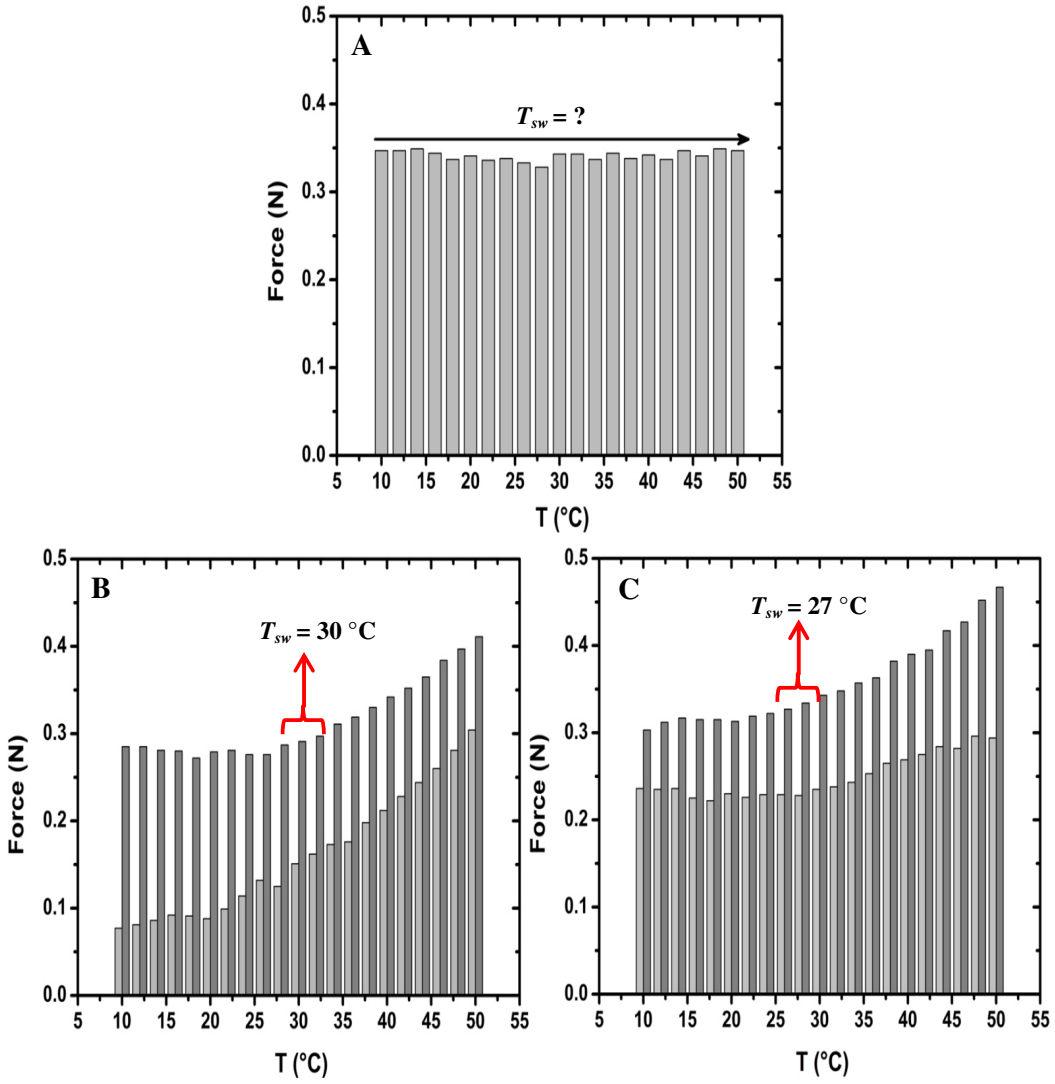

Figure 53. Measurement of force as a function of temperature by rheology. A. GA200_8x (■). B. GA200-*g*-EPE28_3X (■) and GA200-*g*-PEPE28_8X (■). C. GA200-*g*-PEPE34_3X (■) and GA200-*g*-PEPE34_8X (■).

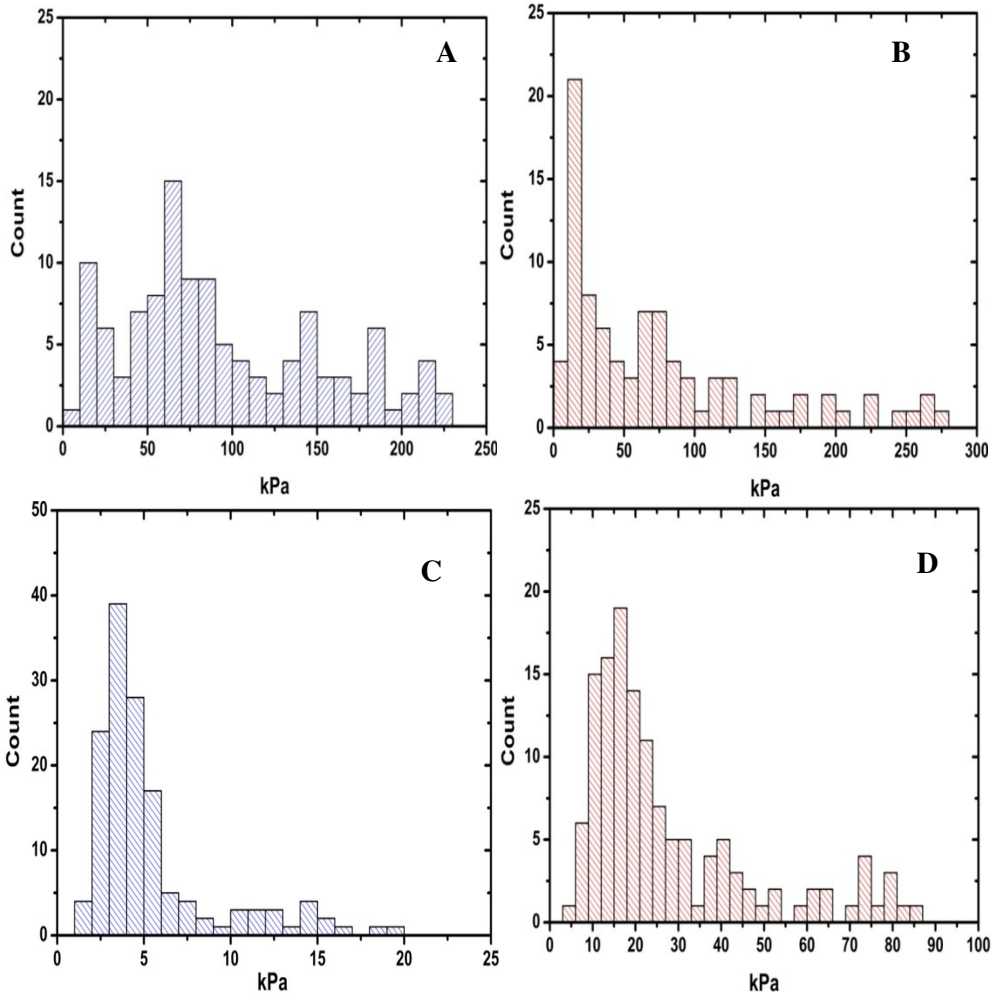

Figure 54. Mechanical properties of T-ArcGel in wet condition, Young's modulus *E* determined by AFM by varying the temperature and LDI content. **A.** GA200-*g*-PEPE28_3X_25 ℃ (≡), **B.** GA200-*g*-PEPE28_3X_37 ℃ (≡), **C**. GA200-*g*-PEPE28_8X_25 ℃ (≡), **D**. GA200-*g*-PEPE28_8X_37 ℃ (≡).

Furthermore, shape-memory experiments were conducted with GA-*g*-PEPE T-ArcGel samples to utilise the effect of thermo-reversible enhancement of mechanical properties, e.g. elastic modulus (G′), which was induced by grafting PEPE to gelatin and further crosslinking of gelatin to fix the structure of hydrogel, which retrieve the effect from grafted PEPE (Figure 56). Following set of experiments were conducted,

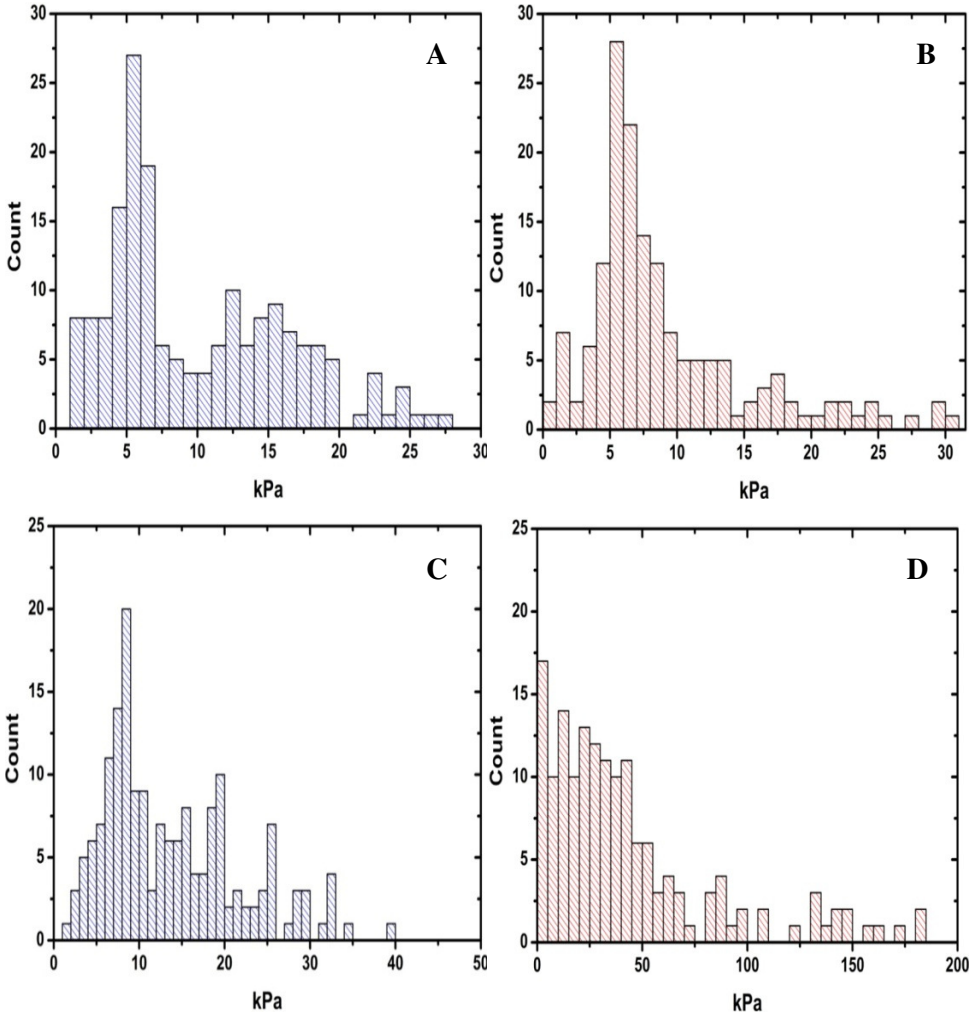

Figure 55. Mechanical properties of T-ArcGel in wet condition, Young's modulus *E* determined by AFM by varying the temperature and LDI content. **A**. GA200-*g*-PEPE34_3X_25 ℃ (≡), **B**. GA200-*g*-PEPE34_3X_37 ℃ (≡), **C**. GA200-*g*-PEPE34_8X_25 ℃ (≡), **D**. GA200-*g*-PEPE34_8X_37 ℃ (≡).

Experiment 1: Sample was equilibrated at 25 ℃ and compressed at 25 ℃. The compressed sample was then equilibrated at 50 ℃. When stress was released, the sample swelled. (The temporary compressed shape is not fixed at 50 ℃, although micellization occurred and the mechanical properties increased).

Experiment 2: Sample was equilibrated at 25 ℃, placed in 50 ℃ water for 5 min and compressed. The compressed sample was then equilibrated in 25 ℃ water. When stressed is released, the sample is fixed, but only for ~1h. This was in contrast

to non-grafted systems, however, which immediately recovered when the compression stress was released.

Experiment 1:

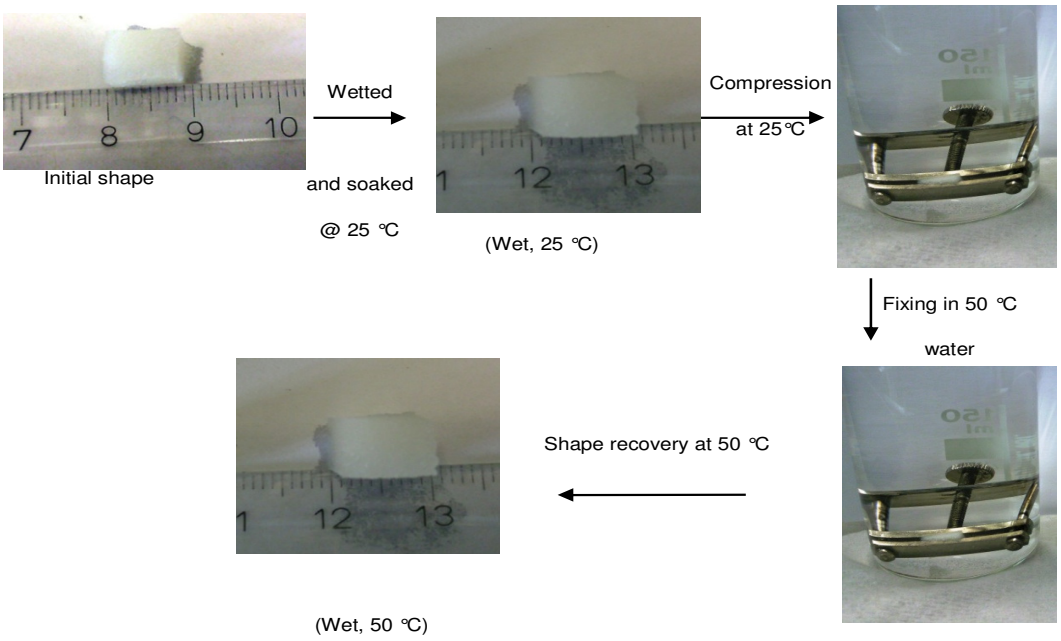

Experiment 2:

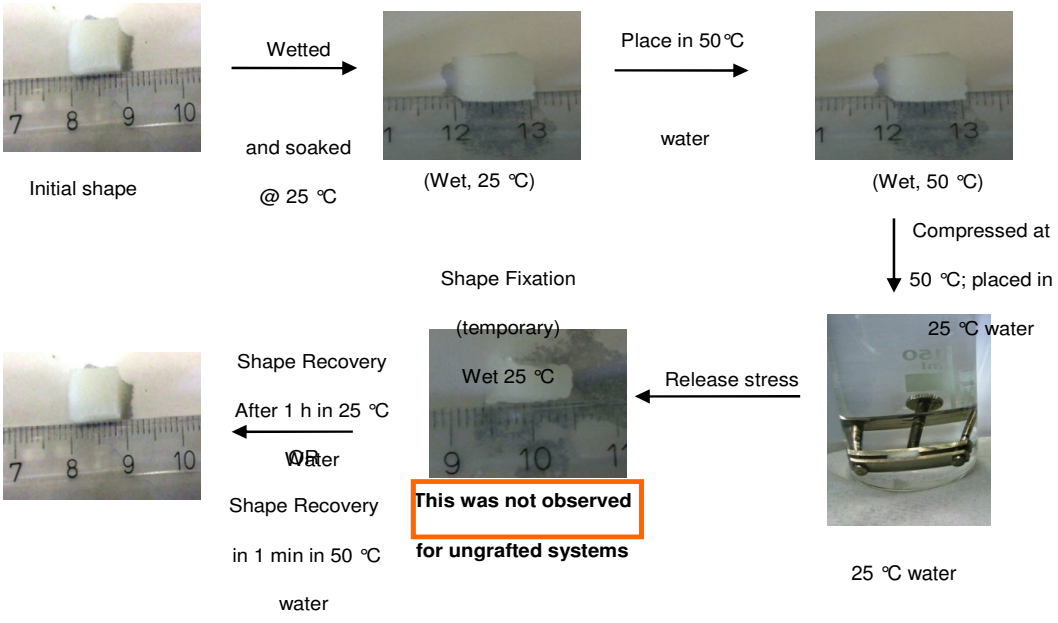

Figure 56. GA-*g*-PEPE T-ArcGel reversible shape memory experiment.

Experiment 3: Sample was equilibrated at 25 °C and compressed at 25 °C. When stress is released, the sample recovered after 1 hr.

Crosslinked GA-*g*-PEPE T-ArcGel did not show inverse shape-memory effect (Experiment 1). However, a shape could temporarily (time = 1 h) be fixed at 25 °C when deformed at 50 °C, which was not possible for only gelatin systems (Experiment 2). This temporary shape could only be realized by fixing at 50 °C and cooling to 25 °C (Experiment 3). The temporary fixation may be due to the micelle-linear chain transition of the PEPE chains, which may cause an increase in entropy of the system. Hence, the desire inverse shape memory effect was not observed in GA-*g*-PEPE T-ArcGel though, the material was possible to fix the temporary shape which was not seen in pure gelatin ArcGel.

6.4 Hydrolytic degradation of T-ArcGel

The GA-*g*-PEPE T-ArcGel were also studied by the hydrolytic degradation process. For any material with future *in vivo* application, it could be very important that the material is degradable either by hydrolytic or enzymatic process. Here the hydrolytic degradation of GA-*g*-PEPE T-ArcGel with different gelatin bloom and PEPE content was investigated at 25 and 37 °C. As these porous materials are based on chemically crosslinked gelatin, the hydrolytic cleavage of gelatin backbone could occur. But, compared to pure gelatin, PEPE grafted to gelatin could influence the degradation behavior. As, PEPE is known to form micelles at higher temperature, at this temperature it may influence the water uptake by the T-ArcGel and hence slower the rate of degradation of the material.

As shown in figure 57, GA200-*g*-PEPE24 and GA90-*g*-PEPE37 were tested for hydrolytic degradation over the period of 8 weeks. Both samples show higher degradation at 25 ℃ in case of total mass loss at different time-point. The reason might be, at 25 ℃ the gelatin and GA-*g*-PEPE ArcGel were found to have more water uptake then at 37 ℃. Thus, the higher water content in the sample may trigger the hydrolytic degradation process faster. It is also to be noted that at 25 ℃ the PEPE is not in the form of micelles thus, more water is regulated through the pores of the T-ArcGel leading the higher degradation rate and mass loss.

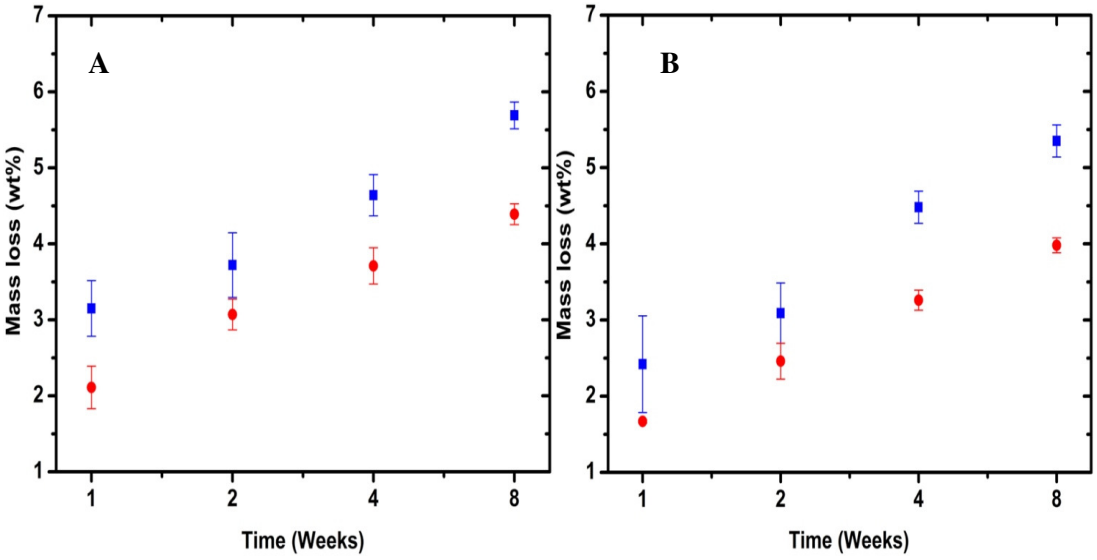

Figure 57. The mass loss during the hydrolytic degradation of GA-*g*-PEPE T-ArcGel in PBS (7.4 pH). A. GA200-*g*-PEPE24 (25 ℃ =■ and 37 ℃ = ●) and B. GA90-*g*-PEPE37 (25 ℃ =■ and 37 ℃ = ●).

In contrast, at 37 ℃ the PEPE form micelles, this could prevent the diffusion of water in to the porous matrix. Hence by controlling the water diffusion the hydrolytic degradation of the T-ArcGel could be controlled. Moreover, no significant difference was observed in degradation of different bloom of gelatin so, the degradation controlling factor could be the PEPE. However, the grafting density of PEPE in GA-*g*-EPEP T-ArcGel does not show influence on the degradation behavior and hence showing similar rate of degradation in both cases (figure 58). Moreover

the SEM investigation showed that there was no significant difference in the morphology of samples before and after degradation (Figure 59).

The ArcGel without PEPE have shown dramatic mass loss up to 80-90 wt% in 5-6 weeks' time and as previously reported[71], thermosensitive T-ArcGel of polyNIPAM show a mass loss of 60 wt% at 25 C within 30 h. and around 30 wt% within 10 h in alkaline solution of 0.7mmol NaOH.

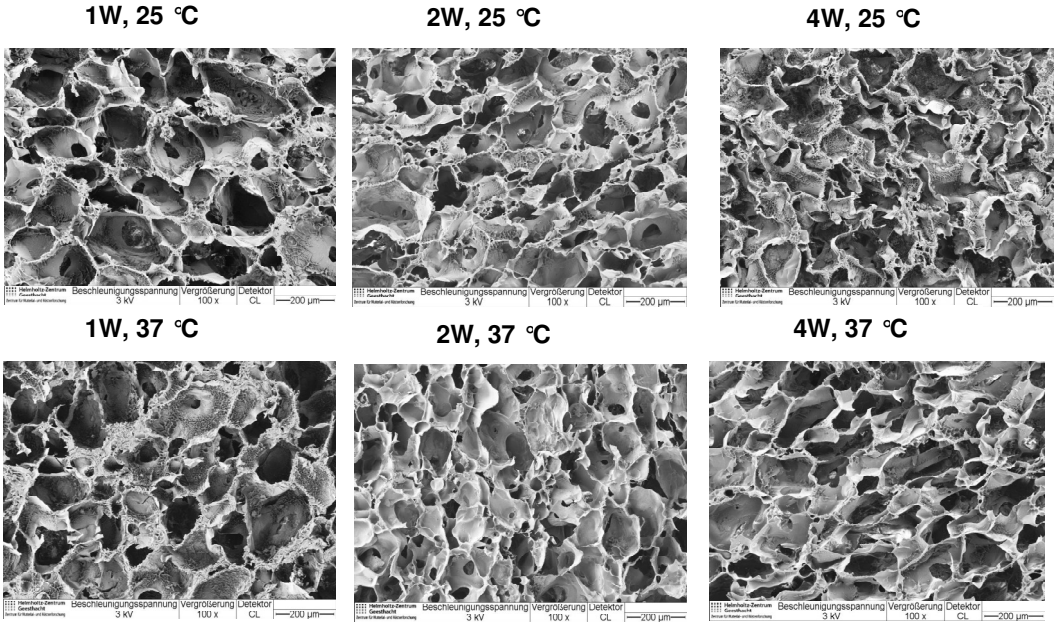

Figure 58. SEM morphology of degradation studies of GA90-*g*-PEPE37 T-ArcGel at, **A.** 25 ℃ and **B.** 37 ℃.

However, the GA-*g*-PEEP T-ArcGel shows a maximum mass loss of around 6 wt% in 8 weeks. Thus, by grafting PEPE to gelatin not only the thermosensitivity but also controlled degradability was induced in the ArcGel.

The grafting of PEPE to gelatin chain resulted as an additional parameter, which could control the water uptake of the system by formation and deformation of PEPE micelles depending upon the temperature of the environment. Thus, the structural

changes in such system show a better control over the water uptake, degradation and importantly, the temperature dependent tunability of viscoelastic properties.

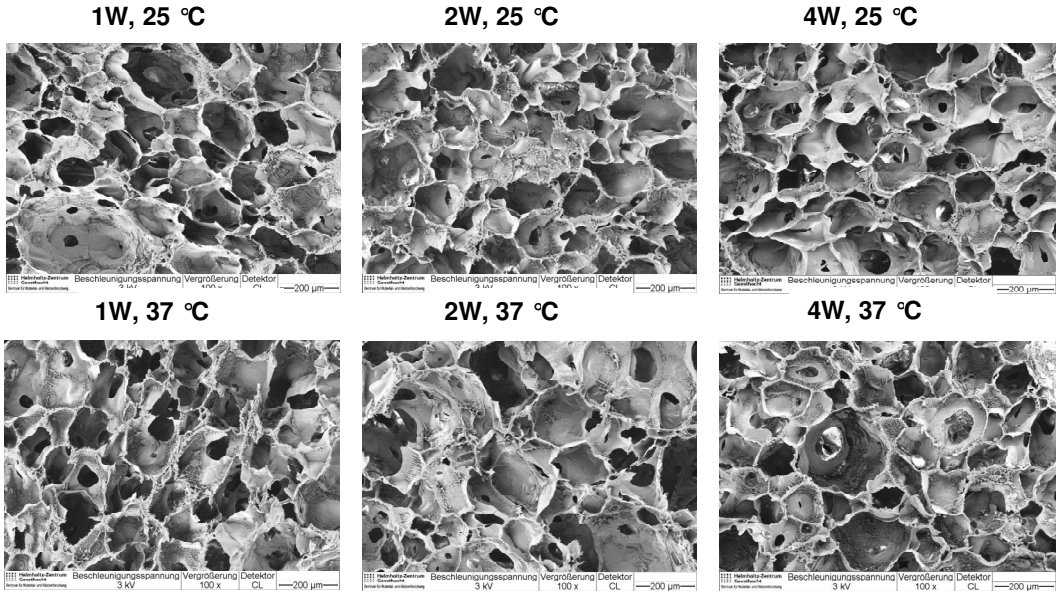

Figure 59. SEM morphology of degradation studies of GA200-*g*-PEPE24 T-ArcGel at, **A.** 25 °C and **B.** 37 °C.

6.5 Summary

A gelatin based T-ArcGel system with tunable mechanical properties was successfully synthesized and characterized. The thermosensitivity was successfully introduced in the rigid porous system by grafting PEPE to gelatin before covalent crosslinking by LDI. The thermo-mechanical properties before grafting was dominated by gelatin which normally became sol at higher temperature (> 37 °C) but slightly shifted the T_{sw} after PEPE grafting. But even at this stage, the triple helix formation of gelatin was affected by PEPE which was shown by WAXS analysis. Further, the thermosensitivity of the system was realized only after covalent crosslinking of gelatin by LDI and further the T_{sw} was tunable by the amount of PEPE grafting to the gelatin. Moreover, the grafting density of PEPE was an important factor in the water uptake and hydrolytic degradation of T-ArcGel. As with

incorporation of PEPE in the rigid structure controlled the diffusion of water at higher temperature by formation of micelles and hence gave longer stability compare to pure gelatin porous material. Thus porous, thermosensitive, tunable mechanical and degradation properties made this system a promising material for future investigation as an biomaterial.

7. Summary and Outlook

Biopolymer based thermosensitive hydrogels with tunable thermo-mechanical properties were prepared by either physical or covalent coupling. In the first part, mono and di-amine PEPE were synthesized by controlling the mole ratio of reactants to have predominately the mono or di-PEPE (even though the final product was having small amount of unreacted PEPE, mono/di-PEPE, which was unable to remove from the product). The amine functionalization of PEPE has slightly influenced the thermo-mechanical properties. A shift in T_m (from 62 to 58 °C) and a decrease in T_{gel} (36 to 30 °C) were determined. Furthermore, these aminated PEPEs were used in physical mixing as well as covalent coupling with polysaccharides.

The hydrogels obtained by physical mixing of hyaluronic acid with amine terminated PEPE showed an enhancement of shear viscosity and also form a transparent gel near body temperature. The ionic interaction between amino groups of PEPE (especially di-PEPE) and carboxylic group of HA show an increase in mechanical properties (elastic modulus; G′, viscosity, and T_{gel}) and lower T_{gel} compared to the mono-PEPE and non-functionalized PEPE hydrogels of same concentration. Moreover, it was possible to tune T_{gel} of these hydrogels by varying the amount of PEPE in the composition. The overall mechanical properties of these hydrogels were observed to be not largely affected by varying the molecular weight of HA. In addition, the gelation mechanism of these hydrogels was determined by SAXS and the micelles were directly visualised by performing Cryo-TEM analysis (average micelle size = 20-30 nm), which gave an additional understanding of the system by knowing the gelation mechanism.

In addition, HA·di-PEPE hydrogels were demonstrated to closely fit the required properties such as, pH (7.1-7.3), optical transparency of >90% at 37 °C (in gel state) and at wavelength of 430-800 nm, a refractive index of 1.358, injectability through a 27G needle, steam sterilizability for a potential application as vitreous body substitute. The cytotoxicity studies (direct cell test) show that these hydrogels are slightly toxic but in vitro studies with mouse fibroblast cells show a promising biocompatibility of the hydrogel. Thus the physical mixing strategy was not only used successfully in these hydrogels but also investigated in detail to understand the physical interactions and thermo-mechanical properties of these thermosensitive hydrogels.

The covalent coupling of the thermosensitive unit PEPE to HA leads to materials, which show an increase in the viscoelastic modulus at much lower concentrations compared to the physical mixtures. This increase was achieved by an efficient covalent coupling of amine terminated PEPE to HA to form a thermosensitive hybrid. DMTMM showed to be a much more effective coupling agent than EDC. Purification by ultrafiltration was necessary to remove unreacted PEPE quantitatively from the final hydrogel. In contrast to physical mixtures of the same components, all synthesized compounds were in the gel state already in low concentration at room temperature, which is likely due to a small degree of crosslinking. The covalent coupling of HA and amine terminated PEPE was shown by FT-IR, and TGA was a suitable method for the determination of the composition of HA and PEPE in the system. The covalently coupled hydrogels showed enhanced mechanical properties when heated near body temperature (37 °C), with the mechanical properties (elastic modulus; G′) being tailorable by the covalent coupling strategy, PEPE content, concentration of the hydrogel, and the degree of functionalization. Interestingly, the thermosensitive behavior could be demonstrated even at a very low concentration of

these hydrogels in water (2.5-10 wt%), in contrast to physical mixtures of the same components, which need a concentration of more than 16 wt%. Thus, covalent coupling of amine terminated PEPE to HA with DMTMM provides a sufficiently high local concentration of PEPE segments, which show thermosensitivity near body temperature. These tunable and reversible mechanical properties (e.g. elastic modulus; G′) make the hydrogels as a potential candidate for drug release systems due to the expected control on the rate of diffusion.

Finally, a gelatin based T-ArcGel system with tunable viscoelastic properties was successfully synthesized and characterized. The thermosensitivity was successfully introduced in the porous system by grafting PEPE to gelatin before covalent crosslinking by LDI. The thermo-mechanical properties before grafting was dominated by gelatin, which normally became a sol at higher temperature (> 37 °C) but slightly shifted the T_{sw} after PEPE grafting. But even at this stage, the triplex helix formation of gelatin was affected by PEPE, which was shown by WAXS analysis. Furthermore, the thermosensitivity of the system was realized only after covalent crosslinking of gelatin by LDI and further the T_{sw} was tunable by the amount of PEPE grafting to the gelatin. Moreover, the grafting density of PEPE was an important factor in the water uptake and hydrolytic degradation of T-ArcGel. As with incorporation of PEPE in the rigid structure controlled the diffusion of water at higher temperature by formation of micelles and hence gave longer stability compare to pure gelatin porous material.

The thermosensitive hydrogels were synthesized by using three different approaches, which can show the thermosensitive effect by physically mixing of aminated PEPE with 1. polysaccharide (HA), 2. covalent coupling with Pectin and chondroitin sulphate (using EDC method) and covalent coupling with HA (using DMTMM) and 3. covalent coupling with gelatin and further crosslinking with LDI to

obtain a 3D T-ArcGel. In all different polymer architectures, the thermosensitive effect was observed via enhancement in the mechanical properties especially in the elastic modulus (G′), T_{sw}, and viscosity, when the samples were heated near body temperature.

8. Materials and Methods

Materials: Pectin (from citrus peel, galacturonic acid content ≥ 74.0 wt%, methoxy content 6.7 mol%, molecular weight 60,000 - 90,000 g/mol, *N*-(3-Dimethylaminopropyl)-*N'*-ethylcarbodiimide hydrochloride (EDC· HCl), Poly(ethylene glycol)-*block*-poly(propylene glycol)-*block*-poly(ethylene glycol) (PEPE) average M_n ~14,600 g/mol (ca. $PEO_{132}PPO_{50}$-PEO_{132}), 4-Nitrophenyl chloroformate (4NCP, 96%), 1,3-Diaminopropane (DAP) (> 99%), Hexane (≥ 95%), Dichloromethane (DCM, ≥ 99.5%), 1,3-Diphenyl-1,3,5-hexatriene(DPH) (98%), 2,4,6-trinitro-benzensulfonic acid (TNBS), and dimethylsulfoxide (DMSO). All chemicals were purchased from Sigma Aldrich (Schnelldorf, Germany) and all the reagents and solvents were of analytical grade and were used without further purification

8.1 ATR-FTIR analysis

ATR-FTIR measurements were performed by using [Bruker Optics Alpha-P (Ettlingen, Germany) and Shimadzu FTIR-8400S (Duisburg, Germany)] in the range 400 - 4000 cm^{-1}. The samples were dried under vacuum to remove residual moisture prior to measurement.

8.2 Nuclear Magnetic Resonance (NMR) spectroscopy

Nuclear Magnetic Resonance spectra were recorded on a NMR Bruker system (DRX 500 Avance, Bruker Biospin GmbH, Rheinstetten, Germany) and analyzed with Topspin (version 1.3). D_2O or $CDCl_3$ was used as a solvent for the dissolution of samples.

8.3 Wide-angle X-ray Scattering

WAXS measurements were carried out using the X-ray diffractometer Bruker D8 Discover with a two dimensional detector (HIStar) operating in 1024*1024 pixel

mode. The X-ray generator was operated at a voltage of 40kV and a current of 20 mA. A copper anode and a graphite monochromator produced Cu Kα radiation with a wavelength (*λ)* of 0.154 nm. WAXS images were collected from all samples in transmission geometry with a collimator-opening of 0.8 mm at a sample-to-detector distance of 15 cm. The exposure time employed was 600 s. Integration of the two-dimensional scattering data gave the intensity as a function of the scattering angle 2*θ*. A beam stop was placed immediately after the sample to avoid air scattering. Two procedures were tested for the extraction of the individual peak areas. A peak fitting program (TOPAS, from Bruker) inserted peaks at the desired positions and fit them to the total scattering curve, and then the peak areas were calculated. A second method consisted of cutting the helix-peaks from the curve and fit the residual data points with a spline function (leading in the pure amorphous scattering), after subtraction from the total scattering, the helix-peaks were obtained and the areas were calculated by integration.

8.4 Small-angle X-ray Scattering

SAXS measurements were performed using a Bruker AXS Nanostar diffractometer equipped with a two dimensional VANTEC-2000 detector (68 µm pixel size) at a wavelength of 0.154 nm. The distance sample to detector was 1070 mm, the beam size 400 µm. The minimum *s* value determined by the beam stop was *s* = 0.015 nm^{-1} and the maximum resolution in real space was 65 nm. In addition SAXS data with short exposure times were recorded at the µSpot beam line at BESSYII (Berlin, Germany) with a sample to detector distance of 810 mm and 0.15418 nm wavelength on a MAR-CCD detector (73.242 µm pixel size). Machine background weighted by the absorption factor was subtracted from the raw data. Invalid pixels (e.g. beam stop) were masked.

8.5 Cryo-TEM analysis

For Cryo-TEM analysis, aqueous polymer solutions with a concentration of 15 wt% are used. Droplets of the sample solution (5 µL) were applied to perforated (1µm hole diameter) carbon film covered 200 mesh grids (R1/4batch of Quantifoil Micro

Tools GmbH, Jena, Germany), which had been hydrophilized prior to use by a 60 s plasma treatment at 8 W in a BALTEC MED 020 (Leica Micro-systems, Wetzlar, Germany) device. The supernatant fluid was removed with a filter paper until an ultra-thin layer (100 – 200 nm) was obtained spanning the holes of the carbon film. The samples were immediately vitrified by propelling the grids into liquid ethane (-190 °C) operating a guillotine-like plunging device. The vitrified samples were transferred under liquid nitrogen into a Tecnai F20 FEG transmission electron microscope (FEI Company, Oregon, USA) using the Gatan (Gatan Inc., California, USA) cryo-holder and -stage (Model 626). Microscopy was carried out at -180 °C sample temperature using the microscopes low dose protocol at a calibrated primary magnification of 62,000x and an accelerating voltage of 160 kV (FEG-illumination). Images were recorded using an EAGLE 2k-CCD de-vice (FEI Company, Oregon, USA) at 2048 by 2048 pixel size.

8.6 Thermo-mechanical Tests

Rheological behavior was investigated with a stress controlled rheometer MARS (Thermo Haake, Germany) in parallel plate-plate geometry (20 mm), equipped with a solvent trap to minimize solvent evaporation. Preliminary stress-sweep experiments were carried out to determine the linear viscoelastic range. All experiments were performed in oscillation mode at 3 Hz by applying a constant stress of 3 Pa in a frequency range from 0.1-100 Hz. The temperature was varied from 0 to 45 °C during the temperature ramp measurements of hydrogels.

8.7 Temperature modulated DSC (TMDSC)

The thermal properties of gelatin films were measured using a Phönix DSC 204 F1 (Netzsch) apparatus. Dry gelatin-network samples were sealed in a hermetic pan during TM-DSC measurements. Two consecutive heating runs from -20 to 150 °C in the first heating run and up to 250 °C in the second heating run were performed with a modulated heating rate with a period of 60 s, amplitude of 0.5 °C, and a heating rate of 5 °C·min^{-1}. Between heating runs, the samples were quickly cooled at a rate of 10 °C·min^{-1}. The melting temperature (T_m) was measured during the first

heating, while the glass transition temperature (T_g) was determined during the second heating run.

8.8 Thermo gravimetric analysis (TGA)

Thermal stability of all polymers and starting materials was carried out by using thermo microbalance [Netzsch GmbH TG 209C (Selb, Germany)] under nitrogen atmosphere within the temperature range of 0 to 700 ℃ with the heating rate of 10 $K \cdot min^{-1}$.

8.9 Imaging with confocal laser scanning microscope (CLSM)

The critical micelle temperature and critical micelle concentration (CMT and CMC) values of amine terminated PEPE and HA hydrogels were characterized by using a confocal laser scanning microscope (CLSM 510, Carl Zeiss). The solution of all samples were placed between two glass slides and excited by using 405 nm laser and imaged in the blue channel.

8.10 Gel electrophoresis

The 0.5% agarose gel was prepared by dissolving 0.2 g of agarose in 40 ml 1% TAE buffer (Tris-Acetate-EDTA buffer) and the gel was kept overnight in the chamber containing 1% TEA buffer at room temperature. On the next day, the samples were loaded (13 µl sample + 2 µl tracking dye = 15 µl each) in the gel with the DNA standard and Hyaluronic acid as a reference sample. The electrophoresis was initially run for 30 min. at 20 V and afterwards at 40 V for 3 h. After that, the gel was kept in the staining medium (0.05% stains all solution in 50% EtOH) for 12 h to stain the gel. After staining the gel was destained by using 10% EtOH for one day (the 10% EtOH was changed once). On the next day the gel was kept under normal light for 2 h to do the final destaining. After finishing the destaining the gel pictures was taken by computer operated camera system in house.

8.11 Mass Spectrometry

The Mass spectra reported in the chapter 4 were acquired in positive ion mode using an integrated ESI-Q-TOFmicro quadruple time-of-flight mass spectrometer (Micromass, Manchester, UK) equipped with an ESI source. The MALDI-TOF spectrum of PEPE, PEPE1, and PEPE2 reported in figure 8 (chapter 4) were measured using a MALDI-TOF/TOF (Ultraflextreme MALDI-TOF/TOF, Bruker Daltonics).

8.12 TNBS assay procedure

11 mg of solid sample were placed in a 50 mL centrifuge tube, followed by addition of 1 mL of 4% $NaHCO_3$ (pH 8.5) and 1 mL of 0.5 % TNBS. The reaction mixture was kept 40 ℃ for 4 hours with mild shaking. Then HCl (6M, 3 mL) was added and the mixture was heated at 110 ℃ for 1 h to hydrolysed and dissolve any insoluble material. The samples were cooled down to room temperature and diluted with 5 mL of water. The hydrolysed dilution was extracted with 20 mL (3x) of anhydrous ethyl ether to remove excess of unreacted TNBS. A 5 mL aliquot of the aqueous phase was removed and heated for 20 min in a hot water bath to evaporate residual ether. The aliquot was diluted with 15 mL of water and the absorbance measured at 346 nm. All samples were read against a blank, prepared by the same procedure as the samples. However the HCl was added before the addition of TNBS to avoid any reaction of TNBS with the protein.

In this spectrophotometric method TNBS (as a UV-chromophore) reacts with primary amino groups of PEPE at an alkaline pH to form a trinitrophenyl derivative and a sulfate ion. By determination of the yellow absorbance of the trinitrophenyl derivative, the number of amino groups in PEPE can be calculated, by using an equation,

$$\frac{moles\ NH_2}{g\ PEPE} = \frac{2\,(absorbance)\,(0.020\,liters)}{(1.4\times10^4\,liters/mole\cdot cm)\,(b)\,(x)} \qquad (8.1)$$

Where, $1.4\cdot10^4$ is the absorption coefficient for 2,4,6-trinitrophenyl derivative, *b* is the cell path length in cm, and *x* is the sample weight in g.

8.13 Critical Micelle Concentration (CMC) and Critical Micelle Temperature (CMT)

The critical micelle concentration and critical micelle temperature was determined by UV spectrophotometer [uvikon 931 UV/VIS spectrophotometer (Leeds, GB)]. The dye used in these measurements was diphenyl hexatriene (DPH). All measurements were performed at 15-45 °C at 5 °C intervals. The sample were prepared in the range of 0.05 – 20 w/v%. To each sample 25 µL 0.004 mM DHP solution (in methanol) was added and the samples were stirred at room temperature (for 2-3 h.) in a dark room. Further, the samples were measured in a temperature range of 15 – 45 °C with 5 °C interval and corresponding UV absorption was recorded to evaluate the CMC and CMT values.

8.14 Water uptake

Freeze dried T-ArcGel samples (of size 1cm X 1 cm X 0.8 cm) were used for this study. The samples were immersed in PBS buffer (7.4 pH) of 25 °C and 37 °C temperature. The water uptake (*H*) was measured by using eq. 6.1. The water uptake was determined by using 4 replicas of each samples. The data points described the median.

8.15 Endotoxin tests (Quanti-Blue Assay)

The material bound microbial products were analysed by a cell based assay. In order to determine the endotoxin content, $5x10^6$ RAW-Blue™ cells (InvivoGen, San Diego, USA) were cultured 1 mL VLE-RPMI (Biochrom®) supplemented with 200 ìg/mL Zeocin (InvivoGen, San Diego, USA) and100 ìg/mL in a 24-well flat-bottom plate in the presence of PEI membranes for 24 hours. As positive control, 10 ìg/mL LPS (O111:B4) was added to the culture. Directly after incubation, 40 ìl of cell culture supernatants were added to 160 ìl Quanti-BlueTM solution (InvivoGen, San Diego, USA) in a 96-well plate and incubated for 3 hours at 37 °C. Secreted embryonic

alkaline phosphatase (SEAP) catalyzed color change was measured at620 nm using a TECAN-InfiniteM200pro (Tecan, Männedorf, Switzerland).

8.16 LAL test

A Limulus amebocyte lysate test (LAL-test) was performed. The here used LAL is a standard test to determine several bacterial endotoxins or lipopolysaccarides (LPS; compounds of the outer membranes) of gram negative bacteria. The test is based on an aqueous extract of lysated blood cells (amoebocytes) from the horseshoe crab (*Limulus polyphemus*) which contains a clotting factor. If endotoxins like LPS are present in the test solution, coagulation will occur and the extent of coagulation can be related to the endotoxin contamination of the sample. The material eluates were prepared according to ISO10993–12. The eluates were analyzed for lipopolysaccharide contamination using the LAL-Test (Lonza, Cologne, Germany), which was performed according to manufacture instructions.The values are given in endotoxin units (EU) per milliliter.

8.17 Synthesis of Mono-amine terminated PEPE

12 g (0.816 mmol) of PEPE was dissolved in 200 ml dichloromethane; 4-nitrophenyl chloroformate (198 mg, 0.979 mmol) was added in the presence of triethylamine (0.113 ml, 0.979 mmol) at room temperature. The reaction was stirred overnight and precipitated in 8 fold hexane. The vacuum dried intermediate was dissolved in 200 ml dichloromethane and reacted with excess of diaminopropane (0.206 ml, 2.44 mmol) overnight under stirring at room temperature, and the mixture was precipitated in 8 fold hexane. The precipitated product was dried under vacuum at 40 ℃ for 24 h. It was re-dissolved in dichloromethane and passed through an alumina (Al_2O_3) column to remove the side-product (p-nitrophenol), re-precipitated in 8 fold hexane and vacuum dried before use. The degree of functionalization was determined by TNBS colorimetric assay (80-85 mol%). IR (υ_{max}/cm^{-1}), 3300-3600 (-OH), 2900 (C-H stretch), 1720 (C=O stretching), 1640 (N-H bending), and 1050-1150 (C-O-C stretching). ^{1}H-NMR (500 MHz, $CDCl_3$) δ = 9.76 (m, O=C–NH- (amide), 2.55

(m, -CH_2- of biaminopropane), 1.1 (s, 3H, -CH_3 of PPG), and 3.55-3.74 (m, 27H, CH_2-O of PEG and PPG, -CH-O- of PPG) ppm.

8.18 Synthesis of di-amine terminated PEPE

After dissolving 12 g (0.816 mmol) PEPE in 200 ml dichloromethane, an excess of 4-nitrophenyl chloroformate (493 mg, 2.448 mmol) was added in the presence of triethylamine (0.283 ml, 2.448 mmol) at room temperature. The reaction mixture was stirred overnight and precipitated in 8 fold hexane. The vacuum dried intermediate was dissolved in 200 ml dichloromethane and reacted with excess of biaminopropane (0.274 ml, 3.26 mmol) overnight at room temperature. Further workup was identical with workup of mono-amine terminated PEPE. The degree of functionalization was determined by TNBS colorimetric assay (85-90 mol%). IR (υ_{max}/cm^{-1}), 3300-3600 (-OH), 2910 (C-H stretch), 1715 (C=O stretching), 1646 (N-H bending), and 1040-1150 (C-O-C stretching). ^{1}H-NMR (500 MHz, $CDCl_3$) δ = 9.72 (m, O=C–NH- (amide), 2.5 (m, -CH_2- of di-amine), 1.13 (s, 3H, -CH_3 of PPG), and 3.52-3.78 (m, 27H, -CH_2-O- of PEG and PPG, -CH-O- of PPG) ppm.

8.19 Synthesis of Pectin-*g*-PEPE hydrogels

Pectin (453 mg, corresponding to 1.9 mmol of free carboxylic acid groups) was dissolved in 300 ml of distilled water with continuous stirring for 4 h to obtain a homogeneous solution, then EDC·HCl (633 mg, 4.08 mmol) was added and the pH was adjusted to 4.6 - 4.7 with 0.1 M HCl. Then, the aminated PEPE (12 g, ca. 0.367 mmole amino groups) was added. The reaction was stirred overnight at room temperature (pH = 4.6 – 4.7). The crude solution was dialyzed against water by using cellulose membrane (Spectra/Por® MWCO 25000 Da) with water changes each hour for the first 12 h and then dialyzed for 2 days. Lyophilization gave a white solid.

8.20 Synthesis of Chondroitin sulfate-*g*-PEPE hydrogels

Chondroitin sulfate (337 mg, corresponding to 0.816 mmol of free carboxylic acid groups) was dissolved in 300 ml of distilled water with continuous stirring for 4 h to obtain a homogeneous solution, then EDC·HCl (633 mg, 4.08 mmol) was added and the pH was adjusted to 4.6 - 4.7 with 0.1 M HCl. Then, the aminated PEPE (12 g, ca. 0.367 mmole amino groups) was added. The reaction was stirred overnight at room temperature (pH = 4.6 – 4.7). The crude solution was dialyzed against water by using cellulose membrane (Spectra/Por® MWCO 25000 Da) with water changes each hour for the first 12 h and then dialyzed for 2 days. Lyophilization gave a white solid.

8.21 Preparation of physical mixtures of amine terminated PEPE and HA hydrogels

The physical mixtures of HA and mono/di-amine terminated PEPE were prepared by using different wt% of PEPE. The general procedure for physical mixture of mono-PEPE is, 322 mg (0.816 mmol) of HA was pre dissolved in distilled water by stirring at room temperature for 6 h. and followed by addition of EDC 633 mg (4.08 mmol) then, 12 g (0.816 mmol) of mono-PEPE were added to the solution. The mixing was performed for 12 h. at room temperature and dialysed by using cellulose membrane of MWCO of 25,000 for 2 days with changing the surrounding water for 7-8 times. Further the product was freeze dried for 2 days to obtain a dry polymer.

The physical mixture of di-amino PEPE and HA was prepared by dissolving 640 mg (1.62 mmol) of HA in 350 ml of distilled water at room temperature for 6 h. and 1.26g of EDC and then 12 g of di-amino PEPE were added. The solution was stirred at room temperature for 12 h. and dialysed by using cellulose membrane of MWCO of 25,000 for 2 days with changing the surrounding water for 7-8 times. Further the product was freeze dried for 2 days to obtain a dry polymer.

8.22 Synthesis of HA-*g*-PEPE hydrogels

HA (320 mg, 0.81 mmol) was dissolved in 190 ml of distilled water with continuous stirring for 6 h. to obtain a homogeneous solution, then DMTMM (672 mg, 2.43 mmol) was added and stirred for 2 h. After addition of mono-amino PEPE (12 g, 0.81 mmol), the reaction was stirred overnight at room temperature. The crude product was purified by ultrafiltration and then freeze-dried for 2 days to obtain a white product. IR (u_{max}/cm^{-1}) 3300-3600 (-OH), 2910 (C-H stretch), 1740 (C=O stretching), 1660 (N-H bending, amide I), 1555 (amide II), and 1030-1145 (C-O-C stretching).

8.23 Synthesis of HA-*x*-PEPE hydrogels

HA (320 mg, 0.81 mmole) was dissolved in 190 ml of distilled water with continuous stirring for 6 h. to obtain a homogeneous solution, then DMTMM (672 mg, 2.43 mmole) was added and stirred for 2 h. After addition of bi-amino PEPE (6 g, 0.405 mmole), the reaction was stirred overnight at room temperature. The crude product was purified by ultrafiltration and then freeze-dried for 2 days to obtain a white product. IR (u_{max}/cm^{-1}) 3300-3600 (-OH), 2915 (C-H stretch), 1740 (C=O stretching), 1658 (N-H bending, amide I), 1558 (amide II), and 1040-1150 (C-O-C stretching).

8.24 Synthesis of p-nitrophenylformate substituted PEPE

12 g (0.816 mmol) of PEPE was dissolved in 200 ml dichloromethane; 4-nitrophenyl chloroformate (198 mg, 0.979 mmol) was added in the presence of triethylamine (0.131 ml, 0.979 mmol) at room temperature. The reaction was stirred overnight and precipitated in 8 fold hexane followed by vacuum drying before use. By this method we can achieve predominantly the mono-substituted PEPE. Moreover, this approach may produce a certain amount of di-substituted PEPE. The content of bi-substituted could not be determined, one of the reasons being the high polydispersity of the starting materials.

8.25 Synthesis of GA-*g*-PEPE hydrogels

15 g of Gelatin was dissolved in 350 ml of DMSO at 45 ℃ in an oil bath. Dry PEPE-4NCP (9 g) was added to gelatin solution slowly, the colour of solution changed from colourless to light yellow (Due to the elimination of 4-nitrophenol as a side product). The reaction mixture was stirred at 45 ℃ for 3-4 h, then at room temperature overnight. The reaction mixture was precipitated in 10 fold ethanol to remove unreacted PEPE-4NCP. The compound was dried under high vacuum at 40 ℃ for 2 days and used for further analysis and crosslinking reaction.

8.26 Synthesis of GA-*g*-PEPE Scaffolds

11.11 g of Gelatin functionalized with PEPE was dissolved in 100 ml water (to get 10 wt% concentration) at 45 ℃ by using a mechanical stirrer at 500 rpm. After complete dissolution, the solution was stirred at 1500 rpm for 20 minutes to get stable foam and then 8 fold L-Lysine Diisocyanate ethyl ether (LDI) was added and stirring was continued for 90 sec. to crosslink the foam. Afterwards, the foam was collected in small portions and kept immediately in the freeze at -20 ℃ to allow the remaining crosslinking and also to stabilize the foam. The next day the scaffolds were washed several times with water to remove unreacted PEPE functionalized gelatin and lyophilised for 3 days to obtain dry T-ArcGel.

9. References

(1) Ifkovits, J. L.; Burdick, J. *Tissue Engineering* **2007**, *13*, 2369–2385.

(2) Seeberger, P. H.; Werz, D. B. *Nature* **2007**, *446*, 1046–1051.

(3) Stuart, M. C.; Huck, W. T. S.; Genzer, J.; Müller, M.; Ober, C.; Stamm, M.; Sukhorukov, G. B.; Szleifer, I.; Tsukruk, V. V; Urban, M.; Winnik, F.; Zauscher, S.; Luzinov, I.; Minko, S. *Nature Materials* **2010**, *9*, 101–113.

(4) Makadia, H. K.; Siegel, S. J. *Polymers* **2011**, *3*, 1377–1397.

(5) Nair, L. S.; Laurencin, C. T. *Progress in Polymer Science* **2007**, *32*, 762–798.

(6) Huebsch, N.; Mooney, D. J. *Nature* **2009**, *462*, 426–432.

(7) Wang, C.; Stewart, R. J.; Kopecek, J. *Nature* **1999**, *397*, 417–420.

(8) Kim, T. G.; Chung, H. J.; Park, T. G. *Acta Biomaterialia* **2008**, *4*, 1611–1619.

(9) Tibbitt, M. W.; Anseth, K. S. *Biotechnology and Bioengineering* **2009**, *103*, 655–663.

(10) Jeong, B.; Kim, S. W.; Bae, Y. H. *Advanced Drug Delivery Reviews* **2002**, *54*, 37–51.

(11) He, C.; Kim, S. W.; Lee, D. S. *Journal of Controlled Release* **2008**, *127*, 189–207.

(12) Namgung, R.; Nam, S.; Kim, S. K.; Son, S.; Singha, K.; Kwon, J.S.; Ahn, Y.; Jeong, M. H.; Park, I.-K.; Garripelli, V. K.; Jo, S.; Kim, W. J. *Biomaterials* **2009**, *30*, 5225–5233.

(13) Jeong, B.; Gutowska, A. *Trends in Biotechnology* **2002**, *20*, 305–311.

(14) Chitosan, F.; Zhang, W.; Gilstrap, K.; Wu, L.; C, R. B. K.; Moss, M. A.; Wang, Q.; Lu, X.; He, X. **2010**, *4*, 6747–6759.

(15) Park, K. M.; Lee, S. Y.; Joung, Y. K.; Na, J. S.; Lee, M. C.; Park, K. D. *Acta Biomaterialia* **2009**, *5*, 1956–1965.

(16) Ahn, S.; Kasi, R. M.; Kim, S.-C.; Sharma, N.; Zhou, Y. *Soft Matter* **2008**, *4*, 1151-1157.

(17) Janmey, P.; McCulloch, C. *Annual review of biomedical Engineering* **2007**, *9*, 1–34.

(18) Yu, L.; Ding, J. *Chemical Society Reviews* **2008**, *37*, 1473–1481.

(19) Ifkovits, J. L.; Burdick, J. *Tissue Engineering* **2007**, *13*, 2369–2385.

(20) Miyata, T.; Uragami, T.; Nakamae, K. *Advanced Drug Delivery Reviews* **2002**, *54*, 79–98.

(21) Oh, E. J.; Park, K.; Kim, K. S.; Kim, J.; Yang, J.-A.; Kong, J.-H.; Lee, M. Y.; Hoffman, A. S.; Hahn, S. K. *Journal of Controlled Release* **2010**, *141*, 2–12.

(22) Habas, J.-P.; Pavie, E.; Lapp, A.; Peyrelasse, J. *Journal of Rheology* **2004**, *48*, 1–21.

(23) Katono, H.; Maruyama, A.; Sanui, K.; Ogata, N.; Okano, T.; Sakurai, Y. *Journal of Controlled Release* **1991**, *16*, 215–227.

(24) Chung, H. J.; Lee, Y.; Park, T. G. *Journal of controlled release* **2008**, *127*, 22–30.

(25) Collins, M. N.; Birkinshaw, C. *Journal of Applied Polymer Science* **2008**, *109*, 923–931.

(26) Hennink, W. E.; Van Nostrum, C. F. *Advanced Drug Delivery Reviews* **2002**, *54*, 13–36.

(27) Jeong, B.; Bae, Y. H.; Lee, D. S.; Kim, S. W. *Nature* **1997**, *388*, 860–862.

(28) Dayananda, K.; He, C.; Park, D. K.; Park, T. G.; Lee, D. S. *Polymer* **2008**, *49*, 4968–4973.

(29) Choi, K. Y.; Min, K. H.; Yoon, H. Y.; Kim, K.; Park, J. H.; Kwon, I. C.; Choi, K.; Jeong, S. Y. *Biomaterials* **2011**, *32*, 1880–1889.

(30) Kraehenbuehl, T. P.; Zammaretti, P.; Van der Vlies, A. J.; Schoenmakers, R. G.; Lutolf, M. P.; Jaconi, M. E.; Hubbell, J. A. *Biomaterials* **2008**, *29*, 2757–2766.

(31) Jin, R.; Moreira Teixeira, L. S.; Krouwels,; Dijkstra, P. J.; Van Blitterswijk, C.; Karperien, M.; Feijen, J. *Acta Biomaterialia* **2010**, *6*, 1968–1977.

(32) Lin, C.-H.; Lin, W.-C.; Yang, M.-C. *Colloids and surfaces. B, Biointerfaces* **2009**, *71*, 36–44.

(33) Seo, B.-B.; Park, M.-R.; Chun, C.; Lee, J.-Y.; Song, S.-C. *Biomaterials* **2011**, *32*, 8271–8280.

(34) Zhu, J.; Beamish, J. A.; Tang, C.; Kottke-Marchant, K.; Marchant, R. E. *Macromolecules* **2006**, *39*, 1305–1307.

(35) Pritchard, C. D.; Crafoord, S.; Andréasson, S.; Arnér, K. M.; O'Shea, T. M.; Langer, R.; Ghosh, F. K. *Acta Biomaterialia* **2011**, *7*, 936–43.

(36) Segura, T.; Anderson, B. C.; Chung, P. H.; Webber, R. E.; Shull, K. R.; Shea, L. D. *Biomaterials* **2005**, *26*, 359–371.

(37) Ehrbar, M.; Rizzi, S. C.; Schoenmakers, R. G.; Miguel, B. S.; Hubbell, J. A.; Weber, F. E.; Lutolf, M. P. *Biomacromolecules* **2007**, *8*, 3000–3007.

(38) Shu, X. Z.; Liu, Y.; Palumbo, F.; Prestwich, G. D. *Biomaterials* **2003**, *24*, 3825–3834.

(39) Pouyani, T.; Harbison, G. S.; Prestwich, G. D. **1994**, 7515–7522.

(40) Joshi, H. N.; Stella, V. J.; Topp, E. M. *Journal of Controlled Release* **1992**, *20*, 109–121.

(41) Van Beek, M.; Jones, L.; Sheardown, H. *Biomaterials* **2008**, *29*, 780–789.

(42) Homma, A.; Sato, H.; Okamachi, A.; Emura, T.; Ishizawa, T.; Kato, T.; Matsuura, T.; Sato, S.; Tamura, T.; Higuchi, Y.; Watanabe, T.; Kitamura, H.; Asanuma, K.; Yamazaki, T.; Ikemi, M.; Kitagawa, H.; Morikawa, T.; Ikeya, H.; Maeda, K.; Takahashi, K.; Nohmi, K.; Izutani, N.; Kanda, M.; Suzuki, R. *Bioorganic & Medicinal Chemistry* **2009**, *17*, 4647–4656.

(43) Ohya, S.; Nakayama, Y.; Matsuda, T. *Biomacromolecules* **2001**, *2*, 856–863.

(44) Kuo, J. *Hyaluronic Acid*; Elsevier Ltd., 2011; pp. 239–259.

(45) Wang, B.; Zhu, W.; Zhang, Y.; Yang, Z.; Ding, J. *Reactive and Functional Polymers* **2006**, *66*, 509–518.

(46) Heskins, M.; Guillet, J. E. *Journal of Macromolecular Science: Part A - Chemistry* **1968**, *2*, 1441–1455.

(47) Schild, H. G. *Progress in Polymer Science* **1992**, *17*, 163–249.

(48) Neugebauer, D. *Polymer International* **2007**, *56*, 1469–1498.

(49) Alexandridis, P.; Holzwarth, J. F.; Hatton, T. A. *Macromolecules* **1994**, *27*, 2414–2425.

(50) Alexandridis, P.; Alan Hatton, T. *Colloids and Surfaces A: Physicochemical and Engineering Aspects* **1995**, *96*, 1–46.

(51) Booth, C.; Attwood, D. *Macromolecular Rapid Communications* **2000**, *21*, 501–527.

(52) Paterson, I. F.; Chowdhry, B. Z.; Leharne, S. A. *Langmuir* **1999**, *15*, 6187–6194.

(53) Holland, R. J.; Parker, E. J.; Guiney, K.; Zeld, F. R. *The Journal of Physical Chemistry* **1995**, *99*, 11981–11988.

(54) Lopes, J. R.; Loh, W. *Langmuir* **1998**, *14*, 750–756.

(55) Haque, M. A.; Kurokawa, T.; Gong, J. P. *Soft Matter* **2013**, *9*, 5223–5230.

(56) Emoto, K.; Iijima, M.; Nagasaki, Y.; Kataoka, K. *Journal of the American Chemical Society* **2000**, *122*, 2653–2654.

(57) Lu, C.; Yoganathan, R. B.; Kociolek, M.; Allen, C. *Journal of Pharmaceutical Sciences* **2013**, *102*, 627–637.

(58) Reinicke, S.; Döhler, S.; Tea, S.; Krekhova, M.; Messing, R.; Schmidt, A. M.; Schmalz, H. *Soft Matter* **2010**, *6*, 2760–2773.

(59) Li, F.; Danquah, M.; Mahato, R. I. *Biomacromolecules* **2010**, *11*, 2610–2620.

(60) Cohn, D.; Sosnik, A.; Levy, A. *Biomaterials* **2003**, *24*, 3707–3714.

(61) Cohn, D.; Lando, G.; Sosnik, A.; Garty, S.; Levi, A. *Biomaterials* **2006**, *27*, 1718–1727.

(62) Sosnik, A.; Cohn, D. **2004**, *25*, 2851–2858.

(63) Li, T.; Lin, J.; Chen, T.; Zhang, S. *Polymer* **2006**, *47*, 4485–4489.

(64) Ma, Y.; Cao, T.; Webber, S. E. *Macromolecules* **1998**, *31*, 1773–1778.

(65) De Cock, L. J.; De Wever, O.; Hammad, H.; Lambrecht, B. N.; Vanderleyden, E.; Dubruel, P.; De Vos, F.; Vervaet, C.; Remon, J. P.; De Geest, B. G. *Chemical Communications* **2012**, *48*, 3512–3514.

(66) Wolf, M. T.; Daly, K. a; Reing, J. E.; Badylak, S. F. *Biomaterials* **2012**, *33*, 2916–2925.

(67) Weigel, T.; Schinkel, G.; Lendlein, A. *Expert Review of Medical Devices* **2006**, *3*, 835–851.

(68) Frisman, I.; Seliktar, D.; Bianco-Peled, H. *Acta Biomaterialia* **2012**, *8*, 51–60.

(69) Velema, J.; Kaplan, D. **2006**, 187–238.

(70) Huang, X.; Zhang, Y.; Donahue, H. J.; Lowe, T. L. *Tissue Engineering* **2007**, *13*, 2645–2652.

(71) Galperin, A.; Long, T. J.; Ratner, B. D. *Biomacromolecules* **2010**, *11*, 2583–2592.

(72) Duarte, A. R. C.; Mano, J. F.; Reis, R. L. *Acta Biomaterialia* **2011**, *7*, 526–529.

(73) Fu, S.; Ni, P.; Wang, B.; Chu, B.; Zheng, L.; Luo, F.; Luo, J.; Qian, Z. *Biomaterials* **2012**, *33*, 4801–4819.

(74) Kim, D. H.; Heo, S.-J.; Shin, J.-W.; Mun, C. W.; Park, K. M.; Park, K. D.; Jee, K. S. *Macromolecular Research* **2010**, *18*, 387–391.

(75) Baino, F. *Acta Biomaterialia* **2011**, *7*, 921–35.

(76) Gao, Q.; Mou, S.; Ge, J.; To, C.-H.; Hui, Y.; Liu, A.; Wang, Z.; Long, C.; Tan, J. *Eye* **2008**, *22*, 461–468.

(77) Soman, N.; Banerjee, R. *Bio-medical Materials and Engineering* **2003**, *13*, 59–74.

(78) Nickerson, C. S.; Park, J.; Kornfield, J. a; Karageozian, H. *Journal of Biomechanics* **2008**, *41*, 1840–1846.

(79) Gao, Q.; Mou, S.; Ge, J.; To, C.; Hui, Y.; Liu, A.; Wang, Z.; Long, C.; Tan, J. *Eye* **2008**, *22*, 461–468.

(80) Annaka, M.; Mortensen, K.; Vigild, M. E.; Matsuura, T.; Tsuji, S.; Ueda, T.; Tsujinaka, H. *Biomacromolecules* **2011**, *12*, 4011–4021.

(81) Chirila, T. V.; Hong, Y. *Polymer International* **1998**, *46*, 183–195.

(82) Hsu, S.-H.; Leu, Y.-L.; Hu, J.-W.; Fang, J.-Y. *Chemical & Pharmaceutical Bulletin* **2009**, *57*, 453–458.

(83) Michels, B.; Waton, G.; Zana, R. *Colloids and Surfaces A: Physicochemical and Engineering Aspects* **2001**, *183-185*, 55–65.

(84) Ma, J.-H.; Guo, C.; Tang, Y.-L.; Wang, J.; Zheng, L.; Liang, X.-F.; Chen, S.; Liu, H.-Z. *Langmuir* **2007**, *23*, 3075–3083.

(85) Lam, Y.; Grigorieff, N.; Goldbeck-Wood, G. *Physical Chemistry Chemical Physics* **1999**, *1*, 3331–3334.

(86) Wu, G.; Liu, L.; Buu, V.-B.; Chu, B.; Schneider, D. K. *Physica A: Statistical Mechanics and its Applications* **1996**, *231*, 73–81.

(87) Burdick, J. a; Chung, C.; Jia, X.; Randolph, M. a; Langer, R. *Biomacromolecules* **2005**, *6*, 386–391.

(88) Su, S. H.; Eu, Y. L.; U, J. H.; Ang, J. F. *Chemical & Pharmaceutical Bulletin* **2009**, *57*, 453–458.

(89) K.Y. Choa, T.W. Chungb, B.C. Kimb, M.K. Kim, J.H. Leec, W.R.Weec, C. S. C. *International Journal of Pharmaceutics* **2003**, *260*, 83–91.

(90) Santan, H. D.; Neffe, A. T.; Kamlage, S.; Lendlein, A. *MRS Proceedings* **2012**, *1403*, mrsf11–1403–v17–05.

(91) Ho, E.; Lowman, A.; Marcolongo, M. *Biomacromolecules* **2006**, *7*, 3223–3228.

(92) Chen, C.-C.; Fang, C.-L.; Al-Suwayeh, S. A.; Leu, Y.-L.; Fang, J.-Y. *International Journal of Pharmaceutics* **2011**, *415*, 119–128.

(93) Gajewiak, J.; Cai, S.; Shu, X. Z.; Prestwich, G. D. *Biomacromolecules* **2006**, *7*, 1781–1789.

(94) Lee, H.; Park, T. G. *Journal of Biomedical Materials Research. Part A* **2009**, *88*, 797–806.

(95) Su, S. H.; Eu, Y. L.; U, J. H.; Ang, J. F. *Chemical & Pharmaceutical Bulletin* **2009**, *57*, 453–458.

(96) Harley, B. A.; Leung, J. H.; Silva, E. C. C. M.; Gibson, L. J. *Acta biomaterialia* **2007**, *3*, 463–474.

(97) Mráz, J.; Boušková, Š. *Chemico-Biological Interactions* **1999**, *117*, 173–186.

(98) Annabi, N.; Mithieux, S. M.; Boughton, E. A.; Ruys, A. J.; Weiss, A. S.; Dehghani, F. *Biomaterials* **2009**, *30*, 4550–4557.

(99) Nowatzki, P. J.; Tirrell, D. A. *Biomaterials* **2004**, *25*, 1261–1267.

(100) EASTOE, J. E. *The Biochemical Journal* **1955**, *61*, 589–600.